

SCHOOL OF  
CIVIL ENGINEERING

INDIANA

DEPARTMENT OF TRANSPORTATION

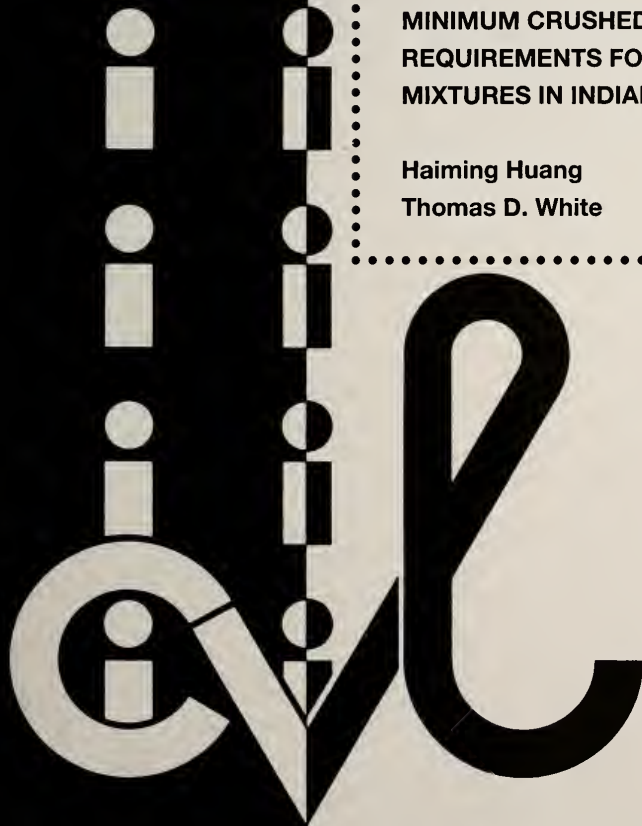
JOINT HIGHWAY RESEARCH PROJECT

FHWA/IN/JHRP-96/23

Final Report

MINIMUM CRUSHED AGGREGATE  
REQUIREMENTS FOR ASPHALT  
MIXTURES IN INDIANA

Haiming Huang  
Thomas D. White



PURDUE UNIVERSITY



FINAL REPORT

**FHWA/IN/JHRP-96/23**

MINIMUM CRUSHED AGGREGATE REQUIREMENTS  
FOR ASPHALT MIXTURES IN INDIANA

by

Haiming Huang  
Graduate Research Assistant

and

Thomas D. White  
Professor of Materials Engineering

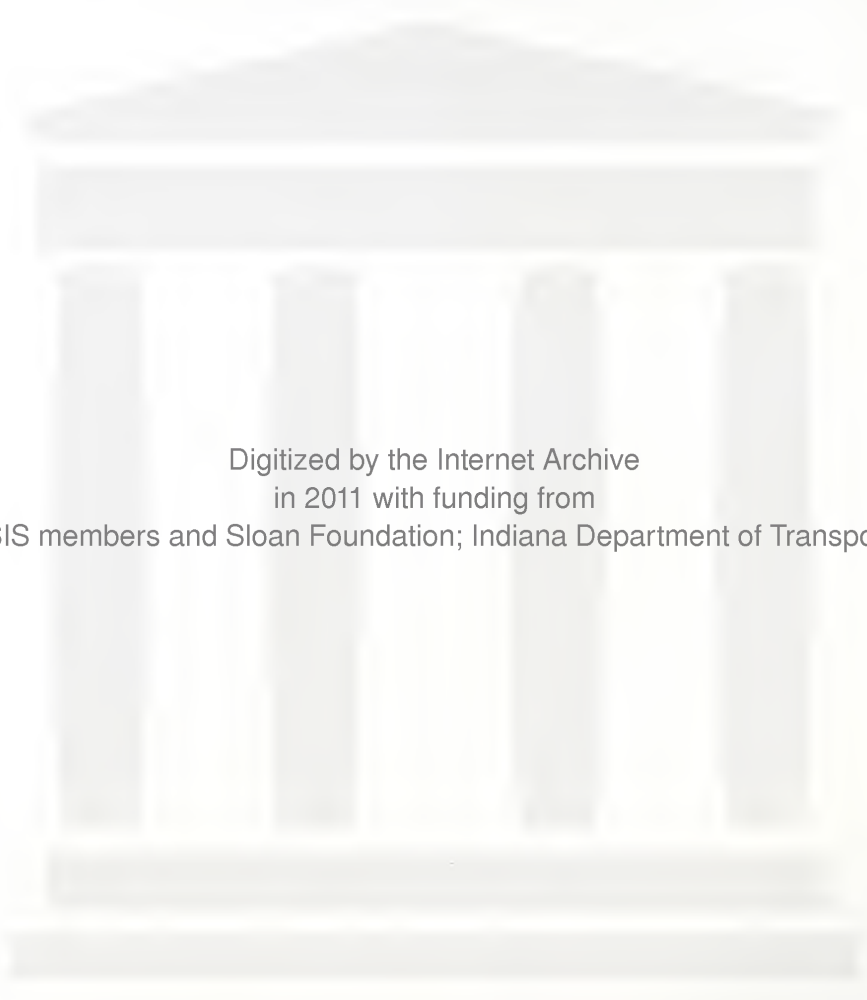
Purdue University  
Department of Civil Engineering

Joint Highway Research Project  
Project No: C-36-55J  
File No: 2-12-10

Prepared in Cooperation with the  
Indiana Department of Transportation and  
the U.S. Department of Transportation  
Federal Highway Administration

The contents of this report reflect the views of the authors who are responsible for the facts and the accuracy of the data presented herein. The contents do not necessarily reflect the official views or policies of the Federal Highway Administration and the Indiana Department of Transportation. This report does not constitute a standard, specification, or regulation.

Purdue University  
West Lafayette, IN 47907  
May 31, 1997



Digitized by the Internet Archive  
in 2011 with funding from  
LYRASIS members and Sloan Foundation; Indiana Department of Transportation



**TECHNICAL REPORT STANDARD TITLE PAGE**

<b>1. Report No.</b> FHWA/TN/JHRP-96/23	<b>2. Government Accession No.</b>	<b>3. Recipient's Catalog No.</b>	
<b>4. Title and Subtitle</b>  Minimum Crushed Aggregate Requirements		<b>5. Report Date</b> May 31, 1997	
		<b>6. Performing Organization Code</b>	
<b>7. Author(s)</b>  H. Huang and T. White		<b>8. Performing Organization Report No.</b> FHWA/TN/JHRP-96/23	
<b>9. Performing Organization Name and Address</b> Joint Highway Research Project 1284 Civil Engineering Building Purdue University West Lafayette, Indiana 47907-1284		<b>10. Work Univ No.</b>	
		<b>11. Contract or Grant No.</b> HPR-2030	
<b>12. Sponsoring Agency Name and Address</b>  Indiana Department of Transportation State Office Building 100 North Senate Avenue Indianapolis, IN 46204		<b>13. Type of Report and Period Covered</b>  Final Report	
		<b>14. Sponsoring Agency Code</b>	
<b>15. Supplementary Notes</b>  Prepared in cooperation with the Indiana Department of Transportation and Federal Highway Administration.			
<b>16. Abstract</b>  <p>An accelerated pavement testing facility has been developed by Purdue University for the Indiana Department of Transportation. The test facility includes a test pit in which prototype scale pavement sections can be installed. The Accelerated Pavement Tester loading system has the capability of applying moving wheel loads to the test sections. An initial study utilizing the accelerated pavement test facility has been conducted at Purdue University to determine the minimum crushed aggregate requirements in asphalt mixtures in Indiana. This study addresses effects of various constituents of the asphalt mixture on pavement rutting. The factors included in this study are aggregate type, percentage of crushed gravel, percentage of natural vs. crushed sand, and asphalt content. Combinations of these factors and their levels resulted in 27 sections being tested.</p> <p>Rutting was documented for each test section during APT operation. Marshall mixture design and laboratory tests provide comprehensive information on mixture properties. As a result of both the laboratory and APT results, recommendations are provided for using gravel in asphalt mixture.</p> <p>A finite element program ABACUS was used in this study to model the pavement structure and permanent deformation. An approximate approach was used to simulate the APT conditions. A creep model was used to represent the actual pavement rutting. Based on the mixture performance in APT, material constants in the creep model were back calculated. Regression analyses were conducted to correlate these material constants with mixture physical properties. Mixtures tested with the APT were also tested in a laboratory wheel track device. After these results were evaluated, two of the original mixtures were retested in the APT.</p>			
<b>17. Key Words</b>  asphalt, crushed, aggregates, mixtures, accelerated, testing, rutting, finite elements.		<b>18. Distribution Statement</b>  No restrictions. This document is available to the public through the National Technical Information Service, Springfield, VA 22161	
<b>19. Security Classif. (of this report)</b>	<b>20. Security Classif. (of this page)</b>	<b>21. No. of Pages</b> 220	<b>22. Price</b>



## TABLE OF CONTENTS

	Page
LIST OF TABLES .....	iv
LIST OF FIGURES .....	vi
IMPLEMENTATION REPORT .....	ix
CHAPTER 1 INTRODUCTION .....	1
CHAPTER 2 LITERATURE REVIEW .....	4
2.1 Causes of Asphalt Pavement Rutting .....	4
2.2 Effects of Mixture Constituents on Rutting .....	6
2.2.1 Asphalt Cement .....	6
2.2.2 Aggregate Angularity .....	7
2.2.3 Aggregate Gradation .....	8
2.2.4 Mineral Filler .....	10
CHAPTER 3 ACCELERATED PAVEMENT TESTING FACILITY .....	11
3.1 System Design Requirements .....	12
3.1.1 Accelerated Damage Due to Load .....	12
3.1.2 Estimate of Rutting Damage .....	12
3.1.3 Structural and Mechanical Design of Accelerated Testing System .....	13
CHAPTER 4 EXPERIMENTAL DESIGN .....	18
CHAPTER 5 TESTING PROCEDURES .....	21
5.1 Mix Designs .....	21
5.1.1 Aggregates .....	21
5.1.2 Asphalt Cement .....	23
5.1.3 Mix Design .....	28
5.1.4 Gyratory Testing Machine Tests .....	29
5.2 Test Section Construction .....	29
5.3 Accelerated Pavement Test .....	30
5.4 Laboratory Tests .....	33
5.4.1 Bulk and Maximum Specific Gravity .....	33
5.4.2 Asphalt Extraction and Recovery .....	36
5.4.3 Sieve Analysis, Crushed Faces, and Flat & Elongated Particles .....	36
5.4.4 Penetration and Viscosity of Recovered Asphalt Cement .....	36
5.4.5 Marshall Recompression Test .....	37
5.4.6 Gyratory Shear Test .....	37
5.5 Laboratory Wheel Tracking Tests .....	37
CHAPTER 6 ANALYSES OF EXPERIMENTAL DATA .....	39
6.1 Results of Marshall Mix Design .....	39
6.2 Air Voids Analysis of In-Situ Pavement .....	46
6.3 Extracted Asphalt Content .....	51
6.4 Penetration and Viscosity .....	54

6.5	Gradation .....	60
6.6	Percentage of Crushed Faces and Flat & Elongated Particles .....	67
6.7	Gyratory Stability Index (GSI) and Shear Strength .....	70
6.7.1	Gyratory Stability Index .....	70
6.7.2	Gyratory Shear Strength of Bulk Mixtures .....	70
6.8	Analysis of Marshall Recompaction .....	76
6.9	Results of Accelerated Pavement Test .....	76
6.10	Statistical Analyses .....	82
6.10.1	40% Crushed Gravel Mixtures .....	82
6.10.2	70% Crushed Gravel Mixtures .....	84
6.10.3	100% Natural Sand Gravel Mixtures .....	87
6.10.4	95% Crushed Gravel, Slag, and Limestone Mixtures .....	89
6.11	WTD Test Results .....	90
6.12	Additional APT Tests .....	91
6.13	Summary .....	103
CHAPTER 7 FINITE ELEMENT ANALYSIS .....		106
7.1	Features of the Finite Element Model .....	107
7.1.1	Material Models .....	107
7.1.2	Boundary Conditions .....	109
7.1.3	Element Types .....	110
7.1.4	Load Models .....	112
7.1.5	Model Responses .....	114
7.1.6	Model Geometry .....	114
7.2	Sensitivity Analysis .....	120
7.3	Backcalculation .....	128
7.4	Summary .....	136
CHAPTER 8 CONCLUSIONS AND RECOMMENDATIONS .....		138
LIST OF REFERENCES .....		142
APPENDICES		
Appendix A	Marshall Mix Design Data .....	146
Appendix B	Mix Rutting Development .....	165
Appendix C	Repeated APT Test Section Rutting Data .....	196

## LIST OF TABLES

	Page
Table 3.1	Estimates of Time to Develop Rutting Damage . . . . . 13
Table 4.1	Experimental Design . . . . . 20
Table 5.1	Mixture Numbering System . . . . . 24
Table 5.2	Target Gradations of Mix Designs . . . . . 24
Table 5.3	Stockpile Gradations . . . . . 25
Table 5.4	Percentage of Stockpiles . . . . . 26
Table 6.1	Summary of Marshall Mix Designs . . . . . 41
Table 6.2	BSG of In-situ Pavement . . . . . 47
Table 6.3	MSG of In-situ Pavement . . . . . 48
Table 6.4	Air Voids of In-situ Pavement . . . . . 49
Table 6.5	ANOVA Results for MSG . . . . . 50
Table 6.6	ANOVA Results for Air Voids . . . . . 50
Table 6.7	Test Section Extracted Asphalt Content . . . . . 52
Table 6.8	ANOVA Results for Extracted Asphalt Content . . . . . 53
Table 6.9	Penetration of Extracted Asphalt (0.01 in.) . . . . . 56
Table 6.10	Kinematic Viscosity of Extracted Asphalt (cSt) . . . . . 57
Table 6.11	ANOVA Results for Penetration . . . . . 58
Table 6.12	ANOVA Results for Viscosity . . . . . 58
Table 6.13	APT Mixture Gradations . . . . . 61
Table 6.14	Percentage of Crushed Faces and Flat & Elongated Particles . . . . . 68
Table 6.15	ANOVA Results for Crushed Percentage . . . . . 69
Table 6.16	Gyratory Stability Index (Laboratory Specimen up to 120 Revolutions) . . . . . 71
Table 6.17	Gyratory Stability Index (Bulk Specimen up to 300 Revolutions) . . . . . 72
Table 6.18	Gyratory Shear Test Results . . . . . 75
Table 6.19	Results of Marshall Recompression . . . . . 78
Table 6.20	Measured Rut Depth at 5000 Load Repetitions . . . . . 79
Table 6.21	Acceptable Mixtures using 0.5 inch Rut Criteria . . . . . 81
Table 6.22	ANOVA Results for 40% Crushed Gravel Mixtures . . . . . 83
Table 6.23	ANOVA Results for 70% Crushed Gravel Mixtures . . . . . 86
Table 6.24	ANOVA Results for 100% Natural Sand Gravel Mixtures . . . . . 89
Table 6.25	ANOVA Results for 95% Crushed Gravel, Slag, and Limestone Mixtures . . . . . 90
Table 6.26	Summary of WTD Sample Physical Properties . . . . . 95
Table 6.27	Summary of WTD Tests . . . . . 96
Table 6.28	Repeated APT Test Section Extracted Asphalt Content . . . . . 99
Table 6.29	Repeated APT Test Section Gradations . . . . . 99
Table 6.30	Repeated APT Test Section BSG . . . . . 101
Table 6.31	Repeated APT Test Section Air Voids . . . . . 101
Table 7.1	Factor Levels for Sensitivity Analysis . . . . . 120
Table 7.2	Backcalculated Material Constants . . . . . 129
Table A.1	MD #1 Marshall Data (Gravel, 95% Crushed and 100% Natural Sand) . . . . . 147
Table A.2	MD #2 Marshall Data (Gravel, 40% Crushed and 100% Natural Sand) . . . . . 149
Table A.3	MD #3 Marshall Data (Gravel, 40% Crushed and 50% Natural Sand) . . . . . 151
Table A.4	MD #4 Marshall Data (Gravel, 40% Crushed and 0% Natural Sand) . . . . . 153
Table A.5	MD #5 Marshall Data (Gravel, 70% Crushed and 100% Natural Sand) . . . . . 155
Table A.6	MD #6 Marshall Data (Gravel, 70% Crushed and 50% Natural Sand) . . . . . 157

Table A.7	MD #7 Marshall Data (Gravel, 70% Crushed and 0% Natural Sand) . . . . .	159
Table A.8	MD #8 Marshall Data (Slag, 100% Crushed and 100% Natural Sand) . . . . .	161
Table A.9	MD #9 Marshall Data (Limestone, 100% Crushed and 100% Natural Sand) . . . . .	163
Table B.1	Rutting Data of MD#1, MD#2, and MD#3 . . . . .	166
Table B.2	Rutting Data of MD#4, MD#4, and MD#6 . . . . .	167
Table B.3	Rutting Data of MD#7, MD#8, and MD#9 . . . . .	168
Table C.1	Rutting Data for Repeated APT Test Sections of MD#4 and MD#7 . . . . .	197

## LIST OF FIGURES

	Page
Figure 3.1	Accelerated Pavement Tester ..... 16
Figure 3.2	View of the INDOT/Purdue APT ..... 17
Figure 5.1	The General Testing Procedure ..... 22
Figure 5.2	Viscosity-Temperature Chart for AC-20 ..... 27
Figure 5.3	APT Tire Print ..... 31
Figure 5.4	Rutting Modes ..... 32
Figure 5.5	Cross Sections Showing Progressive Rutting ..... 34
Figure 5.6	Test Section Sampling Plan ..... 35
Figure 5.7	Test Results for #8 Binder ..... 38
Figure 6.1	Effects of Crushed Level on Asphalt Content ..... 41
Figure 6.2	Effects of Percent Natural Sand on Asphalt Content ..... 42
Figure 6.3	Effects of Crushed Level on Marshall Stability ..... 42
Figure 6.4	Effects of Percent Natural Sand on Marshall Stability ..... 43
Figure 6.5	Effects of Crushed Level on Flow ..... 43
Figure 6.6	Effects of Percent Natural Sand on Flow ..... 44
Figure 6.7	Effects of Aggregate Type on Asphalt Content ..... 44
Figure 6.8	Effects of Aggregate Type on Stability ..... 45
Figure 6.9	Effects of Aggregate Type on Flow ..... 45
Figure 6.10	Extracted vs. Target Asphalt Content ..... 53
Figure 6.11	Relationship Between Retained Penetration and Air Voids ..... 59
Figure 6.12	Relationship Between Viscosity Ratio and Air Voids ..... 59
Figure 6.13	Gradation Curves for Mix #1 ..... 62
Figure 6.14	Gradation Curves for Mix #2 ..... 62
Figure 6.15	Gradation Curves for Mix #3 ..... 63
Figure 6.16	Gradation Curves for Mix #4 ..... 63
Figure 6.17	Gradation Curves for Mix #5 ..... 64
Figure 6.18	Gradation Curves for Mix #6 ..... 64
Figure 6.19	Gradation Curves for Mix #7 ..... 65
Figure 6.20	Gradation Curves for Mix #8 ..... 65
Figure 6.21	Gradation Curves for Mix #9 ..... 66
Figure 6.22	Crushed Percentages of Gravel Mixtures ..... 69
Figure 6.23	Relationship between Plastic Rut Depth and Gyrotory Shear Strength ..... 74
Figure 6.24	Rut Development in the APT ..... 80
Figure 6.25	Response Surface of 40% Crushed Gravel Mixtures ..... 85
Figure 6.26	Response Surface of 70% Crushed Gravel Mixtures ..... 88
Figure 6.27	Rut Depth vs. Relative Asphalt Contents (@800 Loading Cycles) ..... 92
Figure 6.28	Rut Depth vs. Relative Asphalt Contents (@2000 Loading Cycles) ..... 92
Figure 6.29	Rut Depth vs. Relative Asphalt Contents (@3500 Loading Cycles) ..... 93
Figure 6.30	Rut Depth vs. Relative Asphalt Contents (@5000 Loading Cycles) ..... 93
Figure 6.31	Rut Depth vs. Real Extracted Asphalt Contents (@5000 Loading Cycles) ..... 94
Figure 6.32	WTD Creep Slope vs. Percent Coarse Crushed Aggregate and Percent Natural Sand ..... 97
Figure 6.33	WTD Number of Passes to Stripping Inflection Point vs. Percent Coarse Crushed Aggregate and Percent Natural Sand ..... 98
Figure 6.34	Gradation Curves for Repeated Mix #4 ..... 100

Figure 6.35	Gradation Curves for Repeated Mix #7	100
Figure 6.36	Rut Depth vs. Real Extracted Asphalt Contents (@5000 Loading Cycles)	102
Figure 7.1	Cross Section of APT Test Pit	107
Figure 7.2	Fitted Curves of Material Models	111
Figure 7.3	Modeled Contact Areas	113
Figure 7.4	Deformed Cross Section from ABAQUS	113
Figure 7.5	Effects of Mesh Length on Predicted Rut Depth	117
Figure 7.6	Effects of Layer Number on Predicted Rut Depth	117
Figure 7.7	Plan View of Finite Element Mesh	118
Figure 7.8	Side View of Finite Element Mesh	119
Figure 7.9	3-D View of Finite Element Mesh	119
Figure 7.10	Effects of Creep Model Constant, A	122
Figure 7.11	Effects of Creep Model Constant, m	123
Figure 7.12	Effects of Creep Model Constant, n	124
Figure 7.13	Effects of Loading Speed	125
Figure 7.14	Effects of Thickness	126
Figure 7.15	Effects of Load	127
Figure 7.16	Fitted Curves (#2 Mixture, Lean Lane)	130
Figure 7.17	Fitted Curves (#2 Mixture, Optimum Lane)	130
Figure 7.18	Fitted Curves (#2 Mixture, Rich Lane)	131
Figure 7.19	Fitted Curves (#5 Mixture, Optimum Lane)	131
Figure 7.20	Fitted Curves (#6 Mixture, Optimum Lane)	132
Figure 7.21	Fitted Curves (#7 Mixture, Optimum Lane)	132
Figure 7.22	Fitted Curves (#1 Mixture, Optimum Lane)	133
Figure 7.23	Fitted Curves (#8 Mixture, Optimum Lane)	133
Figure 7.24	Fitted Curves (#9 Mixture, Optimum Lane)	134
Figure 7.25	Effects of Aggregate Type on m	134
Figure 7.26	Effects of Relative Asphalt Content on m	135
Figure 7.27	Effects of Percent Passing #4 Sieve on m	135
Figure A.1	MD #1 Marshall Plots (Gravel, 95% Crushed and 100% Natural Sand)	148
Figure A.2	MD #2 Marshall Plots (Gravel, 40% Crushed and 100% Natural Sand)	150
Figure A.3	MD #3 Marshall Plots (Gravel, 40% Crushed and 50% Natural Sand)	152
Figure A.4	MD #4 Marshall Plots (Gravel, 40% Crushed and 0% Natural Sand)	154
Figure A.5	MD #5 Marshall Plots (Gravel, 70% Crushed and 100% Natural Sand)	156
Figure A.6	MD #6 Marshall Plots (Gravel, 70% Crushed and 50% Natural Sand)	158
Figure A.7	MD #7 Marshall Plots (Gravel, 70% Crushed and 0% Natural Sand)	160
Figure A.8	MD #8 Marshall Plots (Slag, 100% Crushed and 100% Natural Sand)	162
Figure A.9	MD #9 Marshall Plots (Limestone, 100% Crushed and 100% Natural Sand)	164
Figure B.1	Rutting of MD#1, Lean Lane	169
Figure B.2	Rutting of MD#1, Opti. Lane	170
Figure B.3	Rutting of MD#1, Rich Lane	171
Figure B.4	Rutting of MD#2, Lean Lane	172
Figure B.5	Rutting of MD#2, Opti. Lane	173
Figure B.6	Rutting of MD#2, Rich Lane	174
Figure B.7	Rutting of MD#3, Lean Lane	175
Figure B.8	Rutting of MD#3, Opti. Lane	176
Figure B.9	Rutting of MD#3, Rich Lane	177
Figure B.10	Rutting of MD#4, Lean Lane	178
Figure B.11	Rutting of MD#4, Opti. Lane	179
Figure B.12	Rutting of MD#4, Rich Lane	180
Figure B.13	Rutting of MD#5, Lean Lane	181
Figure B.14	Rutting of MD#5, Opti. Lane	182
Figure B.15	Rutting of MD#5, Rich Lane	183



Figure B.16	Rutting of MD#6, Lean Lane .....	184
Figure B.17	Rutting of MD#6, Opti. Lane .....	185
Figure B.18	Rutting of MD#6, Rich Lane .....	186
Figure B.19	Rutting of MD#7, Lean Lane .....	187
Figure B.20	Rutting of MD#7, Opti. Lane .....	188
Figure B.21	Rutting of MD#7, Rich Lane .....	189
Figure B.22	Rutting of MD#8, Lean Lane .....	190
Figure B.23	Rutting of MD#8, Opti. Lane .....	191
Figure B.24	Rutting of MD#8, Rich Lane .....	192
Figure B.25	Rutting of MD#9, Lean Lane .....	193
Figure B.26	Rutting of MD#9, Opti. Lane .....	194
Figure B.27	Rutting of MD#9, Rich Lane .....	195
Figure C.1	Rutting of Repeated MD#4, Lean Lane .....	198
Figure C.2	Rutting of Repeated MD#4, Opti. Lane .....	199
Figure C.3	Rutting of Repeated MD#4, Rich Lane .....	200
Figure C.4	Rutting of Repeated MD#7, Lean Lane .....	201
Figure C.5	Rutting of Repeated MD#7, Opti. Lane .....	202
Figure C.6	Rutting of Repeated MD#7, Rich Lane .....	203



## Implementation Report

An accelerated pavement testing facility was developed by Purdue University for the Indiana Department of Transportation. The test facility includes a test pit in which prototype scale pavement sections can be installed. The Accelerated Pavement Tester (APT) loading system has the capability of applying moving wheel loads to the test sections. An initial study utilizing the accelerated pavement test facility was conducted to determine the minimum crushed aggregate requirements in asphalt mixtures in Indiana. This study addresses effects of various constituents of the asphalt mixture on pavement rutting. The factors included in this study were aggregate type, percentage of crushed gravel, percentage of natural vs. crushed sand and asphalt content. Combinations of these factors and their levels resulted in 27 sections being tested.

The INDOT/Purdue APT has been demonstrated to produce accelerated rutting damage. As initially projected, time to develop significant rutting is one to two weeks of testing. Tests conducted include a range of aggregate type (coarse and fine), aggregate size and asphalt contents.

Mix designs for each mixture were conducted using the then current INDOT Marshall procedures and criteria. Each mixture was proportioned to satisfy target percent coarse crushed aggregate, percent natural sand, INDOT #8 binder gradation and optimum and plus and minus 0.5 percent asphalt content. Producing the target mix designs from an asphalt plant proved to be difficult. Also, significant delays in the study resulted from waiting on the contractor to produce the mixtures. It is recommended that future APT work involve a master contract between a contractor and INDOT to produce test mixture within an acceptable time period. Alternatively, a patching plant could be obtained and set up in an INDOT maintenance facility. This latter approach would address test

mixture variability as well as production timeliness. The capability of the APT to evaluate mixture rutting potential suggests that significant experience would result from routinely diverting mixtures from actual paving projects to the APT facility for test section installation. In this case, the diverted mixture would represent in-service mixtures. Such a plan would insure the APT facility would have maximum use.

Laboratory Wheel Tracking Tests (WTD) were conducted on APT mixtures. The results confirmed the concept of using the WTD as a screening tool for studies with the APT. This would allow the tests with the APT to be optimized.

A finite element program, ABAQUS, was used to model the pavement structure and predict permanent deformation. An approximation was used to simulate the APT loading conditions. A creep model was used to characterize the actual pavement material behavior. Based on the rut-depth development data from the APT, material parameters in the creep model were backcalculated. Regression analyses were conducted to correlate these material parameters with mixture physical properties. With the validated/calibrated FEM effects of contact pressure, speed and layer thickness were projected. The FEM should be used to analyze both APT and WTD tests. Future APT tests should include a range of contact pressure and temperature. The speed effect is already modeled. Including temperature would allow the temperature effect to be modeled as well.

Rut depth is more sensitive to asphalt content in the 40% crushed gravel mixtures than in the 70% crushed gravel mixtures. It is noted that 0.5% increase in asphalt content will result in about 0.25 inch increase in total rut depth of 40% crushed gravel mixtures and about 0.09 inch increase in total rut depth of 70% crushed gravel mixtures. The slag and limestone mixtures are also much less sensitive to asphalt content variation.

Percent natural sand is not significant in 40% crushed gravel mixtures but is significant in 70% crushed gravel mixtures. It is noted that 50% increase in natural sand will result in about 0.13 inch increase in total rut depth of 70% crushed gravel mixtures. Also, as noted in the WTD test results, rutting potential increases significantly with more than 50 percent natural sand (uncrushed). When gravel mixtures are utilized minimums of 70 percent coarse crushed particles and 50 percent crushed sand size particles are warranted. In the study, rutting of slag and limestone mixtures is much less than all gravel mixtures. WTD test results from other studies indicate that rutting/stripping potential of such mixtures is further enhanced by use of crushed sand size aggregate.

From the report recommendations for the following items are suggested for implementation:

1. The Accelerated Pavement Tester (APT) proved to be very effective in evaluating rutting potential of asphalt mixtures. Several years of inservice rutting performance can be compressed into a few days of testing. As a result, the APT can and should be utilized to evaluate rutting performance of Superpave mixtures being utilized in Indiana.
2. There is no reason for the APT to be idle. As long as mixtures are being produced for existing construction projects there is opportunity to divert one or two truck loads for APT testing. This includes both Superpave and non-Superpave projects.
3. The finite element model is capable of capturing the permanent deformation response of asphalt layers and can be used to predict permanent deformation.
4. Additional tests should be conducted over a range of temperatures and tire pressures. These tests would define the effect of temperature and tire pressure on rutting performance of asphalt mixtures as well as define the temperatures and stress functions in the theoretical rutting model.

5. The type of coarse crushed aggregate has a significant effect on rutting. Rutting of limestone and slag mixtures is much less than gravel mixtures with 95 percent one crushed face, all with 100 percent natural sand. The past requirements on limiting gravel on high volume roads is valid from a rutting perspective.
6. High percentages of natural sand increased rutting potential of gravel mixtures. Even for non-Superpave mixtures the sand fraction should be 50 percent or less natural sand.
7. Future tests should be planned that complete the matrix with tests of limestone, slag and 95 percent coarse crushed gravel. This would include these coarse aggregate and zero and 50 percent natural sand, respectively.
8. Tests were conducted at asphalt contents of optimum and  $\pm 0.5$  percent of optimum. Asphalt content proved to be very significant with respect to rutting. Similar tests should be conducted to validate Superpave optimum asphalt content criteria.
9. The PURWheel laboratory wheel track tester in large part mirrored the APT results. The PURWheel should be utilized to screen materials to be tested in the APT. Subsequent use of the APT will be more efficient and cost effective.

## CHAPTER 1

### INTRODUCTION

Rutting or permanent deformation is one of the most significant problems associated with asphalt pavement performance. Rutting is characterized by depressions in the wheel path and has become a prevalent form of pavement distress. Rutting is also a safety concern because water collects in the depression causing high speed vehicles to hydroplane or freezes in cold weather.

Loading factors associated with rutting are the axle load, tire pressure and volume of truck traffic. Environmental factors such as moisture and temperature also have significant influence on rutting. The rutting resistance of conventional asphalt mixtures depends on a number of factors related to constituents of the asphalt mixtures, such as aggregate type and gradation, sand angularity and asphalt content. One important factor related to the aggregate constituent is the nature and amount of crushed aggregate. In general, a mixture with a higher percentage of crushed aggregate shows a higher resistance to rutting. However, it is important to consider economy and the use of local materials, such as sand and gravel. Economy may result from lower cost of sand and gravel or short hauling distance. The desire for economy and use of local materials is offset by the need to insure that asphalt mixtures used in surfacing and resurfacing highway pavements will provide the level of performance required. Because resistance to rutting can be increased by the addition of crushed aggregate, a need exists to be able to

determine the required amount of crushed aggregate and the characteristics of that crushed material to optimize performance and economy.

Tests on small, laboratory size specimens do not scale reliably to prototype pavements. Prototype pavement test sections can solve the problem of scale; however, differences in performance may take many years to develop. An alternative testing procedure is to test a small section of pavement with prototype loads. Time can be scaled to reduce the time for performance differences to develop. Structural damage can be scaled by increasing the load so that greater pavement damage is incurred by each pass of the load. Rutting distress can be scaled by increasing asphalt mixture temperature and thereby decreasing the mixture stiffness. Reduced stiffness increases rutting distress with each load pass. Slower speed increases the time of loading and therefore increases rutting distress.

An accelerated pavement testing facility has been developed by Purdue University for the Indiana Department of Transportation (INDOT). The facility is located at the INDOT Division of Research in West Lafayette, Indiana. Prototype scale pavement sections can be installed in a test pit in the facility. The Accelerated Pavement Tester (APT) loading system has the capability of applying moving wheel loads to the pavement test sections.

An initial study utilizing the accelerated pavement test facility has been conducted at Purdue University to determine the minimum crushed aggregate requirements in asphalt mixtures in Indiana. This study addresses effects of various constituents of the asphalt mixture on pavement rutting. The factors included in the study were aggregate type, percentage of crushed gravel, percentage of natural vs. crushed sand and asphalt content. Combinations of these factors and their levels resulted in 27 sections being tested in this study. Rutting was documented for each test section during APT operation. Marshall mixture design and laboratory tests provide comprehensive information on mixture



properties. As a result of both the laboratory and APT results, recommendations are provided for using gravel in asphalt mixture.

A finite element program ABAQUS [ABAQUS, 1994] was used in this study to model the pavement structure and permanent deformation. An approximate approach was used to simulate the APT loading conditions. A creep model was used to represent the actual pavement rutting. Based on the mixture performance in APT, material constants in the creep model were backcalculated. Regression analyses were conducted to correlate these material constants with mixture physical properties.

The objectives of this study included designing, fabricating and implementing a prototype scale accelerated pavement tester (APT). Inherent in the design would be the capability to accelerate the rate of asphalt pavement rutting and structural deterioration of asphalt and concrete pavements. Other pavement features subject to vehicular loads could also be installed and tested, i.e. load transfer devices, culverts and bridge components. Implementation of the APT would result from a study to determine the minimum coarse crushed aggregate requirements for asphalt mixtures in Indiana. The primary aggregate in the study was gravel.



## CHAPTER 2

### LITERATURE REVIEW

Asphalt pavement rutting is a longitudinal surface depression in the wheel path as a result of traffic loads. Rut depth is defined as the vertical distance between the valley and the crest of a rut and is measured by laying a straightedge transverse to the rut and measuring the distance to the lowest point. Rut severity is determined by the mean rut depth, which is calculated by averaging the rut measurements taken along the length of the rut. Mean rut depths less than 0.5 inch are considered as low severity [PAVER], mean rut depths between 0.5 inch and 1 inch are considered as medium severity and mean rut depth greater than 1 inch as high severity.

Significant rutting can cause safety problems. For example, when the rut depth is severe enough, water begins to pond in the wheel path. Possible hydroplaning of fast moving vehicles jeopardizes the safety of the motoring public. In cold climates this water may freeze. Therefore, the cross-slope of the pavement section is the controlling factor in determining the critical rut depth which causes water accumulation in the wheel paths.

#### 2.1 Causes of Asphalt Pavement Rutting

Rutting stems from a permanent deformation in any of the pavement layers or subgrade, usually caused by densification or shear failure of the materials due to traffic loading. Three basic types of rutting can develop in bituminous mix [Dawley et al, 1990].

Wear rutting is caused by the progressive loss of coated aggregate particles from the asphalt pavement surface. It is caused by a combination of environmental and traffic influences.

Structural rutting is caused by permanent vertical deformation of the pavement structure under repeated traffic loads. Permanent vertical deformation can be caused by continued densification due to insufficient initial compaction and/or by plastic deformation in one or more of the pavement layers or the subgrade.

Instability rutting is caused by lateral movement of material within the asphalt concrete layer. Instability rutting is characterized primarily by plastic flow in an unstable mixture.

Recent work by Eisenmann and Hilmer [1987] shows that densification occurs in the initial stage of trafficking. After the initial stage, compaction under traffic is completed for the most part and further rutting is caused essentially by plastic flow of asphalt mixture. Total rutting was mainly caused by this plastic deformation without volume change. Dawley, Hogewiede, and Anderson [1990] also stated that the majority of HMA rutting is due primarily to instability rutting.

There is a strong relationship between in-place air voids and rutting in a bituminous mixture. Brown [1990] indicated that initial air voids of HMA pavements are approximately 7-8% but densify further under traffic loads. Also, mix stability increases during the densification process, which in turn resists further densification. A rut-resistant mix will reach equilibrium at approximately 4% air voids. The air voids of a rut prone mixture typically do not stabilize but continue to decrease. Sousa [1994] concluded that when air void contents drop below 2-3% the binder acts as a lubricant between the aggregates and reduces point to point contact pressure, resulting in flow.

Ford [1988] studied the relationship between in-place air voids and instability rutting. Cores were taken from 24 test sites to represent the various types of HMA

pavement in the State of Arkansas. The service life of selected pavements ranged from 3 to 22 years and the number of total accumulated 18-kip Equivalent Single Axle Loads (ESAL) ranged from 110,000 to 3,064,000. Air voids of the surface layers were determined from in-place pavements inside wheel path and compared with measured rut depths. Statistical analysis was conducted to establish relationships between asphalt pavement rutting and physical properties of the pavement cores. It was concluded that the air voids in the pavement were indicative of the measured rut depth. Mixture air voids of 2.5 to 5 percent were indicative of asphalt mixtures with an acceptable level of rutting. Severe ruts were associated with mixtures having air voids of less than 1.0 percent.

## 2.2 Effects of Mixture Constituents on Rutting

Asphalt cement and aggregate are the two major components in a hot mix asphalt (HMA) mixture. The rut resistance of a HMA mixture is greatly affected by properties and proportions of these two constituents. With proper control of these constituents in mix design and construction, the HMA rutting problem can be minimized. Factors related to these two constituents and rutting performance are viscosity and volume of asphalt, aggregate angularity, gradation and proportion of mineral filler.

### 2.2.1 Asphalt Cement

Asphalt cement viscosity and asphalt content affect the rutting resistance of a mix. Decker and Goodrich [1989] studied the effect of asphalt cement physical properties on rutting. They found that a high viscosity asphalt cement resulted in a stiffer mix at a given temperature and loading rate. This stiffer mix exhibits better rutting resistance. At high ambient temperature, mix stiffness is dominated by aggregate properties and asphalt content. Asphalt viscosity becomes less important and asphalt elastic modulus becomes

more important. Asphalt cement with high elastic modulus increases the mix resistance to permanent deformation. Decker and Goodrich concluded that the balance between an asphalt's viscous modulus and its elastic modulus is an important physical property influencing the contribution of the asphalt cement to rutting.

Excessive asphalt content is the most common cause for lateral plastic flow of HMA. The excess asphalt cement causes the loss of internal friction between aggregate particles and results in the load being carried by the asphalt cement rather than the aggregate skeleton. There are several causes that contribute to the selection of a design asphalt content that is too high [Roberts et al, 1991]. One such cause is low compaction effort during Marshall mix design and quality control testing. A low compactive effort in the laboratory results in a density lower than the ultimate in-service density. As a result, the asphalt content selected to satisfy other mix design criteria will likely be too high.

### 2.2.2 Aggregate Angularity

Aggregate with rough surface texture results in higher internal friction and stronger bond with the asphalt cement, which provides better stability and rut resistance. Therefore, mixtures with manufactured sand and crushed coarse aggregate have high stability and resistance to rutting. Since percent fracture of aggregate significantly affects the properties of asphalt concrete mixtures, a number of studies have been conducted to examine the effects and desired threshold levels of fracture.

Kalcheff and Tunncliffe [1982] evaluated effects of crushed aggregate size and shape on mixture permanent deformation. They found that asphalt mixes containing greater amounts of crushed coarse aggregate were more resistant to permanent deformation. Also, mixtures containing manufactured sand were more resistant to permanent deformation than mixtures containing natural sand

Brown, McRae, and Crawley [1989] conducted a study of the effects of aggregates on the performance of bituminous concrete. They reported that HMA mixes containing crushed aggregates had better resistance to rutting than those containing little or no crushed aggregates.

Lundy, Hicks, and McHattie [1989] investigated the effects of aggregate percent fracture faces on the laboratory performance of asphalt mixtures. The percent crushed faces examined were 50, 70, 90 percent. Aggregate from Anchorage, Fairbanks, and Juneau were included in the study. The results from repeated load diametral tests showed that the effect of percent fractured faces on permanent deformation are not consistent across the aggregate types tested. The mixture with Juneau aggregate shows little reduction in permanent deformation with increasing fracture level. Mixtures using the anchorage aggregate show the greatest reduction in permanent deformation with increasing percent fractured faces. It is suspected that the contradictory results may be attributed to the lower asphalt contents associated with all Anchorage mixtures.

### 2.2.3 Aggregate Gradation

Aggregate gradation is the distribution of particle sizes expressed as a percent of the total weight. In general, aggregate gradations are described as dense-graded, uniformly-graded (open), and gap-graded. Gradation controls many of the important properties of an asphalt mixture including rutting resistance.

Monismith, Epps and Finn [1985] recommended that dense aggregate gradation be used to mitigate the effects of rutting. They showed that mixtures with dense gradation close to the FHWA 0.45 power curve tend to have higher stiffness and thus higher resistance to rutting.

Evans and Ott [1986] studied gravel, slag, and limestone. They reported that aggregate gradation had a significant effect on rutting performance of uncrushed gravel

but a minor effect on slag rutting performance and no significant effect on crushed limestone rutting performance.

The maximum aggregate particle size in a mixture is also related to performance. A mixture with large maximum size may cause workability and segregation problems. However, a small maximum size may result in an unstable mixture. Brown and Bassett [1990] conducted a laboratory analysis of the effect of varying the maximum aggregate size on rutting potential and on other properties of asphalt/aggregate mixtures. A 100 percent crushed limestone was used in this study and maximum aggregate sizes of 3/8, 1/2, 3/4, 1 and 1½ inch were evaluated. The general trend of the data in this study showed that mixes with larger aggregate size with an air voids content of 4 percent were generally stronger than mixes prepared with small aggregate. Static creep tests of 6 in. cores showed that increase of maximum aggregate size in a mix increased the mix's resistance to rutting.

Asphalt mixtures that are not stable when compacted or are prone to rutting are classified as "tender". Tender mixtures are associated with a hump in the gradation curve near the No. 40 sieve as plotted on the FHWA 0.45 power curve. In a study conducted by Carpenter and Enockson [1987], 92 different uniform sections in 32 overlay projects placed over Portland cement concrete pavements were visually surveyed to obtain performance data. The data were analyzed to develop regression relations between rutting and mixture properties of the asphalt concrete overlays. The analysis clearly showed that gradation parameters were related to measured rutting. The most influential variable appeared to be the hump in gradation on the No. 40 Sieve. The percentage passing the No. 40 sieve and retained on the No. 80 sieve in the surface mixture also influenced degree of rutting.



#### 2.2.4 Mineral Filler

Mineral filler is the material passing the No. 200 sieve. Mineral filler characteristics vary with the size of the filler particles. If the size of the filler particle is less than the asphalt film thickness (about 10 microns), the filler acts as part of the binder in the mixture. If the mineral filler size is larger than 10 micron, it acts more like an aggregate particle.

The amount of mineral filler in a mixture greatly affects the mixture performance. An increase in filler results in a corresponding decrease in optimum asphalt content. The results of laboratory tests conducted by Brown, McRae, and Crawley [1989] indicated that a mixture designed with higher filler content will result in a significantly higher stability than that with low filler content. They reported that there is evidence that the optimum filler content is between 3 to 6 percent for well-graded bituminous concrete.

Lundy, Hicks, and McHattie [1989] studied the effects of mineral filler content on the laboratory performance of asphalt mixtures. Three levels of mineral filler content were included in their study, namely 3%, 6%, 10%. They reported that permanent deformation decreases with increasing fines at 10,000 repetitions of indirect tensile repeated load tests.



### CHAPTER 3

#### ACCELERATED PAVEMENT TESTING FACILITY

A "Traffic Simulator" or Accelerated Pavement Tester (APT) system has been designed and fabricated with which simulated truck traffic can be applied to a small section of pavement. Material used in the test section as well as environment and loading conditions can be controlled. A number of pavement materials, structure and loading factors can be evaluated in the facility.

The accelerated pavement testing facility is located at the INDOT Research Division in West Lafayette, Indiana. A pit within the test facility allows prototype scale pavement sections to be installed. The APT spans the pit and incorporates the capability to apply moving wheel loads.

A review of literature and evaluation was made of loading mechanisms, power systems and test facility configuration options. A mass loading system was considered to have liabilities of size and requirements for controlling momentum. Hydraulic loading systems can leak and cause test section contamination. The mechanical loading concept selected was projected to be reasonably compact, low cost, and simple to operate and maintain. Linear loading was considered desirable and loading in one or two directions was easy to implement as a result of the overall sequence of operation of the proposed system. The test pit in which pavement test sections are built is 20 ft x 20 ft x 6 ft deep.

### 3.1 System Design Requirements

The design of the accelerated pavement testing system was based on estimates of the capacities and operating conditions that would effect the desired accelerated rutting and structural damage.

#### 3.1.1 Accelerated Damage Due to Load

Pavement structural damage can be accelerated by increasing loads. For example, the effects of increasing an 18,000 pound axle load (9000 per half-axle) were estimated using the AASHTO load equivalency factors, LEF, [Yoder & Witczak, 1975]. With increased load the damage per pass is increased. As a result, the time to achieve a given amount of damage can be reduced.

Use of serviceability based LEF to predict structural damage has some limitation. However, the estimates are considered reasonable for preliminary planning. If the estimates are too conservative, structural damage can be further accelerated by installing and testing underdesigned pavement sections.

#### 3.1.2 Estimate of Rutting Damage

In addition, traffic speed and pavement temperature are two major factors expected to contribute to compression of time to develop rutting damage. A reduction of speed will increase the loading time and the viscous component of deformation. An increase in temperature has the same effect. The magnitude of the speed and temperature effect was estimated using the Shell method [Claessen, et al, 1977].

In current tests with the APT a 3 inch bituminous layer is placed on a base concrete slab. Hot water flowing through conduits in the concrete slab provides heating of the

bituminous surfacing. The heating system is capable of holding the asphalt layer at the target temperature of  $38 \pm 1.1^\circ\text{C}$ .

Using the temperature regime and characteristics of materials in Indiana [Coree and White, 1989] estimates of time of rutting were made as shown in Table 3.1. These estimates are considered to be approximate but do indicate that rutting damage can be developed with the APT in a reasonable period of time. Load and tire pressure are two other factors that could be varied and factored into the APT tests to further accentuate rutting damage.

Table 3.1 Estimates of Time to Develop Rutting Damage.

Temperature °C	$\eta$ poise	Cycles of Loading	Hours of Operation @ 5 mph	Number 8 Hr. Days
38	10,500	36,353	101	12.6
60	4,000	13,849	38	4.8
82.2	850	2,943	8	1.0

### 3.1.3 Structural and Mechanical Design of Accelerated Testing System

The APT is designed to apply up to a 20,000 pound load on a dual wheel or super single assembly as it moves across a section of test pavement at 5 mph. The design is unique in that it uses a mechanical linkage and springs to develop and maintain a constant force. Energy requirements for starting and stopping such a system are much less than a system using a 20,000 pound mass for load generation as noted above.

Reaction forces generated by the constant force loading system are transmitted to the foundation using the structure shown in Figure 3.1. Figure 3.1 is a conceptual

drawing of the APT system. A pair of beams run horizontally across the test pit with support structures at each end. The support structures are on rollers so the system can be moved laterally to different lanes of the test pavement. Clamps are used at each end of the structure so that the reaction force of the wheel assembly does not lift the rollers off their tracks. Figure 3.2 shows a view of the APT system.

Traffic wander can be accounted for by lifting and transversely positioning the APT wheel assembly before each pass across the pavement. Lift is provided by pneumatic cylinders acting on the constant force mechanism. Transverse positioning between cycles is provided by an electric motor driving a pair of ball screws.

Longitudinal motion of the wheel assembly along the test lane is provided by a cable drive system which is powered by a 30 hp, 480 volt, 3 phase electric motor. The motor is located on one of the structure end supports along with the gear box which connects the motor to the cable drum.

The entire operation of the APT, as well as all data acquisition, is controlled by a micro-computer. A data acquisition board is used to interface with the motor controllers and all required sensors. Variable frequency controllers with reversing and soft start options are used for both the main and lateral drive systems. Position of the system is monitored with encoders. Limit switches are used to shut down the system if the wheel assembly should exceed its normal operating zone.

The APT became operational in the summer of 1992. Several design modifications have been implemented resulting in increasing reliability of the system.

Initial application of the APT was for the study of crushed aggregate requirements to provide an acceptable resistance to permanent deformation (rutting) of gravel asphalt mixtures used in Indiana. Indiana has an abundance of glacio-fluvial gravel which are universally rounded in shape. Currently, state specifications require a relatively high degree of particle crushing to minimize permanent deformation. This research project was

developed to incorporate mineral aggregate type, degree of coarse particle crushing, percent natural vs. manufactured sand. The aggregate factors in combination with asphalt content were considered significant in determining the rutting potential of asphalt mixtures.

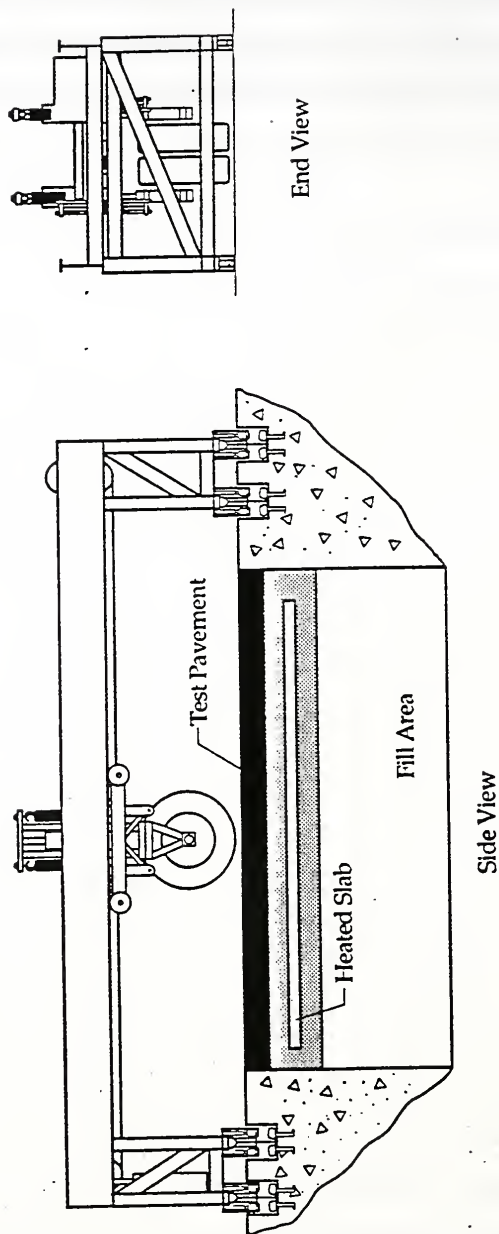


Figure 3.1 Accelerated Pavement Tester



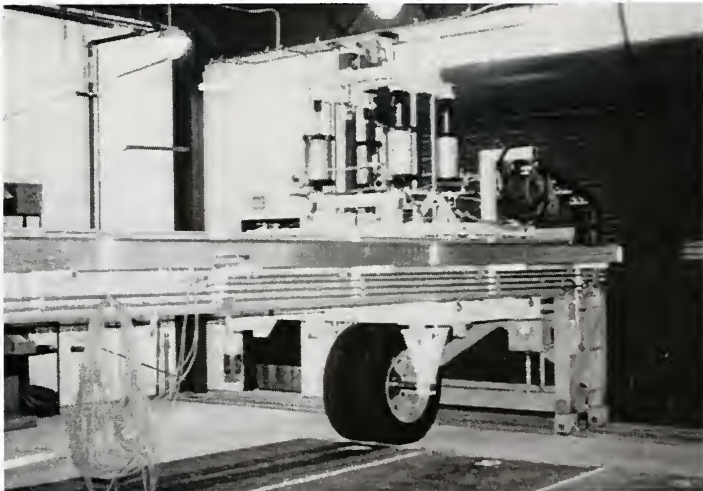
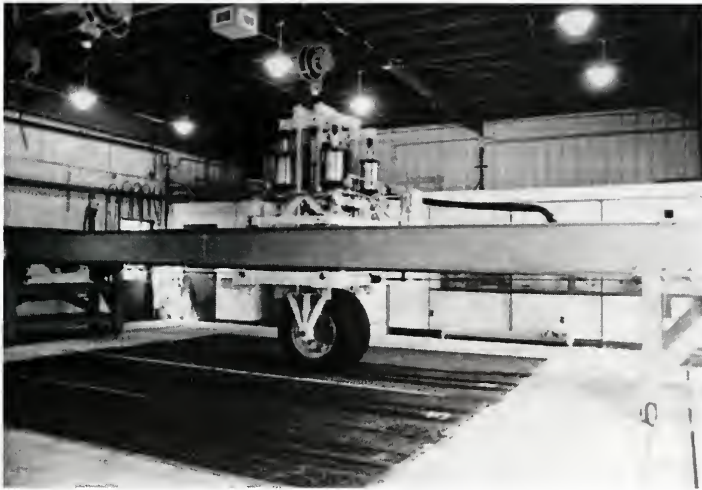


Figure 3.2 View of the INDOT/Purdue APT



## CHAPTER 4

### EXPERIMENTAL DESIGN

From meetings and discussions within INDOT and with the mineral aggregate industry the following factors were identified as significant to determining the effect of crushed aggregate on rutting potential of bituminous mixtures.

- (1) Maximum Aggregate Size
- (2) Bitumen Content
- (3) Aggregate Type
- (4) Coarse Crushed Aggregate
- (5) Crushed and Uncrushed Sand

To control the size of the experimental design a decision was made to use one maximum aggregate size (1 inch). Asphalt content also affects rutting potential. Rather than incorporating mix design criteria into the experimental design the question is addressed by conducting a standard Indiana mix design for each aggregate combination and then testing sections 0.5 percent above and below this optimum asphalt content. As a result, the effectiveness of the current mix design criteria would be evaluated. More detailed studies of mix design criteria are possible in the future. As planned, three test sections are installed at the same time for consecutive testing with the APT. Since the bituminous mixture is plant produced, the logical process is to calibrate the plant for one aggregate combination and gradation and then vary the bitumen content (-0.5 percent, optimum, +0.5 percent). Asphalt source was not included as a factor in the study.

In this study gravel was the primary aggregate of interest. Other predominate aggregates used in Indiana, limestone and slag, are known to provide acceptable rutting

resistance under current specifications. Therefore, the experimental design was developed to focus on gravel mixtures but include a series of limestone and slag mixtures for comparison purposes.

In Indiana, degree of crushing is specified based on percentage of one crushed face. To examine the effect of percent coarse crushed particles, three levels of crushed particles were adopted for the study; 40, 70 and 95 percent, respectively. These three levels were selected after considering available aggregates and at the same time maintaining as broad of a range of percent crushed faces as possible.

Typically, asphalt mixture rutting resistance is increased by incorporating more crushed sand and less natural sand. As a result, percentage of natural sand was considered as a factor in the study. Three levels; 0, 50 and 100 percent of the sand fraction, respectively, were utilized. Only one source of either natural sand or crushed sand was considered. The limestone and slag mixtures were included with 100 percent uncrushed fine aggregate.

Indiana has significant lane miles of concrete pavement that have exceeded original design life. One frequently specified rehabilitation option for concrete pavements is an asphalt overlay. Early rutting of such overlays has been a particular problem. Consequently, tests in the APT were conducted with an asphalt overlay applied on the base concrete slab in the APT test pit. Thickness of the overlay was a potential variable but a decision was made to use a single overlay thickness of three inches. This was a reasonable thickness for a binder course. Mixture gradation also affects mixture rutting potential. Variation of this factor was eliminated by using a single gradation, Indiana No. 8 binder.

The experimental design developed for the study, considering the above discussion is given in Table 4.1. There is a total of twenty-seven test items represented in the experimental design. The experimental design is very efficient. Combinations of the





## CHAPTER 5

### TESTING PROCEDURES

Marshall mix designs were conducted for gravel mixtures with each combination of crushed level and percentage of natural sand. Mix designs were also conducted for the limestone and slag coarse aggregate and natural sand. Subsequently, mixtures were prepared by local contractors and delivered to the APT site for installation. Bulk sample was obtained during installation for laboratory evaluation. After traffic tests, cores were taken from each test lane for subsequent testing. The general testing sequence followed in this study is shown in the Figure 5.1 and is discussed briefly below.

#### 5.1 Mix Designs

Asphalt mixture designs were conducted using the manual Marshall hammer with a 75 blow compactive effort. Subsequently, optimum asphalt content was selected using Indiana mix design criteria. For binder course mixtures this involves selecting an asphalt content at six percent air voids and confirming that the Marshall Stability is greater than 1200 lbs. and the minimum voids in the Mineral Aggregate (VMA) are satisfied.

##### 5.1.1 Aggregates

The first step in the mix design process involved selecting aggregate sources that would satisfy the crushed aggregate requirements, percents of natural and crushed sand and the No. 8 binder gradation. Significant help was provided in this process by the Indiana aggregate industry as well as the Indiana DOT Division of Materials and Tests.

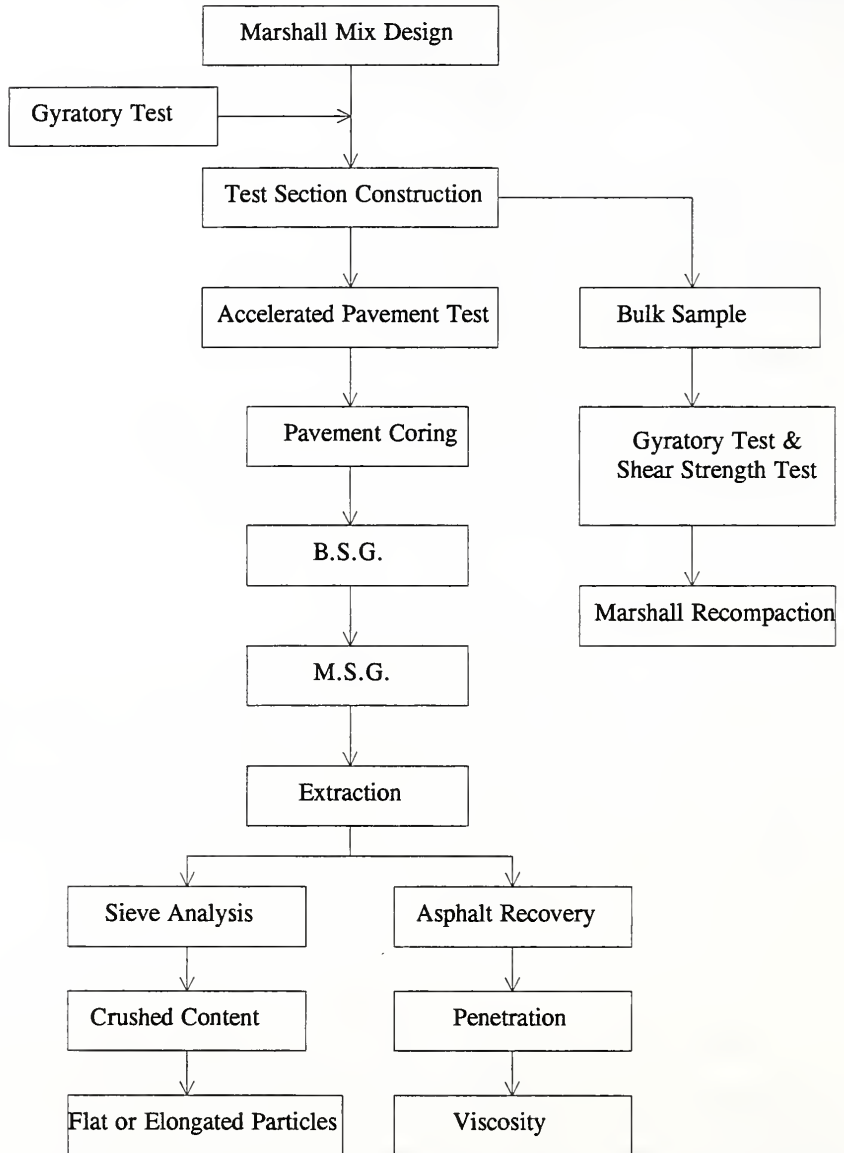


Figure 5.1 The General Testing Procedure



Subsequently, samples of the various stockpiles were obtained and sieved to obtain material for each sieve size. These materials were combined for individual aggregate batches matching the desired gradation. Enough aggregate batches were prepared for at least three samples at five asphalt contents. For reference in subsequent discussions, the mixture numbering system in Table 5.1 was utilized.

Using this mix design designation, the target gradations for each mix design are given in Table 5.2. Gradations for each stockpile material used are given in Table 5.3. Percent crushed particles are also given for each stockpile. The percentage of each stockpile used for each mix gradation is shown in Table 5.4.

#### 5.1.2 Asphalt Cement

AC-20 asphalt used in this study was from Ashland Petroleum, Indianapolis. The asphalt viscosity and specific gravity are listed below:

Viscosity	@ 60°C:	2275.2 Poise
	@ 135°C:	397.4 cSt (4.09 Poise)
Penetration	@ 25°C:	62
Specific Gravity:		1.03

Figure 5.2 shows the viscosity temperature relationship for this asphalt. The temperature to which the asphalt must be heated to produce kinematic viscosity of  $170 \pm 20$  centistokes and  $280 \pm 30$  centistokes was chosen as the mixing temperature and compaction temperature, respectively. The resulting mixing temperature is  $145 \pm 1.1^\circ\text{C}$  and the compaction temperature is  $139 \pm 1.1^\circ\text{C}$ .



Table 5.1 Mixture Numbering System

Mix Design Number	Coarse Aggregate Type	Percent Coarse Crushed (%)	Percent Natural Sand* (%)
1	Gravel	95	100
2	Gravel	40	100
3	Gravel	40	50
4	Gravel	40	0
5	Gravel	70	100
6	Gravel	70	50
7	Gravel	70	0
8	Slag	100	100
9	Limestone	100	100

\* Complementary sand is crushed

Table 5.2 Target Gradations of Mix Designs

Sieve Size	Mix Design #								
	1	2	3	4	5	6	7	8	9
1"	100.0%	100.0%	100.0%	100.0%	100.0%	100.0%	100.0%	100.0%	100.0%
3/4"	93.3%	95.1%	94.6%	94.6%	95.0%	95.1%	95.1%	94.2%	94.0%
1/2"	71.0%	78.9%	77.0%	77.0%	76.9%	77.4%	77.4%	75.7%	74.0%
3/8"	53.1%	68.1%	65.2%	65.2%	62.3%	63.0%	63.0%	59.1%	61.0%
#4	31.7%	38.1%	38.7%	38.7%	33.2%	34.2%	34.2%	32.7%	34.8%
#8	22.3%	21.3%	23.6%	22.6%	23.5%	23.3%	22.4%	25.3%	22.7%
#16	16.8%	15.9%	15.8%	13.1%	17.9%	15.7%	13.0%	18.3%	16.6%
#30	12.0%	10.3%	10.5%	9.1%	11.9%	10.8%	9.4%	11.5%	10.2%
#50	6.7%	4.9%	6.0%	6.6%	5.7%	6.4%	6.9%	4.5%	4.4%
#100	3.5%	2.5%	3.7%	4.8%	2.8%	3.9%	5.0%	2.8%	2.6%
#200	2.7%	1.8%	2.7%	3.5%	1.9%	2.7%	3.6%	1.7%	1.9%



Table 5.3 Stockpile Gradations

Size	Gravel				Slag		Lime Stone			Sand		
	IND #8	IND #8	IND #11	IND #12	IND #8	IND #11	IND #8	IND #11	IND #24	IND #24	IND #24	FA-20
Source	VMC <sup>1</sup>	INT ST. <sup>2</sup>	INT ST.	VMC	LEVY <sup>3</sup>	LEVY	DELPHI <sup>4</sup>	DELPHI	FAIRFIELD <sup>5</sup>	FAIRFIELD	BARKER PIT	INT ST.
% Crushed	48%	97%	100%	22%	100%	100%	100%	100%				
Sieve Size	% Passing by Weight											
1"	100.0%	100.0%	100.0%	100.0%	100.0%	100.0%	100.0%	100.0%	100.0%	100.0%	100.0%	100.0%
3/4"	89.0%	90.0%	100.0%	100.0%	87.0%	100.0%	88.0%	100.0%	100.0%	100.0%	100.0%	100.0%
1/2"	53.0%	57.0%	100.0%	100.0%	46.0%	100.0%	48.0%	100.0%	100.0%	100.0%	100.0%	100.0%
3/8"	29.0%	32.0%	90.0%	100.0%	23.0%	79.0%	29.0%	86.0%	100.0%	100.0%	100.0%	100.0%
#4	2.0%	10.0%	24.0%	47.0%	7.0%	16.0%	6.0%	28.0%	100.0%	99.0%	100.0%	100.0%
#8	1.5%	2.0%	4.0%	5.0%	5.0%	6.0%	1.0%	3.0%	90.0%	85.0%	79.0%	79.0%
#16	1.0%	1.5%	3.0%	3.0%	4.0%	5.0%	1.0%	2.0%	65.0%	60.0%	49.0%	49.0%
#30	1.0%	1.0%	2.5%	1.0%	4.0%	4.0%	1.0%	1.0%	43.0%	34.0%	31.0%	31.0%
#50	0.7%	0.8%	2.3%	0.8%	3.0%	3.0%	1.0%	1.0%	17.0%	9.0%	19.0%	19.0%
#100	0.6%	0.6%	2.0%	0.7%	3.0%	3.0%	1.0%	1.0%	2.0%	2.0%	10.0%	10.0%
#200	0.3%	0.3%	1.9%	0.5%	1.9%	2.3%	0.5%	0.5%	0.7%	0.7%	4.0%	4.0%

Notes: 1. Vulcan Materials Co., West Lafayette, IN

4. Delphi Limestone, Delphi, IN

2. Roger's Group Inc., Williamsport, IN

5. Fairfield Builders Supply Corp., Lafayette, IN

3. Levy Co., Portage, IN



Table 5.4 Percentage of Stockpiles

Stockpile				Mix Design #								
	SIZE	SOURCE	% CRUSHED	MD1	MD2	MD3	MD4	MD5	MD6	MD7	MD8	MD9
Gravel	IND #8	VMC	48%		45.0%	49.0%	49.0%	40.0%	39.0%	39.0%		
	IND #8	INT ST.	97%	67.5%				10.0%	10.0%	10.0%		
	IND #11	INT ST	100%	10.0%				25.0%	25.0%	25.0%		
	IND #12	VMC	22%		33.5%	25.0%	25.0%					
Slag	IND #8	LEVY	100%								45.0%	
	IND #11	LEVY	100%								30.0%	
Lime	IND #8	DELPHI	100%									50.0%
	IND #11	DELPHI	100%									25.0%
Sand	IND #24	FAIRFIELD (MODIFIED)		20.0%	20.0%	12.0%		23.5%	12.0%			
	IND #24	FAIRFIELD (BARKER PIT)									25.0%	23.5%
	FA-20	INT ST.				12.0%	23.5%		12.0%	23.5%		
	M.Filler			2.5%	1.5%	2.0%	2.5%	1.5%	2.0%	2.5%	0.0%	1.5%





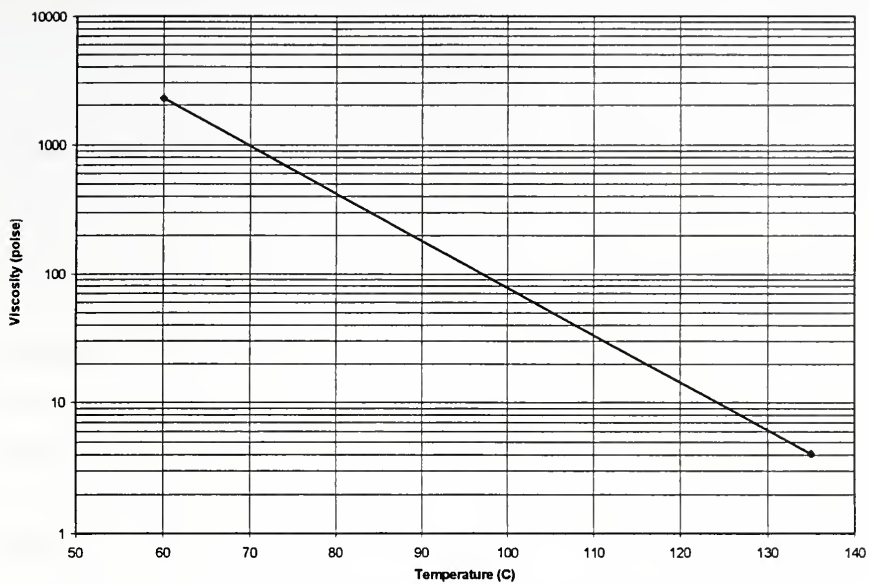


Figure 5.2 Viscosity-Temperature Chart



### 5.1.3 Mix Design

Mix designs were conducted by preparing samples in increments of one-half percent asphalt content to span an expected optimum. At least three specimens were compacted at each asphalt content using the 75 blows Marshall hand hammer. Bulk specific gravity tests were performed on compacted Marshall samples in accordance with ASTM 2726-90. Then the Marshall Stability and flow tests were conducted following the procedures described in ASTM D1559-82. After completion of the stability and flow tests, the theoretical maximum specific gravity of mixtures was determined in triplicate at three asphalt contents in accordance with ASTM D2041-90. Supplemental procedure of ASTM D2726-90 for mixture containing porous aggregate not completely coated was followed in determining the maximum specific gravity for the slag mixture. The maximum specific gravities for any other asphalt contents were calculated using the following equation:

$$G_{mm} = \frac{P_{mm}}{\frac{P_s}{G_{se}} + \frac{P_b}{G_b}} \dots\dots\dots(5.1)$$

Where,

- $G_{mm}$  = Maximum specific gravity of mixture,
- $P_{mm}$  = Total loose mixture, 100 percent,
- $P_s$  = Aggregate, percent by total weight of mixture,
- $P_b$  = Asphalt content, percent by total weight of mixture,
- $G_{se}$  = Effective specific gravity of aggregate,
- $G_b$  = Specific gravity of asphalt cement.

#### 5.1.4 Gyratory Testing Machine Tests

The U.S. Corps of Engineers Gyratory Machine (Model 4C) was used to compact mixtures at the optimum asphalt content and 0.5 percent above and below the selected optimum asphalt content. Three samples at each asphalt content were compacted at one degree angle of gyration, 120 psi normal pressure, 120 revolutions, and 283°F compaction temperature. The primary purpose of this test was to evaluate the gyratory stability index (GSI) for the mixtures.

#### 5.2 Test Section Construction

Mixtures #1 through #3 were prepared by a local contractor in a batch plant. The contractor replaced the batch plant with a drum mix plant which was used to prepare mix #4. As a result of concern with mixture variation and a significant increase in aggregate required to produce the mix through the drum mix plant, arrangements were made with a second contractor to produce mixtures #5 through #9 in another batch plant.

Indiana Department of Transportation trucks were used to deliver appropriate stockpiles to the contractor's plant site. The plant was calibrated for the stockpile aggregate to produce the desired combined mix design gradation. Initial mixture was produced at the one-half percent lower than optimum asphalt content. Subsequently, mixtures were produced at optimum and one-half percent higher than optimum. One truck of mixture was produced at each asphalt content and delivered to the APT facility.

Mixture was placed with an asphalt laydown machine and compacted with a vibratory steel wheel roller in the "static" mode. A tack coat was applied to the concrete surface in preparation for placement of the asphalt layer. The first truck load of mixture was placed in the laydown machine hopper and the laydown machine was backed into the APT facility. A 10 foot wide, 3 inch thick layer was laid. Compaction was applied to

achieve 96 percent density of 75 blow manual Marshall compaction or until refusal. Density was monitored with a nuclear gage. After compaction, five feet of the lane was removed. The second and third mixtures were constructed using the same procedure except that the third lane was left ten feet wide. In summary, three test sections were constructed. The first two sections were five feet wide and the third section was ten feet wide.

### 5.3 Accelerated Pavement Test

Accelerated traffic was applied with the Indiana DOT/Purdue accelerated pavement test (APT) device. APT loading for this series of tests was applied at 5 mph. A 9000 lb. constant force was applied to dual wheels. Traffic was applied in a single wheel path and in only one direction. The loading cycle is approximately 15 s. Tires are Michelin radial, 11R 24.5XTA inflated to 90 psi. Figure 5.3 shows the tire print of one tire. During tests, temperature of the asphalt layer was held at  $38^{\circ}\text{C} \pm 1.1^{\circ}\text{C}$ ). This temperature was essentially constant through the depth of the asphalt.

An analog to digital board in a PC is used to interface with sensors. The sensors are monitored and sampled, converted to engineering units and stored. Data for traffic tests basically consisted of temperature, load cycle event and transverse surface profile.

Transverse profile was initially recorded with a Rainhart Model 865 modified to a six foot length. On the original device, the profile was recorded on graph paper. The graph consisted of transverse position and vertical displacement. This graph was digitized for analysis. Subsequently, the profiler was retrofitted with LVDTs and the data was collected, processed and stored for analysis.

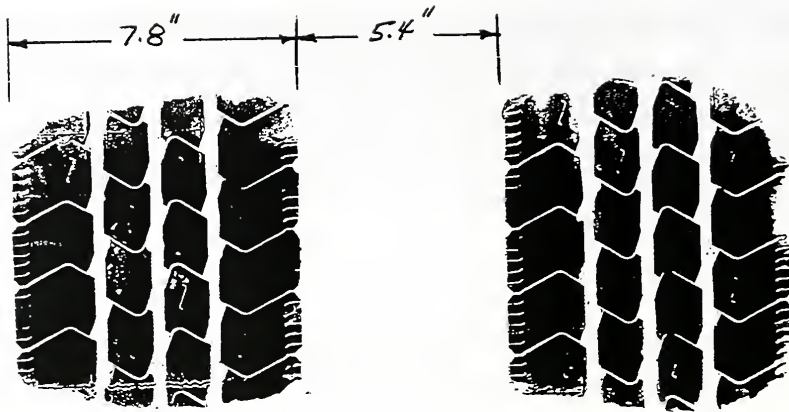


Figure 5.3 APT Tire Print

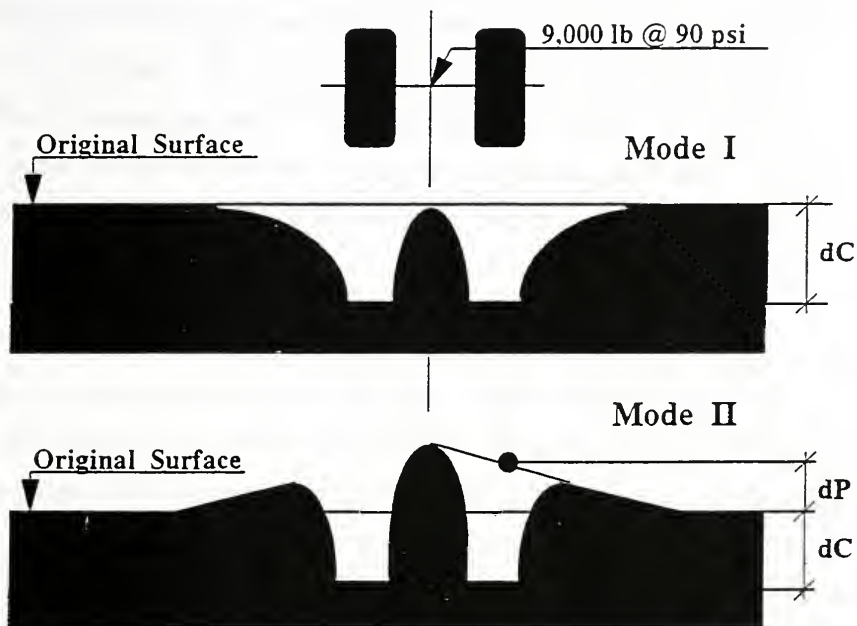
Data was recorded for nine transverse sections of each lane using the transverse profilometer. Transverse profiles were recorded at each of the nine cross-sections at 100, 300, 800, 1500, 2000, 2500, 3000, 3500, 4000, 4500 and 5000 repetitions of load, or until the measured rut exceeded 0.75" (20 mm), whichever came first.

Permanent deformation was noted in all mixture tests. Two mixtures (both at 0.5% over design optimum asphalt content) were terminated at less than 5000 repetitions due to excessive deformation.

Two modes of rutting have been observed. These modes are shown in Figure 5.4 and described as follows:

**Compactive:** Permanent deformation due to densification, and is identified where the deformed surface is lower than the original, undisturbed surface.

**Plastic:** Permanent deformation with shear failure and flow, and is evidenced by the deformed surface being higher than the original surface. The uplift typically occurs both between and outside the wheel paths.



**Mode I: Primarily Compactive (dC), Stable, Limited rut**

**Mode II: Compactive (dC) and Plastic (dP), Unstable, Unlimited rut**

Figure 5.4 Rutting Modes

Prior to traffic tests, locations for transverse profiles were marked on the test section surface. The sections were located at a spacing of two feet, starting from the end of the test sections. The transverse profilometer is six feet long so that the end supports are outside of the rutted area. As a result, rutting measurements were made referenced to a fixed datum. Subsequently, the data were processed to determine the "stringline" rut. "Stringline" rutting is the difference between the highest and lowest point on the profile.

Figure 5.5 shows the rut development with increasing traffic. Data and plots of the individual modes of rutting and the combined "stringline" rutting are shown for individual test lanes in Appendix B. "Stringline" rutting is the difference between the highest and lowest point on the profile. Each plot represents the average rutting of each test section.

#### 5.4 Laboratory Tests

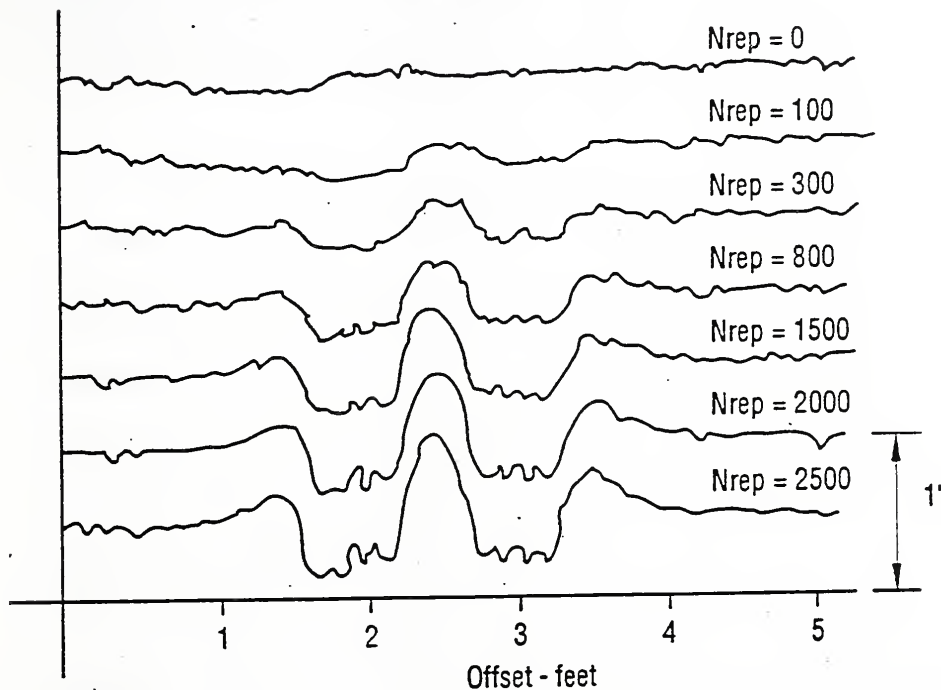
A number of tests were conducted to document the as-placed test sections as well as determine the properties of mixtures. Bulk samples were taken of the material placed in the test sections. Also, upon completion of traffic tests, 4" cores and block samples were taken from each section. These samples were retained for detailed destructive and non-destructive testing. Cores were cut from in the wheel paths, between the wheel paths and outside the wheel paths. Figure 5.6 shows the sampling plan. Bulk and maximum specific gravity, asphalt extraction and recovery, sieve analysis, crushed content, flat & elongated particles, penetration and viscosity, and Marshall and Gyratory recompaction were performed on the samples from each test lane.

##### 5.4.1 Bulk and Maximum Specific Gravity

Bulk specific gravity was performed on all 4 inch cores from each test lanes in accordance with ASTM D2726-90. A total four 4 inch cores from each lane (Two from the wheel paths, two from outside the wheel paths) were tested for maximum specific



gravity in accordance with ASTM D2041-90. Supplemental procedure of ASTM D2726-90 for mixture containing porous aggregate not completely coated was followed in determining the maximum specific gravity for the slag mixture.



MD#1, Rich Lane: Asphalt Content = 4.9%

Figure 5.5 Cross Sections Showing Progressive Rutting

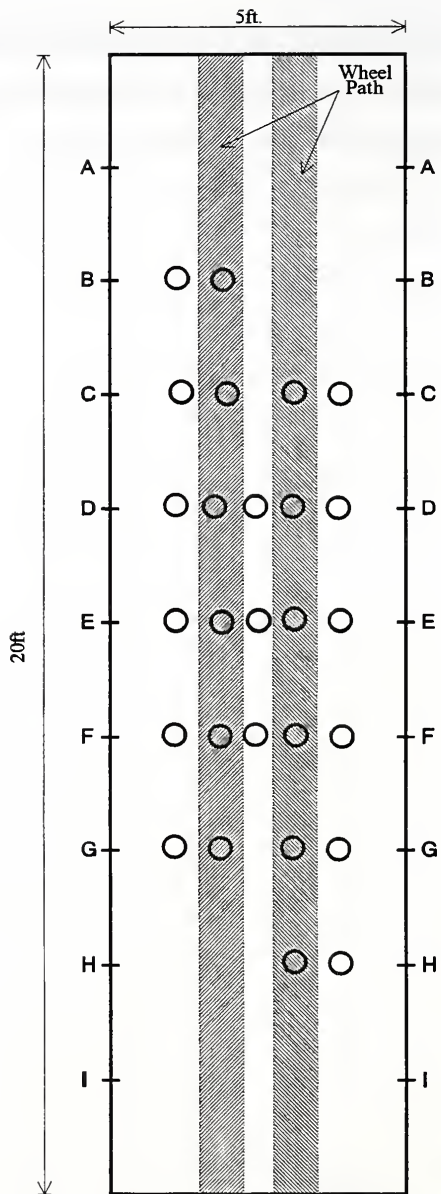


Figure 5.6 Test Section Sampling Plan

#### 5.4.2 Asphalt Extraction and Recovery

Asphalt extraction was performed in accordance with Test Method A of ASTM D2172-88. The same samples tested for maximum specific gravity were air-dried to constant weight and used in this test. Therefore, 4 samples were extracted for each lane. Two of the samples were from the wheel paths and another two were from out of the wheel paths. Asphalt was recovered in accordance with ASTM D1856-79. A rotary evaporator was used to concentrate the solution to about 200 ml, which speeds up the whole distillation procedure significantly.

#### 5.4.3 Sieve Analysis, Crushed Faces, and Flat & Elongated Particles

A sieve analysis was performed on recovered aggregates from the extraction tests in accordance with ASTM C136. After sieve analysis, crushed faces of the gravel were determined in accordance with IND. 204.86 Test Method for determining percentage of crushed particles in coarse aggregates. A particle having one or more fractured faces is considered as a crushed particle. The crushed percentage is calculated by weight ratio.

Determination of the flat or elongated particles in the coarse aggregate was performed in accordance with ASTM D4791-89. An aggregate particle having a ratio of width to thickness or length to width greater than 4:1 is considered as a flat or elongated particle according to INDOT's specification. The percentage of these particles is determined by dividing the weight of flat or elongated particles retained on the No.4 sieve by the total weight of material retained on the No.4 Sieve.

#### 5.4.4 Penetration and Viscosity of Recovered Asphalt Cement

The extracted asphalt was used for penetration and viscosity tests. The penetration test was performed in accordance with ASTM D5-86. The testing temperature, load and time were 25°C, 100g and 5s, respectively. The kinematic viscosity was determined after

the penetration test in accordance with ASTM D2170-85. The tests were conducted at 135°C using a Zeitfuchs cross-arm viscometer.

#### 5.4.5 Marshall Recompaction Test

Marshall recompaction was conducted on bulk samples obtained during test section construction. Three samples from each lane were compacted using a Marshall 75 blow compaction effort. Subsequently, bulk specific gravities of these Marshall samples were determined in accordance with ASTM D2726-90. Air voids of each sample were calculated.

#### 5.4.6 Gyratory Shear Test

The gyratory shear modulus was determined using the U.S. Corps of Engineers gyratory testing machine (Model 8A/6B/4C) at the INDOT Research Division. A 4 inch mold was used to compact material from the bulk samples obtained during section installation. Gage reading of 257 psi was set up to obtain 120 psi vertical compressive pressure on specimens. The bulk samples were heated up to 145°C in an oven and compacted at 139°C. The chuck mold temperature was kept at 60°C during compaction. Three hundred revolutions at one degree angle of gyration were applied to each specimen.

### 5.5 Laboratory Wheel Tracking Tests

Significant information was obtained from the APT on the effects of percent coarse crushed aggregate, natural sand and asphalt. However, the plant produced asphalt mixtures varied from the design mixtures. This was true for both asphalt content and gradation. While the APT tests were being conducted, a laboratory scale wheel testing

device (WTD) was designed and fabricated. A proposal was made and accepted to expand the project to include the laboratory WTD testing of all of the mixtures tested in the APT except for the slag mixture.

The advantage of the laboratory WTD testing is that compacted slabs can be prepared in close agreement to the mixture designs. Tests are conducted with the slab submerged in hot water at a temperature of 60 °C for surface mixtures and 57.5°C binder mixtures. A loaded pneumatic wheel is moved back and forth over the center of the slab at a speed of 13 in/sec. The pneumatic wheel load and tire pressure were 240 lb and 120 psi, respectively. Loading cycles are applied until the rut depth is 25.4 mm or until 20,000 cycles. Rutting from an initial zero is measured throughout the test and recorded automatically. A typical data set is plotted in Figure 5.7. Several characteristic features of the plot are indicated on the figure. This test provides a combined measure of the rutting and stripping potential of mixtures.

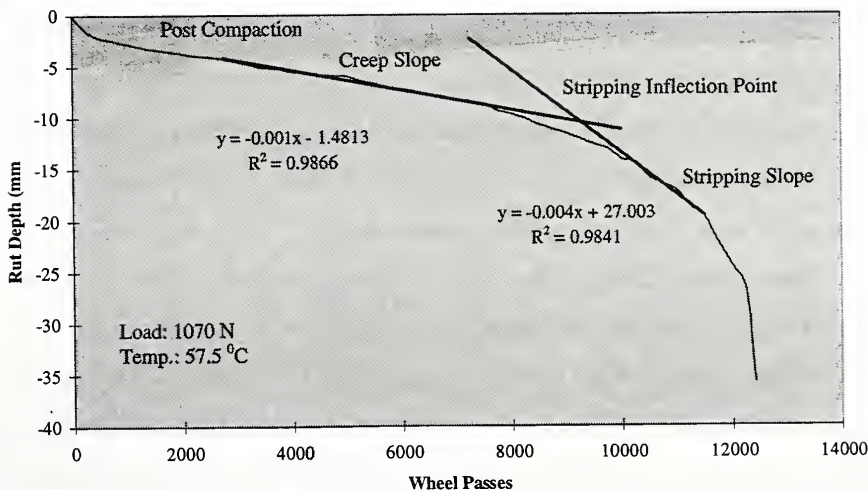


Figure 5.7 Test Results for #8 Binder (70% Crushed Gravel, 100% Natural Sand)



## CHAPTER 6

### ANALYSES OF EXPERIMENTAL DATA

Data collected from APT and laboratory investigations were analyzed with the aid of Statistical Analysis Software (SAS) [SAS Institute, Inc. 1991]. An analysis of variance (ANOVA) was performed in order to determine the significance of certain factors and/or interactions of factors. A discussion of the test data is presented as well as the results of the statistical analysis.

#### 6.1 Results of Marshall Mix Design

Voids and physical test data in tabular and graphical form are given in Appendix A. Optimum asphalt content as well as Marshall stability (lb.) and flow (0.01 in.) for each mix design are listed in Table 6.1.

Optimum asphalt contents for gravel mixtures with 100 percent natural sand are plotted against percentages of coarse crushed aggregate in Figure 6.1. Figure 6.2 shows the relationship between optimum asphalt content and percentage of natural sand at 40% and 70% crushed count. As can be seen, optimum asphalt content increases with increased coarse crushed level and decreases with high percentage of natural sand.

Figures 6.3 and 6.4 show the effects of aggregate angularity on Marshall stability. Marshall stability increases from 850 lbs. to 1700 lbs. when the percentage of coarse crushed gravel increases from 40 % to 95 %. These mixtures contained 100 % natural sand. Effects of percent natural sand on Marshall stability are not consistent at different levels of crushed gravel. For the 70% crushed gravel mixture, as expected, the Marshall stability decreases with increase in percent natural sand. For the 40% crushed gravel, the

mixtures with 50% natural sand have the highest stability of 1387 lbs. Marshall stabilities for mixtures with 0% and 100% natural sand mixtures are lower, 1120 and 850 lbs., respectively. INDOT's mix design criteria requires a minimum 1200 lbs. Marshall stability. The bulk density data shows that the 50% natural sand mixture has the highest bulk density of 147.8 pcf while bulk densities of 0% and 100% natural sand mixtures are 146.6 pcf. and 146.3 pcf, respectively. These results indicate that high bulk density corresponds to high stability.

Flow values of all nine mixtures range from 9 to 16 and meet the flow criteria (6 to 16) in INDOT mix design specification. The effects of coarse crushed aggregate and natural sand on flow are shown in Figures 6.5 and 6.6. Flow appears to be related to both density and asphalt content. High density samples with 70% coarse crushed aggregate and 50% natural sand have relatively low flow. At the same time, samples with low asphalt content and 100% natural sand also have relatively low flow. In both cases, stiffer mixtures with high density and low asphalt content have relatively low flow.

Figure 6.7, 6.8 and 6.9 show the effects of aggregate type on selected asphalt content, Marshall stability and flow, respectively. It is clear that the slag mixture has a much higher optimum asphalt content than limestone and gravel mixtures with 100 % natural sand. Asphalt extraction tests were conducted on the slag mixture and the average asphalt absorption was 0.85%. Therefore, the effective asphalt content would be 5.5% at a 6.35% optimum asphalt content. The more porous slag requires a higher asphalt content. The Marshall stability of slag and limestone mixes is higher than gravel mixtures. The slag mixture stability is two times that of the limestone mixture.



Table 6.1 Summary of Marshall Mix Designs

Mix Design No.	Aggregate Type	Percent Crushed (%)	Percent Natural Sand (%)	Optimum Asphalt Content (%)	Stability (lbs.)	Flow (0.01 in.)
MD1	Gravel	95	100	4.75	1700	11.8
MD2	Gravel	40	100	4.3	850	10.4
MD3	Gravel	40	50	4.5	1387	9
MD4	Gravel	40	0	5.2	1120	11
MD5	Gravel	70	100	4.5	1533	9.5
MD6	Gravel	70	50	5	1800	14
MD7	Gravel	70	0	5.4	1880	16
MD8	Slag	100	100	6.35	4400	14.2
MD9	Limestone	100	100	4.7	2200	11.7

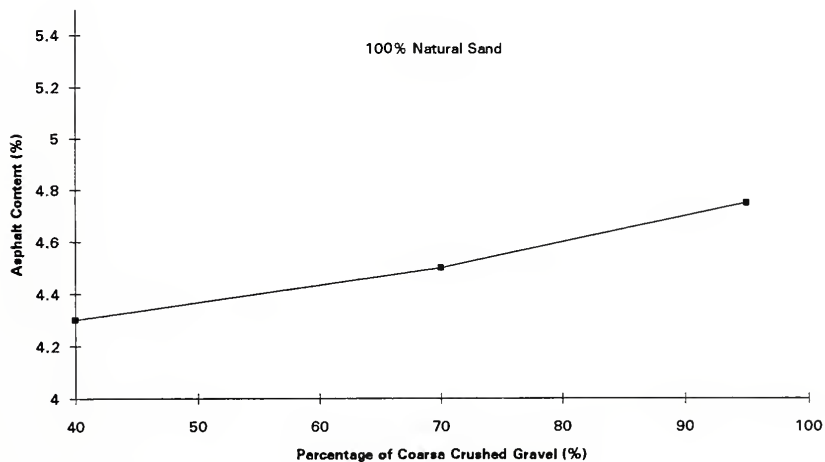


Figure 6.1 Effects of Crushed Level on Asphalt Content



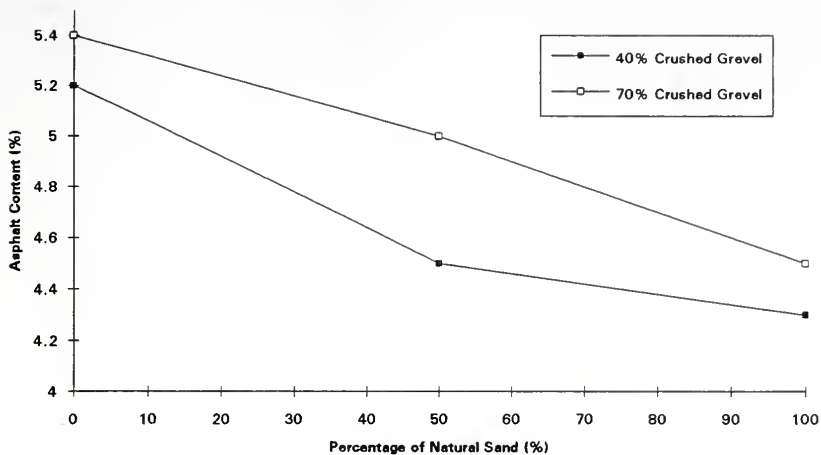


Figure 6.2 Effects of Percent Natural Sand on Asphalt Content

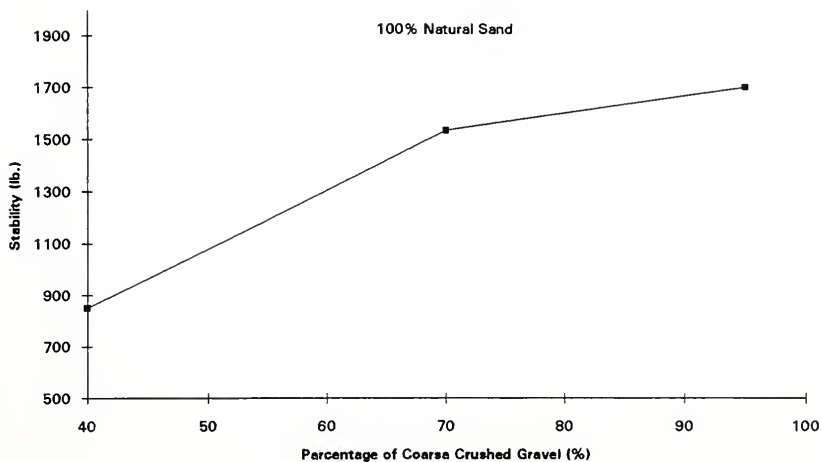


Figure 6.3 Effects of Crushed Level on Marshall Stability



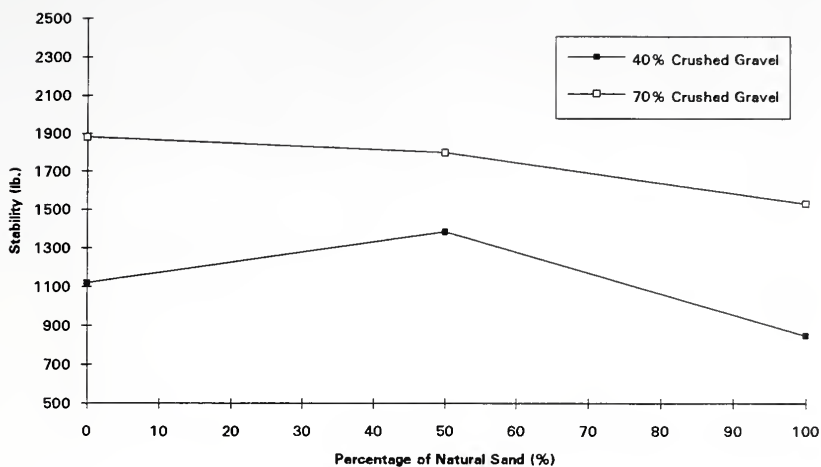


Figure 6.4 Effects of Percent Natural Sand on Marshall Stability

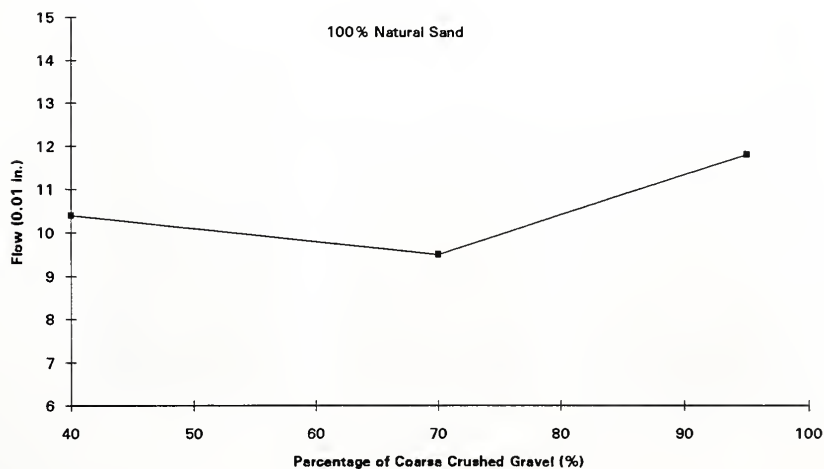


Figure 6.5 Effects of Crushed Level on Flow



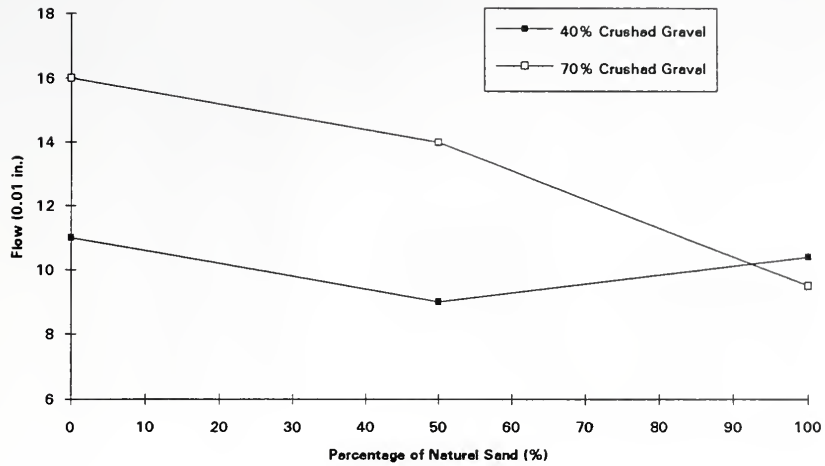


Figure 6.6 Effects of Percent Natural Sand on Flow

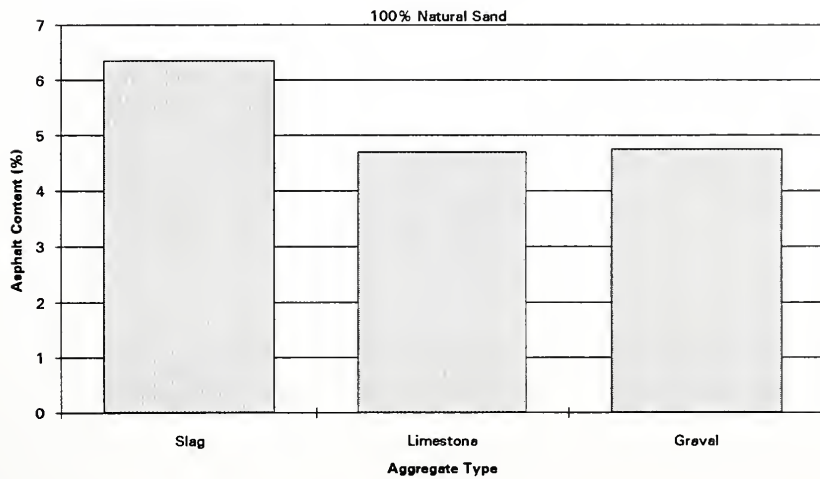


Figure 6.7 Effects of Aggregate Type on Asphalt Content





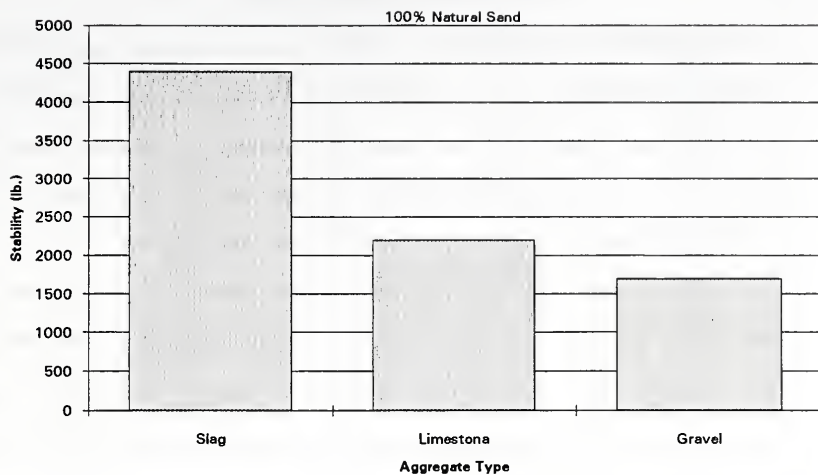


Figure 6.8 Effects of Aggregate Type on Stability

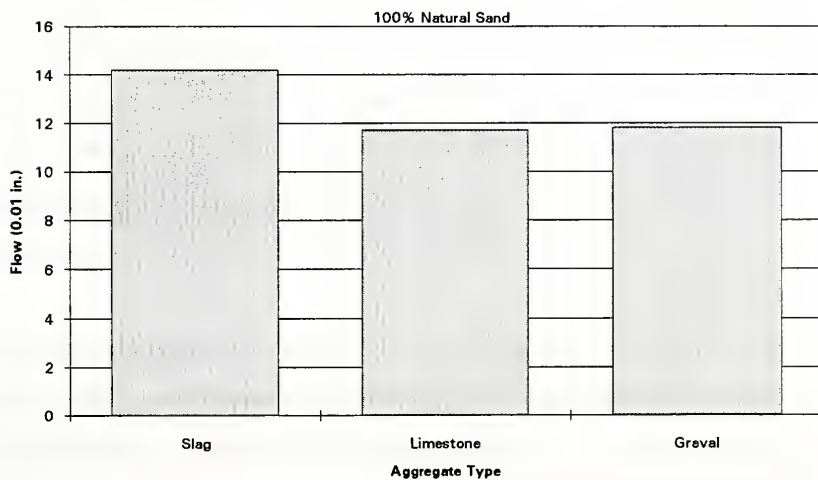


Figure 6.9 Effects of Aggregate Type on Flow

## 6.2 Air Voids Analysis of In-situ Pavement

The average bulk specific gravity (BSG), maximum specific gravity (MSG) and air voids for the APT test sections are listed in Tables 6.2 through 6.4. The BSGs determined are for different locations of each lane, namely in, out, and between wheel paths. The average BSGs in and out of the wheel path are based on tests from 12 cores. The average BSGs for between the wheel path are based on tests from 3 cores.

Replicate MSG tests were conducted on material from in and out of the wheel paths for each test section. An ANOVA was performed and the results are summarized in Table 6.5. The main effect, location, is not significant. This suggests that there is no significant difference of MSG for material taken from in or out of the wheel paths. The MSG was determined by averaging the replicate tests.

The air voids are based on the average MSG and BSG. The air voids out of the wheel path can be considered as initial pavement air voids. An ANOVA was performed and the results are summarized in Table 6.6. The main effect, location, is significant. This suggests that the air voids are significantly different at the three locations on each lane. The air voids between the wheel paths are highest with an average of 11.1%, 10.5%, and 9.7% for the lean, optimum, and rich lanes, respectively. As expected, the air voids out of the wheel paths are higher than those in the wheel paths. The average air voids out of the wheel paths are 9.9%, 9.1%, and 8.1% for lean, optimum, and rich lane, respectively. The average air voids in the wheel paths are 9.2%, 8.0%, and 7.0% for lean, optimum, and rich lane, respectively.

The air voids difference between in and out of the wheel path reflects the mixture densification under repeated traffic. The overall average difference between in and out of the wheel path is 1.0% which would result in 0.03 in. rut depth due to mixture densification of a 3 in. asphalt overlay.

Table 6.2 BSG of In-situ Pavement

		Between	In Wheel Path	Out Wheel Path
MD1	Lean	2.325	2.314	2.320
	Optimum	2.283	2.303	2.301
	Rich	2.216	2.299	2.302
MD2	Lean	2.252	2.314	2.289
	Optimum	2.229	2.292	2.275
	Rich	2.214	2.305	2.244
MD3	Lean	2.245	2.317	2.286
	Optimum	2.258	2.345	2.289
	Rich	2.259	2.358	2.323
MD4	Lean	2.251	2.237	2.270
	Optimum	2.168	2.220	2.229
	Rich	2.223	2.290	2.274
MD5	Lean	2.280	2.344	2.318
	Optimum	2.232	2.349	2.325
	Rich	2.259	2.370	2.326
MD6	Lean	2.204	2.292	2.293
	Optimum	2.266	2.352	2.310
	Rich	—	2.315	2.273
MD7	Lean	2.179	2.252	2.250
	Optimum	2.205	2.272	2.257
	Rich	2.226	2.284	2.270
MD8	Lean	2.113	2.132	2.116
	Optimum	2.142	2.148	2.125
	Rich	2.117	2.168	2.120
MD9	Lean	2.330	2.366	2.340
	Optimum	2.351	2.381	2.355
	Rich	2.374	2.391	2.362

Note: Data is not available for the cell with sign "—".



Table 6.3 MSG of In-situ Pavement

		In Wheel Path	Out Wheel Path	Average
MD1	Lean	2.552	2.555	2.553
	Optimum	2.515	2.524	2.520
	Rich	2.489	2.482	2.485
MD2	Lean	2.531	2.536	2.534
	Optimum	2.511	2.513	2.512
	Rich	2.499	2.495	2.497
MD3	Lean	2.540	2.539	2.539
	Optimum	2.517	2.517	2.517
	Rich	2.494	2.508	2.501
MD4	Lean	2.533	2.545	2.539
	Optimum	2.473	2.488	2.481
	Rich	2.498	2.485	2.492
MD5	Lean	2.539	2.539	2.539
	Optimum	2.498	2.505	2.502
	Rich	2.482	2.479	2.481
MD6	Lean	2.515	2.539	2.527
	Optimum	2.493	2.520	2.507
	Rich	2.505	2.500	2.503
MD7	Lean	2.507	2.513	2.510
	Optimum	2.515	2.506	2.510
	Rich	2.471	2.464	2.468
MD8	Lean	2.376	2.385	2.380
	Optimum	2.373	2.357	2.365
	Rich	2.343	2.350	2.346
MD9	Lean	2.572	2.579	2.575
	Optimum	2.571	2.575	2.573
	Rich	2.559	2.539	2.549



Table 6.4 Air Voids of In-situ Pavement

		Between	In Wheel Path	Out Wheel Path
MD1	Lean	8.9%	9.3%	9.2%
	Optimum	9.4%	8.4%	8.9%
	Rich	10.8%	7.6%	7.3%
MD2	Lean	11.1%	8.6%	9.7%
	Optimum	11.3%	8.7%	9.5%
	Rich	11.3%	7.8%	10.0%
MD3	Lean	11.6%	8.8%	9.9%
	Optimum	10.3%	6.8%	9.1%
	Rich	9.7%	5.4%	7.4%
MD4	Lean	11.3%	11.7%	10.8%
	Optimum	12.6%	10.2%	10.4%
	Rich	10.8%	8.3%	8.5%
MD5	Lean	10.2%	7.7%	8.7%
	Optimum	10.8%	6.0%	7.2%
	Rich	8.9%	4.5%	6.2%
MD6	Lean	12.8%	8.8%	9.7%
	Optimum	9.6%	5.6%	8.3%
	Rich	—	7.6%	9.1%
MD7	Lean	13.2%	10.2%	10.5%
	Optimum	12.2%	9.7%	9.9%
	Rich	9.8%	7.6%	7.9%
MD8	Lean	11.2%	10.3%	11.3%
	Optimum	9.4%	9.5%	9.8%
	Rich	9.8%	7.4%	9.8%
MD9	Lean	9.5%	8.0%	9.2%
	Optimum	8.6%	7.4%	8.5%
	Rich	6.9%	6.6%	7.0%

Note: Data is not available for the cell with sign "—".





Table 6.5 ANOVA Results for MSG

Source of Variation	df	SS	MS	F	Pr>F
LO	1	0.00018	0.00018	1.35	0.2478
LA	2	0.03635	0.01817	134.86	0.0001
MD	8	0.29040	0.03630	269.32	0.0001
LA*LO	2	0.00092	0.00046	3.44	0.0365
LO*MD	8	0.00073	0.00009	0.68	0.7072
LA*MD	16	0.01056	0.00066	4.90	0.0001
Error	89	0.01199	0.00013		

Note: LO = Location, In and out

LA = Lane, Lean, Optimum, and Rich

MD = Mixture, Mixture #1 to #9

Table 6.6 ANOVA Results for Air Voids

Source of Variation	df	SS	MS	F	Pr>F
LO	2	53.349	26.674	12.32	0.0001
LA	2	63.506	31.753	14.67	0.0001
MD	8	76.057	9.507	4.39	0.0001
LA*LO	4	2.499	0.624	0.29	0.8831
LO*MD	16	31.837	1.989	0.92	0.5568
LA*MD	16	24.974	1.560	0.72	0.7529
Error	32	69.264	2.164		

Note: LO = Location, In, Out, and Between

LA = Lane, Lean, Optimum, and Rich

MD = Mixture, Mixture #1 to #9



### 6.3 Extracted Asphalt Content

The extracted asphalt contents from each test section are shown in Table 6.7. In most cases replicate extraction tests were conducted in and out of the wheel paths for each test section. An ANOVA was performed and the results are summarized in Table 6.8. The main effect, location, is not significant. This suggests that there is no significant difference between in and out of the wheel path asphalt contents. The extracted asphalt content was determined by taking the average of all four asphalt contents for each test section. A bar graph of target and actual asphalt contents is given in Figure 6.10.

For gravel mixtures, the differences between target and average extracted asphalt content range from 0.0% to 1.3% with an average difference of 0.4%. Asphalt absorption of gravel mixtures is about 0.2%. Therefore, the real asphalt contents are about 0.2% below the target asphalt contents.

Differences between target and average extracted asphalt content for the slag mixtures range from 0.3% to 0.6% with an average difference of 0.5%. Asphalt absorption of slag mixtures is about 0.85% based on results of two preliminary extraction tests during slag mixture design. Therefore, the real asphalt contents are about 0.35% above target asphalt contents.

Differences between target and average extracted asphalt content for limestone mixtures range from 0.3% to 0.8% with an average difference of 0.5%. Asphalt absorption of limestone mixtures is about 0.2%. Therefore, the real asphalt contents are about 0.3% below the target asphalt contents.

Although target asphalt contents were not achieved in the test sections, the actual asphalt contents did reflect a pattern of increase in asphalt content from lean to rich lanes. Because of this range in asphalt content, the asphalt content effect on mixture rutting should be reflected in the results.

Table 6.7 Test Section Extracted Asphalt Content

		In Wheel Path		Out Wheel Path		Avg.	Target
		1	2	1	2	Extracted	
MD1	Lean	4.11%	4.26%	3.72%	3.89%	4.0%	4.2%
	Optimum	4.62%	4.09%	4.43%	4.21%	4.3%	4.7%
	Rich	4.93%	4.76%	5.40%	4.41%	4.9%	5.2%
MD2	Lean	3.82%	3.25%	3.88%	3.75%	3.7%	3.8%
	Optimum	—	4.38%	4.30%	4.14%	4.3%	4.3%
	Rich	4.10%	4.32%	4.28%	4.78%	4.4%	4.8%
MD3	Lean	4.80%	3.64%	3.63%	3.64%	3.9%	4.0%
	Optimum	3.73%	4.21%	3.80%	3.83%	3.9%	4.5%
	Rich	4.52%	4.60%	4.55%	4.15%	4.5%	5.0%
MD4	Lean	3.50%	3.65%	3.28%	3.31%	3.4%	4.7%
	Optimum	5.29%	4.62%	5.02%	4.96%	5.0%	5.2%
	Rich	4.58%	4.36%	4.78%	4.97%	4.7%	5.7%
MD5	Lean	3.77%	3.65%	3.56%	3.25%	3.6%	4.0%
	Optimum	4.06%	4.44%	4.19%	4.18%	4.2%	4.5%
	Rich	4.90%	4.28%	5.35%	3.96%	4.6%	5.0%
MD6	Lean	4.30%	4.57%	4.21%	3.54%	4.2%	4.5%
	Optimum	5.10%	4.85%	4.62%	4.14%	4.7%	5.0%
	Rich	4.94%	4.71%	4.87%	4.75%	4.8%	5.5%
MD7	Lean	4.91%	4.25%	4.41%	4.64%	4.6%	4.9%
	Optimum	4.80%	4.36%	4.70%	4.95%	4.7%	5.4%
	Rich	5.47%	5.47%	5.55%	5.66%	5.5%	5.9%
MD8	Lean	5.34%	5.05%	5.41%	5.24%	5.3%	5.9%
	Optimum	5.81%	6.10%	5.24%	5.86%	5.8%	6.4%
	Rich	5.91%	7.51%	6.95%	6.11%	6.6%	6.9%
MD9	Lean	4.09%	4.27%	3.74%	3.86%	4.0%	4.3%
	Optimum	4.51%	4.79%	3.89%	3.81%	4.3%	4.8%
	Rich	4.80%	4.28%	4.89%	4.04%	4.5%	5.3%

Note: Data is not available for the cell with sign "—".

Table 6.8 ANOVA Results for Extracted Asphalt Content

Source of Variation	df	SS	MS	F	Pr>F
LO	1	0.070	0.070	0.26	0.6138
LA	2	14.031	7.015	25.74	0.0001
MD	8	36.480	4.560	16.73	0.0001
LA*LO	2	0.472	0.236	0.87	0.4251
LO*MD	8	3.703	0.463	1.7	0.1140
LA*MD	16	6.257	0.391	1.44	0.1511
Error	70	19.076	0.272		

Note: LO = Location, In, and Out

LA = Lane, Lean, Optimum, and Rich

MD = Mixture, Mixture #1 to #9

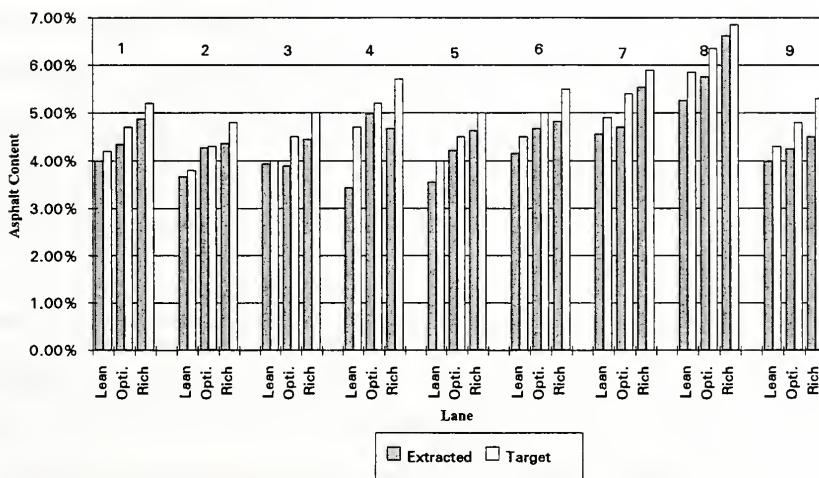


Figure 6.10 Extracted vs. Target Asphalt Content

#### 6.4 Penetration and Viscosity

Asphalt extracted from each test section was tested for penetration and kinematic viscosity. Results of these tests are given in Tables 6.9 and 6.10. In most cases, replicate tests were conducted on material from in and out of the wheel path for each test section. Statistical analyses were conducted to compare mean penetration and viscosity of extracted asphalt in the wheel path with those of extracted asphalt out of the wheel path. An ANOVA was performed and the results are summarized in Tables 6.11 and 6.12. It is found that there was no significant difference. The extracted asphalt penetration and viscosity were determined by taking the average of all four tests for each test section.

The percentage of retained penetration compares extracted asphalt penetration to initial asphalt penetration. The viscosity ratio is the ratio of extracted asphalt viscosity to initial asphalt viscosity. Percent retained penetrations range from 33.8% to 54.9% with an average of 44.1%. Viscosity ratios range from 1.47 to 2.17 with an average of 1.78. The reduction in asphalt penetration or increase in viscosity are significant. Several factors could contribute to this rapid aging process. First of all, the asphalt cement could undergo short-term aging when mixed with hot mineral aggregates in the mixing plant. Secondly, the aging process could continue during the accelerated pavement testing in APT where the temperature was held at 100°F.

Also, the high air voids in the pavement test sections could contribute to the change in the asphalt cement. Regression analysis was performed to determine the relationship between the retained penetration and viscosity of extracted asphalt and air voids in the mixtures. Two regression equations were developed and are briefly discussed below.

##### (1) Retained penetration vs. air voids

$$\text{PEN} = 40.14 + 0.44 \text{ AV} \dots\dots\dots (6.1)$$

Where:

PEN = Percent retained penetration, %,

AV = Air voids, %.

The  $R^2$  correlation coefficient for this equation is 0.01 and the equation is not statistically significant. This indicates that the percent retained penetration is not significantly correlated to the air voids.

(2) Viscosity ratio vs. air voids

$$VIS = 1.16 + 0.07 AV \dots\dots\dots(6.2)$$

Where:

VIS = Viscosity ratio

AV = Air voids, %.

The  $R^2$  correlation coefficient for this equation is 0.21 and the equation is statistically significant. This indicates that the viscosity ratio is significantly correlated to the air voids in mixture. An increase in air voids of 1% will result in approximately 7% increase of the viscosity ratio.

Figure 6.11 shows the relationship between percent retained penetration and initial air voids in the test sections and Figure 6.12 shows the relationship between viscosity ratio and initial air voids. The increase in viscosity with increase in air voids is apparent in Figure 6.12.

Table 6.9 Penetration of Extracted Asphalt (0.01 in.)

		In Wheel Path		Out Wheel Path		Avg.	Percent Retained
		1	2	1	2		
MD1	Lean	25.0	24.2	24.0	23.3	24.1	38.9%
	Optimum	24.0	22.7	33.2	22.7	25.6	41.3%
	Rich	25.7	25.3	27.1	24.7	25.7	41.5%
MD2	Lean	34.8	31.3	26.8	29.2	30.5	49.3%
	Optimum	—	27.0	27.5	19.7	24.7	39.9%
	Rich	24.7	31.5	26.0	29.8	28.0	45.2%
MD3	Lean	41.0	24.7	36.3	21.7	30.9	49.9%
	Optimum	37.2	26.9	37.7	33.3	33.8	54.5%
	Rich	35.3	26.2	39.4	24.5	31.4	50.6%
MD4	Lean	22.3	20.1	20.9	20.6	21.0	33.8%
	Optimum	21.6	21.3	21.4	22.6	21.7	35.1%
	Rich	22.6	21.6	22.7	22.8	22.4	36.1%
MD5	Lean	21.7	23.7	23.5	22.8	22.9	37.0%
	Optimum	23.8	25.3	23.3	25.3	24.4	39.4%
	Rich	27.3	24.3	26.6	23.3	25.4	40.9%
MD6	Lean	24.9	25.7	25.3	22.8	24.7	39.8%
	Optimum	24.8	27.5	26.4	25.3	26.0	41.9%
	Rich	25.6	26.7	27.1	25.2	26.2	42.2%
MD7	Lean	28.3	29.4	25.5	33.8	29.3	47.2%
	Optimum	—	25.6	28.3	26.1	26.7	43.0%
	Rich	36.0	31.6	34.6		34.1	54.9%
MD8	Lean	32.1	33.3	31.3	33.2	32.5	52.4%
	Optimum	31.0	32.8	39.0	32.0	33.7	54.3%
	Rich	30.8	35.0	34.7	30.0	32.6	52.6%
MD9	Lean	26.7	27.7	25.1	29.5	27.2	43.9%
	Optimum	25.8	29.7	21.3	25.6	25.6	41.3%
	Rich	32.3	24.3	27.9	26.7	27.8	44.8%

Note: Data is not available for the cell with sign "—".



Table 6.10 Kinematic Viscosity of Extracted Asphalt (cSt)

		In Wheel Path		Out Wheel Path		Avg.	Ratio
		1	2	1	2		
MD1	Lean	856.9	842.3	877.6	871.0	862.0	2.17
	Optimum	827.1	804.7	722.2	692.1	761.5	1.92
	Rich	737.2	738.1	689.9	680.8	711.5	1.79
MD2	Lean	787.7	802.6	790.7	792.7	793.4	2.00
	Optimum	794.7	806.7	870.7	862.0	833.5	2.10
	Rich	839.0	837.2	775.5	773.6	806.3	2.03
MD3	Lean	710.5	708.5	710.0	707.3	709.1	1.78
	Optimum	690.3	680.1	693.9	700.1	691.1	1.74
	Rich	718.8	704.4	671.5	675.6	692.6	1.74
MD4	Lean	859.4	853.7	831.6	847.4	848.0	2.13
	Optimum	817.3	800.5	777.2	782.9	794.5	2.00
	Rich	755.0	750.2	738.7	737.7	745.4	1.88
MD5	Lean	656.1	659.1	665.2	672.6	663.3	1.67
	Optimum	627.9	630.7	626.7	637.9	630.8	1.59
	Rich	630.8	630.4	647.3	648.7	639.3	1.61
MD6	Lean	698.1	703.4	729.2	717.9	712.1	1.79
	Optimum	674.1	676.0	658.0	665.1	668.3	1.68
	Rich	646.7	663.6	675.3	677.7	665.8	1.68
MD7	Lean	637.6	654.1	716.3	704.0	678.0	1.71
	Optimum	837.3	834.2	713.0	711.4	774.0	1.95
	Rich	582.8	590.0	570.8	597.0	585.2	1.47
MD8	Lean	627.2	624.0	662.0	656.7	642.5	1.62
	Optimum	658.0	655.3	635.8	642.9	648.0	1.63
	Rich	659.5	653.2	695.8	689.7	674.5	1.70
MD9	Lean	664.5	654.8	679.7	676.9	669.0	1.68
	Optimum	588.6	587.5	659.7	658.5	623.6	1.57
	Rich	586.8	584.6	644.1	639.0	613.6	1.54



Table 6.11 ANOVA Results for Penetration

Source of Variation	df	SS	MS	F	Pr>F
LO	1	0.514	0.514	0.04	0.8395
LA	2	34.519	17.259	1.39	0.2569
MD	8	1298.839	162.354	13.05	0.0001
LA*LO	2	15.814	7.907	0.64	0.5329
LO*MD	8	40.402	5.050	0.41	0.9134
LA*MD	16	178.834	11.177	0.90	0.5741
Error	67	833.780	12.444		

Note: LO = Location, In, and Out

LA = Lane, Lean, Optimum, and Rich

MD = Mixture, Mixture #1 to #9

Table 6.12 ANOVA Results for Viscosity

Source of Variation	df	SS	MS	F	Pr>F
LO	1	25.230	25.230	0.05	0.8318
LA	2	45056.327	22528.163	40.57	0.0001
MD	8	444519.455	55564.931	100.06	0.0001
LA*LO	2	4982.821	2491.410	4.49	0.0147
LO*MD	8	17541.085	2192.635	3.95	0.0007
LA*MD	16	115465.739	7216.608	12.99	0.0001
Error	70	38873	555.337		

Note: LO = Location, In, and Out

LA = Lane, Lean, Optimum, and Rich

MD = Mixture, Mixture #1 to #9



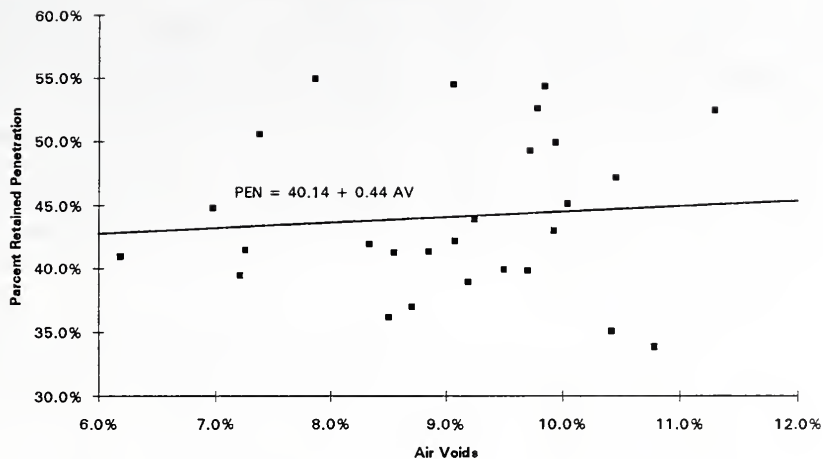


Figure 6.11 Relationship Between Retained Penetration and Air Voids

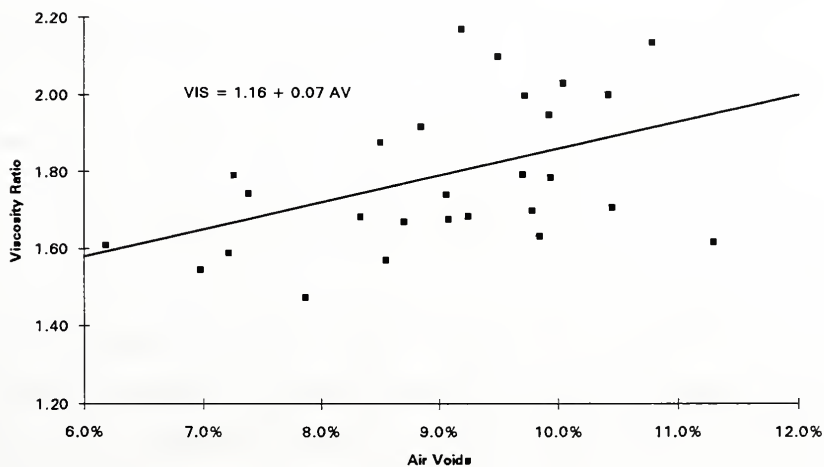


Figure 6.12 Relationship Between Viscosity Ratio and Air Voids

### 6.5 Gradation

Average gradations for each test section are given in Table 6.13. The average was determined by taking the average of all gradations for each sample from a mix. Average gradations determined in and out of the wheel paths for each test section are plotted in Figures 6.13 through 6.21. For relative comparison the Indiana gradation specification limits for the #8 binder mix, the FHWA 0.45 power curve and the target gradation curve are plotted in these figures.

Gradation curves in Figures 6.13 through 6.21 show that there is no significant difference between gradations in and out of the wheel paths. These results indicate there is no significant degradation of aggregate from traffic with the 90 psi tire pressure. In most cases, the gradations conform to the Indiana gradation specification for #8 binder mix. The gradation of mixture #4 shows significant variation which is not unexpected because a drum mix plant was used to prepare this mixture.

Two parameters were derived from mixture gradations for the correlation analysis in Chapter 7:

(1) Percent passing #4 sieve. This parameter defines the proportion of fine aggregate in a mixture.

(2) Fineness modulus (F.M.) of fine aggregate (passing No.4 sieve). It is defined as:

$$\text{F.M.} = \sum (\text{Cumulative Percent Retained on Standard Sieves}) / 100 \dots \dots \dots (6.3)$$

The standard sieves used are No.100, No.50, No.30, No.16, No.8, and No.4. The fineness modulus can be used to check the constancy of grading when relatively small changes are to be expected. A small number indicates a finer grading.

Table 6.13 APT Mixture Gradations

Sieve Size	MD1			MD2			MD3		
	Lean	Opti.	Rich	Lean	Opti.	Rich	Lean	Opti.	Rich
1"	100.0%	100.0%	100.0%	100.0%	100.0%	100.0%	100.0%	100.0%	100.0%
3/4"	90.6%	91.9%	90.4%	96.0%	97.7%	97.6%	96.3%	94.1%	94.8%
1/2"	72.2%	75.1%	71.3%	83.4%	82.9%	84.6%	81.5%	74.9%	77.6%
3/8"	56.4%	57.3%	54.7%	69.5%	69.6%	71.3%	69.9%	59.9%	62.9%
#4	30.7%	30.9%	30.2%	43.3%	46.1%	46.7%	48.1%	37.2%	42.3%
#8	17.3%	17.0%	18.6%	23.7%	24.5%	25.6%	31.3%	26.4%	28.7%
#16	12.4%	12.4%	13.5%	17.0%	16.3%	17.2%	20.9%	20.0%	20.3%
#30	9.7%	9.7%	10.4%	12.1%	10.5%	11.3%	13.4%	14.4%	13.8%
#50	7.0%	7.0%	7.1%	6.1%	5.1%	5.5%	6.8%	7.0%	7.4%
#100	4.7%	4.6%	4.3%	3.1%	2.8%	2.9%	3.6%	2.9%	4.1%
#200	3.3%	3.4%	3.1%	2.1%	2.0%	1.9%	2.3%	1.8%	2.6%
	MD4			MD5			MD6		
	Lean	Opti.	Rich	Lean	Opti.	Rich	Lean	Opti.	Rich
1"	100.0%	100.0%	100.0%	100.0%	100.0%	100.0%	100.0%	100.0%	100.0%
3/4"	97.6%	97.5%	95.6%	94.3%	96.3%	91.1%	94.6%	92.3%	91.7%
1/2"	78.5%	72.3%	77.2%	70.6%	75.4%	71.3%	65.8%	65.4%	62.9%
3/8"	67.7%	60.1%	66.8%	53.4%	59.1%	58.5%	51.8%	52.1%	49.4%
#4	33.5%	33.1%	46.2%	26.4%	29.1%	30.7%	30.8%	30.6%	27.6%
#8	9.8%	16.1%	28.4%	20.4%	22.0%	23.7%	21.1%	21.2%	19.2%
#16	5.4%	9.5%	17.7%	16.5%	17.1%	18.6%	14.1%	15.0%	12.9%
#30	4.0%	6.7%	11.2%	12.4%	12.5%	13.8%	9.5%	10.6%	8.6%
#50	3.0%	5.1%	5.8%	5.8%	5.7%	6.5%	5.3%	6.0%	4.7%
#100	2.3%	3.8%	3.4%	2.2%	2.2%	2.7%	2.9%	3.1%	2.4%
#200	1.7%	2.5%	2.3%	1.3%	1.2%	1.6%	1.8%	1.9%	1.5%
	MD7			MD8			MD9		
	Lean	Opti.	Rich	Lean	Opti.	Rich	Lean	Opti.	Rich
1"	100.0%	100.0%	100.0%	100.0%	100.0%	100.0%	100.0%	100.0%	100.0%
3/4"	91.4%	94.4%	95.3%	95.0%	94.5%	94.9%	96.2%	94.4%	95.6%
1/2"	71.7%	71.7%	70.2%	75.8%	75.1%	77.6%	76.5%	68.8%	72.6%
3/8"	59.0%	58.4%	57.3%	60.6%	59.4%	65.6%	66.1%	58.5%	63.4%
#4	31.2%	29.7%	31.6%	34.2%	33.9%	38.4%	43.3%	38.6%	41.4%
#8	18.6%	18.1%	21.2%	24.4%	25.8%	28.2%	27.8%	25.8%	26.5%
#16	11.3%	11.4%	14.4%	18.2%	19.8%	21.3%	20.1%	19.4%	19.6%
#30	7.7%	7.9%	10.8%	12.3%	13.6%	14.7%	13.1%	13.0%	13.1%
#50	5.5%	5.7%	8.2%	6.1%	6.7%	7.2%	5.9%	5.8%	6.0%
#100	3.9%	4.1%	5.7%	3.0%	3.3%	3.3%	2.7%	2.5%	2.7%
#200	2.7%	2.7%	3.5%	1.7%	1.8%	1.8%	1.8%	1.5%	1.8%





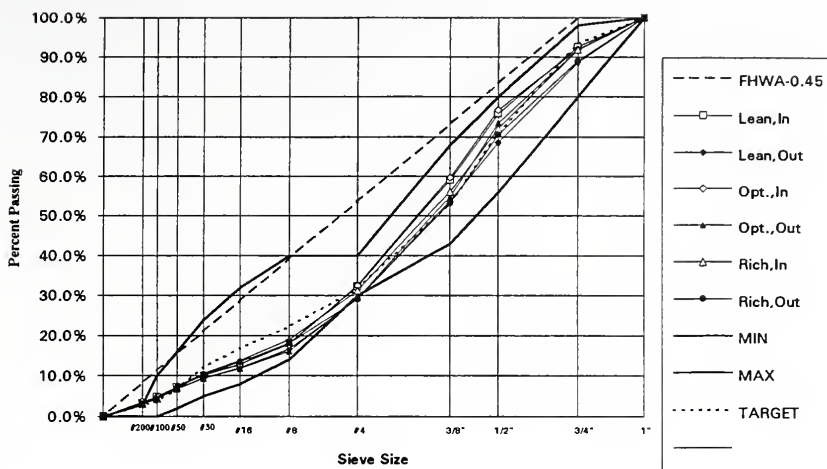


Figure 6.13 Gradation Curves for Mix #1

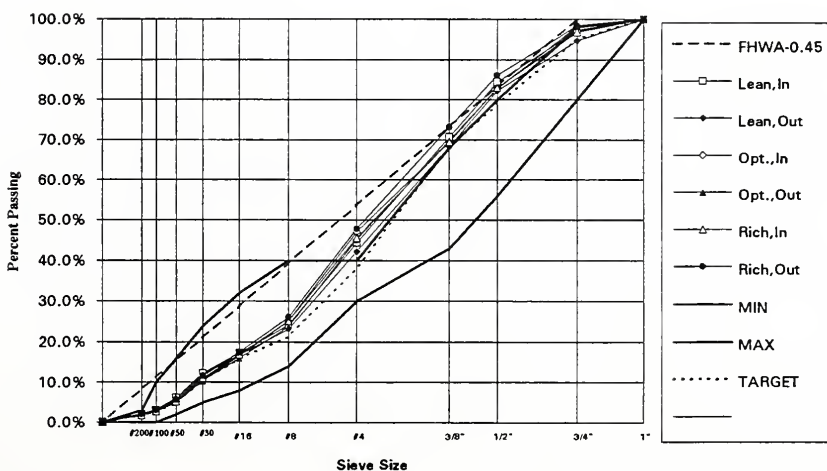


Figure 6.14 Gradation Curves for Mix #2



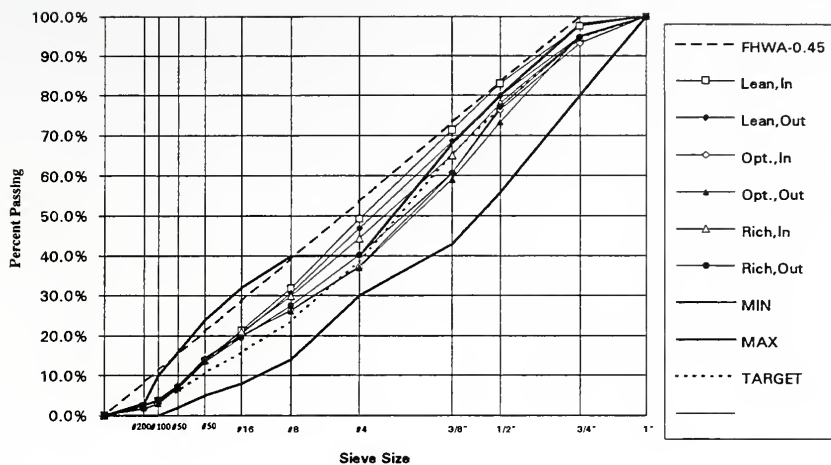


Figure 6.15 Gradation Curves for Mix #3

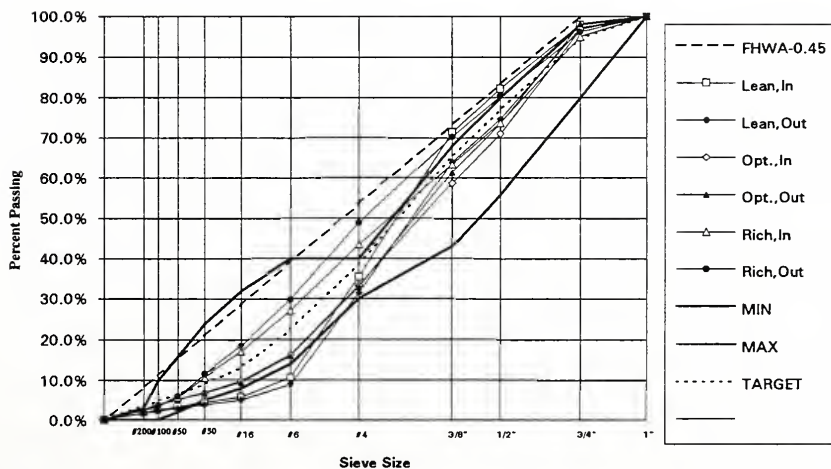


Figure 6.16 Gradation Curves for Mix #4



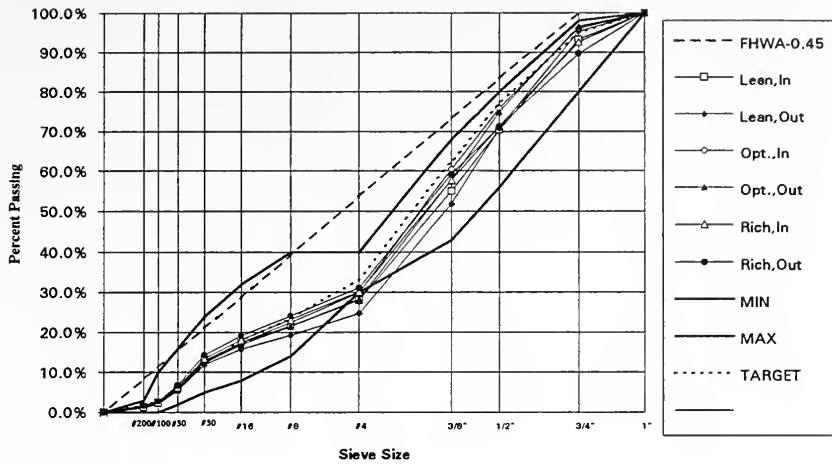


Figure 6.17 Gradation Curves for Mix #5

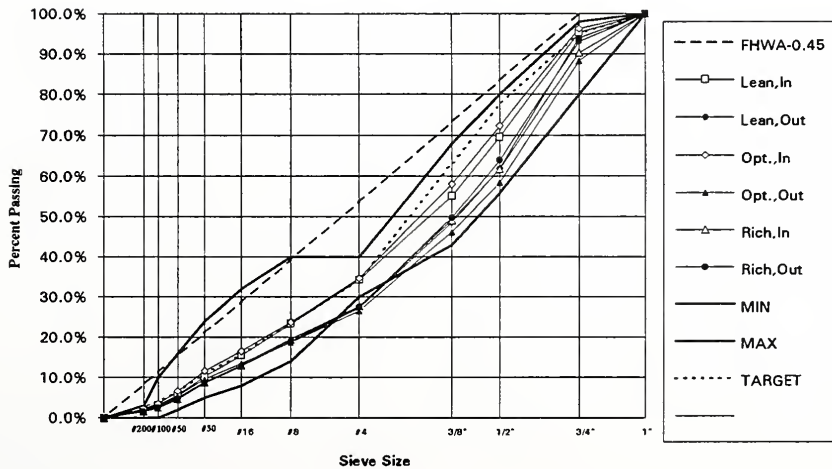


Figure 6.18 Gradation Curves for Mix #6



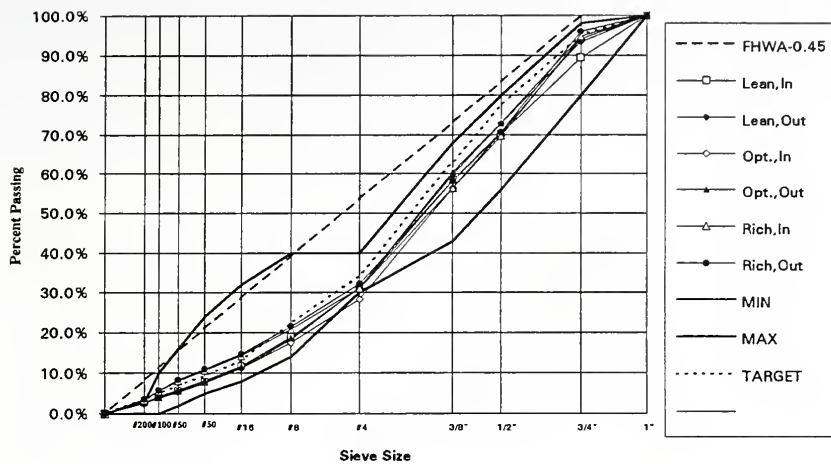


Figure 6.19 Gradation Curves for Mix #7

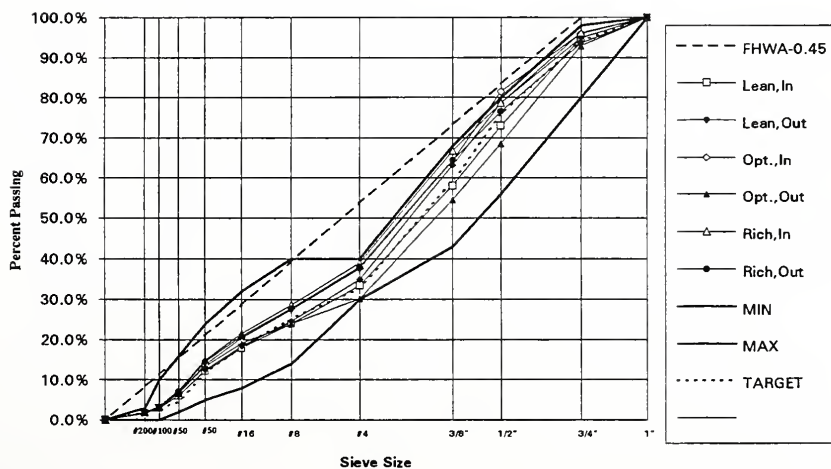


Figure 6.20 Gradation Curves for Mix #8





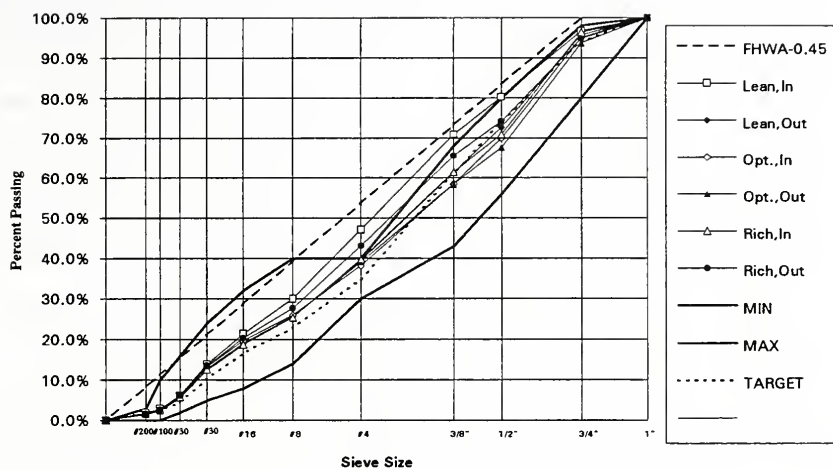


Figure 6.21 Gradation Curves for Mix #9



### 6.6 Percentage of Crushed Faces and Flat & Elongated Particles

Gravel mixtures were blended to achieve various levels of coarse crushed faces. Measured percentage of crushed faces as well as percentage of flat & elongated particles in each test section are listed in Table 6.14. These determinations were made on the material from in and out of the wheel paths. Percentage of flat & elongated particles ranged from 0.0% to 1.2%. This is well below the INDOT limit of a maximum of 15%.

Statistical analyses were conducted to compare mean crushed percentages in the wheel path with those out of the wheel path. An ANOVA was performed and the results are summarized in Table 6.15. The main effect, location, is not significant. This indicates that there was no significant aggregate fracture from traffic. The crushed percentage was determined as the average of two crushed percentages in and out of wheel path for each test section. A bar graph of target and actual crushed percentages is given in Figure 6.22.

The 95% crushed gravel mixtures had actual crushed percentages ranging from 96% to 96.9% with an average of 96.5% which is very close to the target value. The 40% crushed gravel mixtures had actual crushed percentages that were higher than the target percentages. Actual crushed percentages ranged from 40% to 53.6% with an average of 46.2%.

All 70% crushed gravel mixtures except lean and rich sections of MD5 had higher actual crushed percentages than the target percentages. Actual crushed percentages ranged from 61.6% to 81.6% with an average of 74.1%.

Table 6.14 Percentage of Crushed Faces and Flat &amp; Elongated Particles

		% Flat & Elongated			% Crushed			
		In Wheel path	Out Wheel path	Avg.	In Wheel path	Out Wheel path	Avg.	Target
MD1	Lean	0.4%	0.0%	0.2%	97.7%	96.2%	96.9%	95%
	Opt.	0.0%	0.0%	0.0%	96.6%	95.4%	96.0%	95%
	Rich	0.3%	0.1%	0.2%	96.7%	96.3%	96.5%	95%
MD2	Lean	0.0%	0.5%	0.2%	42.3%	44.2%	43.2%	40%
	Opt.	0.3%	0.0%	0.1%	46.9%	48.7%	47.8%	40%
	Rich	0.3%	0.2%	0.2%	40.6%	39.5%	40.0%	40%
MD3	Lean	0.0%	0.2%	0.1%	38.7%	50.3%	44.5%	40%
	Opt.	0.0%	0.8%	0.4%	46.5%	46.0%	46.3%	40%
	Rich	0.4%	0.0%	0.2%	44.3%	41.2%	42.8%	40%
MD4	Lean	0.3%	1.6%	0.9%	44.2%	47.9%	46.0%	40%
	Opt.	1.9%	0.5%	1.2%	51.4%	55.7%	53.6%	40%
	Rich	0.5%	0.5%	0.5%	51.4%	51.9%	51.7%	40%
MD5	Lean	0.0%	0.0%	0.0%	61.9%	64.8%	63.3%	70%
	Opt.	0.3%	0.0%	0.1%	73.2%	68.4%	70.8%	70%
	Rich	0.0%	0.3%	0.1%	59.4%	63.8%	61.6%	70%
MD6	Lean	0.7%	0.0%	0.3%	80.4%	80.2%	80.3%	70%
	Opt.	0.0%	0.2%	0.1%	82.9%	80.4%	81.6%	70%
	Rich	0.9%	0.5%	0.7%	77.8%	78.9%	78.4%	70%
MD7	Lean	0.0%	0.0%	0.0%	74.3%	76.9%	75.6%	70%
	Opt.	0.0%	0.4%	0.2%	78.5%	77.1%	77.8%	70%
	Rich	0.0%	0.3%	0.2%	76.6%	79.0%	77.8%	70%
MD8	Lean	0.0%	0.0%	0.0%	100.0%	100.0%	100.0%	95.0%
	Opt.	0.0%	0.0%	0.0%	100.0%	100.0%	100.0%	95.0%
	Rich	0.0%	0.0%	0.0%	100.0%	100.0%	100.0%	95.0%
MD9	Lean	0.0%	0.0%	0.0%	100.0%	100.0%	100.0%	95.0%
	Opt.	0.0%	0.0%	0.0%	100.0%	100.0%	100.0%	95.0%
	Rich	0.0%	0.0%	0.0%	100.0%	100.0%	100.0%	95.0%

Table 6.15 ANOVA Results for Crushed Percentage

Source of Variation	df	SS	MS	F	Pr>F
LO	1	10.006	10.005	1.54	0.2380
LA	2	114.574	57.287	8.83	0.0044
MD	6	14703.516	2450.586	377.67	0.0001
LA*LO	2	23.846	11.923	1.84	0.2013
LO*MD	6	19.059	3.176	0.49	0.8043
LA*MD	12	132.995	11.082	1.71	0.1833
Error	12	77.863	6.488		

Note: LO = Location, In, and Out  
 LA = Lane, Lean, Optimum, and Rich  
 MD = Mixture, Mixture #1 to #7

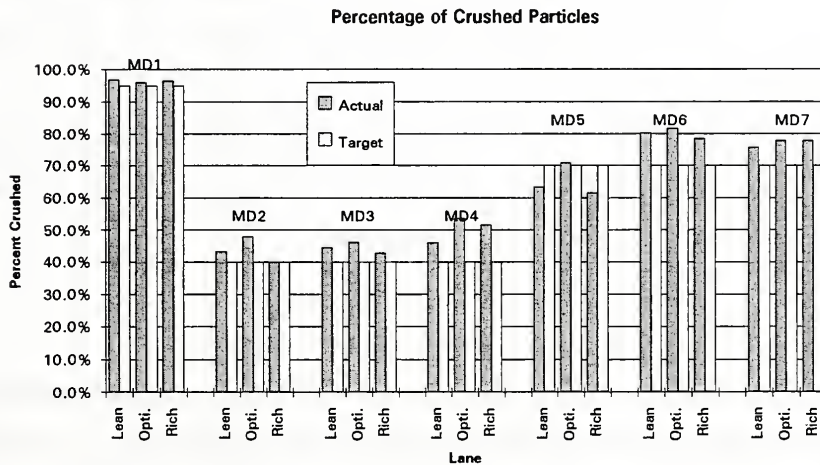


Figure 6.22 Crushed Percentages of Gravel Mixtures

### 6.7 Gyrotory Stability Index (GSI) and Shear Strength

During mix design, the gyratory testing machine (GTM) tests were conducted on laboratory-prepared specimens to evaluate the Gyrotory Stability Index (GSI) prior to test section construction. Bulk samples of material from each test section were retained, GTM compaction and shear tests were conducted on these materials.

#### 6.7.1 Gyrotory Stability Index

Gyrotory Stability Index (GSI) is the ratio of the maximum gyratory angle to the minimum gyratory angle [ASTM D 3387, 1991]. A GSI in excess of unity indicates a progressive increase in plasticity during densification and foretells instability of the bituminous mixture for the loading employed. A GSI of not more than 1.1 was suggested by the Indiana Mineral Aggregate Association as an acceptable stability criteria.

The Gyrotory Stability Index (GSI) of laboratory prepared specimens is given in Table 6.16. The GSI values for all 27 mixtures range from 0.93 to 1.06. In most cases the GSI values are less than unity.

Table 6.17 summarizes the Gyrotory Stability Index (GSI) of specimens prepared from the bulk samples. GSI values range from 0.80 to 1.02. In most cases the GSI values are less than unity which indicates a non-plastic mixture.

#### 6.7.2 Gyrotory Shear Strength of Bulk Mixtures

The Gyrotory Shear Strength ( $S_G$ ) and Gyrotory Shear Modulus ( $G_G$ ) were obtained from gyratory shear tests on specimens prepared from the bulk samples. The formulas developed by McRae [1993] to calculate  $S_G$  and  $G_G$  are briefly discussed below:

Table 6.16 Gyrotory Stability Index (Laboratory Specimen up to 120 Revolutions)

Asphalt Content	Sample #	GSI	Asphalt Content	Sample #	GSI	Asphalt Content	Sample #	GSI
MD1			MD2			MD3		
4.3	A	—	3.8	A	0.97	4.0	A	0.95
	B	—		B	1.00		B	0.98
	C	—		C	1.00		C	0.99
4.8	A	0.98	4.3	A	0.98	4.5	A	0.96
	B	0.98		B	0.98		B	0.93
	C	0.97		C	0.98		C	0.96
5.3	A	—	4.8	A	0.98	5.0	A	1.00
	B	—		B	0.97		B	0.97
	C	—		C	0.98		C	0.97
MD4			MD5			MD6		
4.7	A	0.99	4.0	A	0.98	4.5	A	0.97
	B	0.99		B	0.98		B	1.00
	C	0.94		C	0.99		C	0.96
5.2	A	0.97	4.5	A	0.98	5.0	A	1.02
	B	0.99		B	0.98		B	1.00
	C	0.98		C	0.98		C	0.97
5.7	A	1.00	5.0	A	0.99	5.5	A	1.00
	B	0.99		B	0.95		B	1.06
	C	0.95		C	0.97		C	1.02
MD7			MD8			MD9		
4.9	A	0.99	5.85	A	0.98	4.3	A	1.00
	B	0.96		B	1.02		B	0.97
	C	0.98		C	1.00		C	0.94
5.4	A	1.00	6.35	A	0.96	4.8	A	1.00
	B	1.00		B	1.00		B	1.00
	C	0.99		C	1.02		C	0.98
5.9	A	1.00	6.85	A	0.98	5.3	A	1.00
	B	0.99		B	0.98		B	1.00
	C	1.00		C	0.97		C	1.00

Note: Data is not available for the cell with sign "—".





Table 6.17 Gyrotory Stability Index (Bulk Specimen up to 300 Revolutions)

Asphalt Content	Sample #	GSI	Asphalt Content	Sample #	GSI	Asphalt Content	Sample #	GSI
MD1			MD2			MD3		
4.0	A	0.89	3.7	A	0.89	3.9	A	0.85
	B	0.89		B	0.93		B	0.96
	C	0.90		C	0.94		C	0.93
4.3	A	0.90	4.3	A	0.89	3.9	A	0.93
	B	0.86		B	1.02		B	0.98
	C	0.92		C	1.02		C	0.90
4.9	A	0.93	4.4	A	0.92	4.5	A	0.97
	B	0.94		B	0.95		B	0.91
	C	0.87		C	0.91		C	0.96
MD4			MD5			MD6		
3.4	A	0.85	3.6	A	0.97	4.2	A	0.94
	B	0.91		B	0.87		B	0.87
	C	0.93		C	0.94		C	0.91
5.0	A	0.88	4.2	A	0.97	4.7	A	0.88
	B	0.85		B	0.90		B	0.93
	C	0.89		C	1.00		C	0.93
4.7	A	0.88	4.6	A	0.94	4.8	A	0.94
	B	0.80		B	0.94		B	0.92
	C	0.96		C	0.95		C	0.92
MD7			MD8			MD9		
4.6	A	0.88	5.3	A	0.91	4.0	A	0.98
	B	0.88		B	0.88		B	0.94
	C			C	0.83		C	0.94
4.7	A	0.95	5.8	A	0.85	4.3	A	0.95
	B	0.89		B	0.95		B	0.83
	C	0.90		C	0.90		C	0.85
5.5	A	0.89	6.6	A	0.97	4.5	A	0.98
	B	1.00		B	0.92		B	0.95
	C	1.00		C	0.93		C	0.92



(1) Gyratory Shear Strength ( $S_G$ )

$$S_G = \frac{2(W \times L - F \times a) + N \times b}{A \times h} \dots\dots\dots(6.4)$$

For  $S_G$  at  $\theta_{\max}$ , multiply by  $\frac{\theta_{\max}}{\theta_0}$

Where:

- $S_G$  = Gyratory shear strength,
- $A$  = cross sectional area of specimen, in.<sup>2</sup>,
- $h$  = height of specimen, in.,
- $W$  =  $p \times a$  = load on roller, pound,
- $L$  = length of roller lever arm, in.,
- $F$  = force caused by wall friction, pound,
- $a$  = effective area of roller piston, in.<sup>2</sup>,
- $N$  = vertical load on specimen, pound
- $b$  = arm of vertical force couple =  $h \times \tan\theta_0$ , in.
- $p$  = roller pressure, psi
- $P$  = vertical pressure in GTM test, psi
- $\theta_0$  = initial gyratory angle
- $\theta_{\max}$  = maximum gyratory angle

(2) Gyratory Shear Modulus ( $G_G$ ), psi

$$G_G = \frac{S_G}{\tan\theta_0} \dots\dots\dots(6.5)$$

Tests were conducted with the GTM model 8A/6B/4C. Appropriate factors for this GTM Model were substituted into Equations 6.4 and 6.5 to calculate  $S_G$  and  $G_G$  values.

Three bulk samples were tested for each test lane. Average  $S_G$  and  $G_G$  values were determined by averaging the triplicate results for each mixture which are shown in Table 6.18.

It is believed that the rutting is primarily caused by plastic deformation due to high shear stress in the upper portions of the asphalt layer. An attempt was made to correlate plastic rut depth with mixture  $S_G$ . Figure 6.23 shows the relationship between plastic rut depth and gyratory shear strength. This figure does not indicate any such correlation.

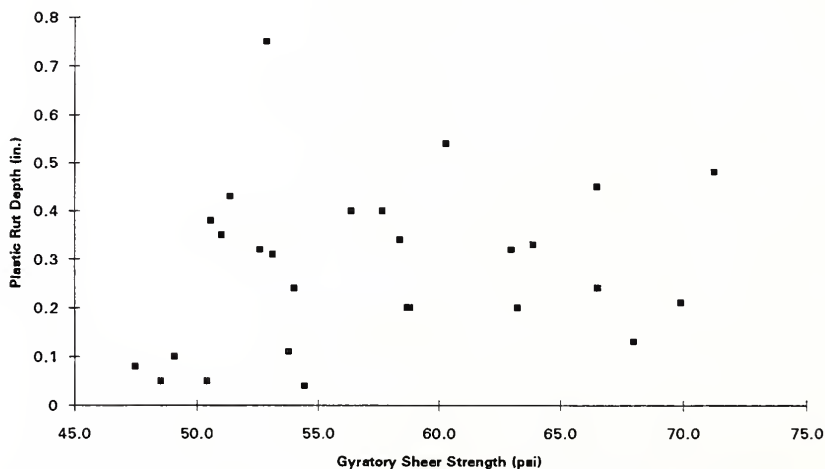


Figure 6.23 Relationship between Plastic Rut Depth and Gyratory Shear Strength

Table 6.18 Gyrotory Shear Test Results

		Asphalt Content		Shear Strength (psi)	
		Extracted	Target	S <sub>G</sub>	G <sub>G</sub>
MD1	Lean	4.0%	4.2%	63.3	3054.7
	Optimum	4.3%	4.7%	69.9	3579.6
	Rich	4.9%	5.2%	56.4	2841.3
MD2	Lean	3.7%	3.8%	58.8	2855.1
	Optimum	4.3%	4.3%	63.0	2973.2
	Rich	4.4%	4.8%	71.2	3145.6
MD3	Lean	3.9%	4.0%	58.7	2946.6
	Optimum	3.9%	4.5%	58.4	2763.5
	Rich	4.5%	5.0%	50.6	2535.9
MD4	Lean	3.4%	4.7%	68.0	3106.6
	Optimum	5.0%	5.2%	63.9	2977.6
	Rich	4.7%	5.7%	52.9	2820.5
MD5	Lean	3.6%	4.0%	57.7	2791.5
	Optimum	4.2%	4.5%	66.5	3242.7
	Rich	4.6%	5.0%	60.3	2877.8
MD6	Lean	4.2%	4.5%	66.5	3211.2
	Optimum	4.7%	5.0%	53.1	2845.7
	Rich	4.8%	5.5%	51.4	2489.4
MD7	Lean	4.6%	4.9%	52.6	2764.5
	Optimum	4.7%	5.4%	54.0	2675.1
	Rich	5.5%	5.9%	51.0	2406.3
MD8	Lean	5.3%	5.9%	48.5	2465.3
	Optimum	5.8%	6.4%	54.4	2853.6
	Rich	6.6%	6.9%	53.8	2691.0
MD9	Lean	4.0%	4.3%	50.4	2770.4
	Optimum	4.3%	4.8%	47.5	2603.7
	Rich	4.5%	5.3%	49.1	2554.6

### 6.8 Analysis of Marshall Recomposition

Air voids from the Marshall Recomposition tests are summarized in Table 6.19. The target and average extracted asphalt contents as well as air voids out of the wheel path are also listed in Table 6.19 for relative comparison.

Air voids from the Marshall recompositions reflect a logical pattern. In general, the air voids decrease with increase of asphalt content. Air voids out of the wheel path are higher than the air voids from Marshall recomposition. The average air voids of the nine mixtures at the target optimum asphalt contents is 5.8% which is close to the 6.0% target air void content. Average air voids of the nine test sections at the target optimum asphalt contents is 9.1%. The difference in air voids reflects the difference in compaction of the Marshall procedure and field compaction. The larger as-constructed air voids indicate that field compactive effort is less than the compactive effort achieved with 75 blows per side of the Marshall manual hammer.

### 6.9 Results of Accelerated Pavement Test

During accelerated pavement tests, rut depths were measured at various levels of repetitions. Data in tabular form and plots of the individual modes of rutting and the combined "stringline" rutting are shown for each test lane in Appendix B. Table 6.20 summarizes the measured rut depths at 5000 load repetitions for all mixtures. The total rut is broken down into compactive rutting and plastic rutting.

Figure 6.24 shows the rutting of all 27 mixtures that were tested in the APT. The number of passes are shown on the X-axis. The Y-axis represents the average rut depth of each test lane. As discussed in Chapter 2, significant rutting can cause safety problems. When rut depth is severe enough, cross drainage of surface water is a problem and water begins to pond in the wheel path, creating a potential for hydroplaning or an icing

condition in cold weather. A 0.5 inch rut depth is used as a limiting criterion by a number of agencies.

Table 6.21 shows the traffic levels at which the various mixtures satisfy the 0.5 inch rut criteria. Cells with an x indicate the mixture has a rut depth less than 0.5 inch. It is clear that the slag and limestone mixtures have low potential for rutting. Of the gravel mixtures, rich mixtures are prone to rutting while in most cases lean mixtures are more rut resistant.

Table 6.19 Results of Marshall Recompaction<sup>1</sup>

		Asphalt Content		Air Voids	
		Extracted <sup>2</sup>	Target <sup>3</sup>	Marshall	Test Section <sup>4</sup>
MD1	Lean	4.0%	4.2%	7.8%	9.2%
	Opt.	4.3%	4.7%	6.0%	8.9%
	Rich	4.9%	5.2%	4.2%	7.3%
MD2	Lean	3.7%	3.8%	7.9%	9.7%
	Opt.	4.3%	4.3%	6.9%	9.5%
	Rich	4.4%	4.8%	5.5%	10.0%
MD3	Lean	3.9%	4.0%	6.8%	9.9%
	Opt.	3.9%	4.5%	4.7%	9.1%
	Rich	4.5%	5.0%	3.4%	7.4%
MD4	Lean	3.4%	4.7%	8.7%	10.8%
	Opt.	5.0%	5.2%	6.8%	10.4%
	Rich	4.7%	5.7%	5.7%	8.5%
MD5	Lean	3.6%	4.0%	5.9%	8.7%
	Opt.	4.2%	4.5%	4.4%	7.2%
	Rich	4.6%	5.0%	1.5%	6.2%
MD6	Lean	4.2%	4.5%	5.4%	9.7%
	Opt.	4.7%	5.0%	4.5%	8.3%
	Rich	4.8%	5.5%	4.6%	9.1%
MD7	Lean	4.6%	4.9%	6.0%	10.5%
	Opt.	4.7%	5.4%	6.0%	9.9%
	Rich	5.5%	5.9%	1.9%	7.9%
MD8	Lean	5.3%	5.9%	7.8%	11.3%
	Opt.	5.8%	6.4%	8.1%	9.8%
	Rich	6.6%	6.9%	3.6%	9.8%
MD9	Lean	4.0%	4.3%	5.6%	9.2%
	Opt.	4.3%	4.8%	5.0%	8.5%
	Rich	4.5%	5.3%	3.6%	7.0%

Notes: 1 = 75 blow hand hammer Marshall compaction.

2 = From test sections.

3 = From laboratory mix design.

4 = From out-wheel-path specimens

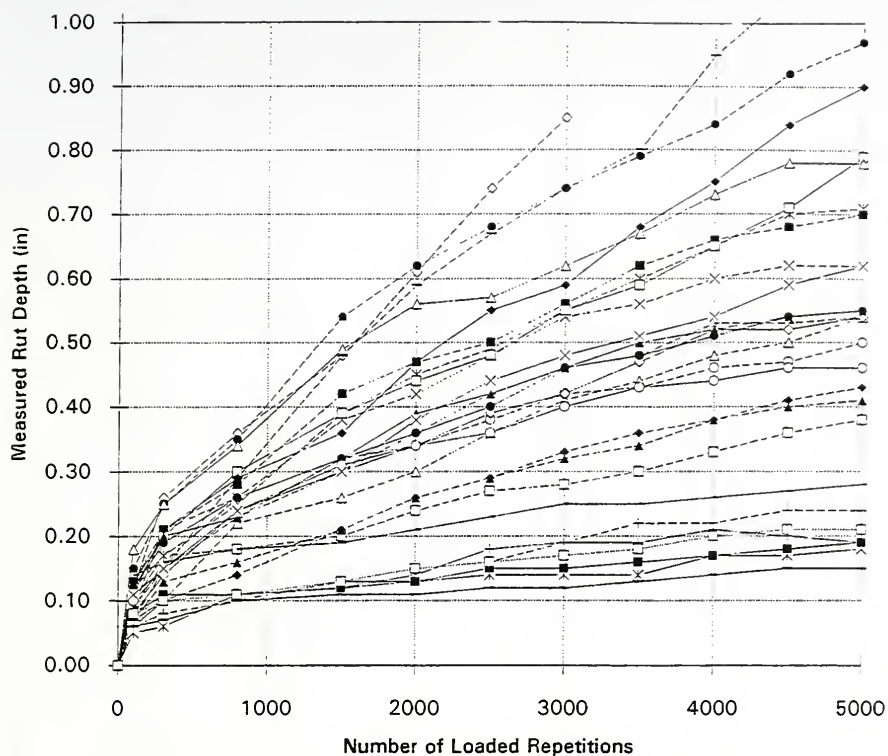


Table 6.20 Measured Rut Depth at 5000 Load Repetitions

		Extracted Asphalt Content	Plastic Rut Depth (in.)	Compactive Rut Depth (in.)	Total Rut Depth (in.)
MD1	Lean	4.0%	0.20	0.18	0.38
	Opt.	4.3%	0.21	0.22	0.43
	Rich	4.9%	—	—	—
MD2	Lean	3.7%	0.20	0.21	0.41
	Opt.	4.3%	0.32	0.22	0.54
	Rich	4.4%	0.48	0.49	0.97
MD3	Lean	3.9%	0.20	0.30	0.50
	Opt.	3.9%	0.34	0.28	0.62
	Rich	4.5%	0.38	0.33	0.71
MD4	Lean	3.4%	0.13	0.11	0.24
	Opt.	5.0%	0.75	0.44	1.19
	Rich	4.7%	0.33	0.21	0.54
MD5	Lean	3.6%	0.40	0.30	0.70
	Opt.	4.2%	0.45	0.34	0.79
	Rich	4.6%	0.54	0.36	0.90
MD6	Lean	4.2%	0.24	0.30	0.54
	Opt.	4.7%	0.31	0.24	0.55
	Rich	4.8%	0.43	0.35	0.78
MD7	Lean	4.6%	0.32	0.23	0.55
	Opt.	4.7%	0.24	0.22	0.46
	Rich	5.5%	0.35	0.27	0.62
MD8	Lean	5.3%	0.05	0.13	0.18
	Opt.	5.8%	0.04	0.15	0.19
	Rich	6.6%	0.11	0.17	0.28
MD9	Lean	4.0%	0.05	0.10	0.15
	Opt.	4.3%	0.08	0.11	0.19
	Rich	4.5%	0.10	0.11	0.21

Note: Data is not available for the cell with sign "—".





Note: L = Lean, O = Optimum, R = Rich.

Figure 6.24 Rut Development in the APT



Table 6.21 Acceptable Mixtures using 0.5 inch Rut Criteria

Number of Pass		1500	2000	2500	3000	3500	4000	4500	5000
Number of ESAL (10 <sup>6</sup> )		1.8	2.4	3	3.6	4.2	4.8	5.4	6
MD1	Lean	x	x	x	x	x	x	x	x
	Opt.	x	x	x	x	x	x	x	x
	Rich	x							
MD2	Lean	x	x	x	x	x	x	x	x
	Opt.	x	x	x	x	x	x		
	Rich								
MD3	Lean	x	x	x	x	x	x	x	
	Opt.	x	x	x					
	Rich	x	x	x					
MD4	Lean	x	x	x	x	x	x	x	x
	Opt.	x	x	x	x	x			
	Rich	x							
MD5	Lean	x	x						
	Opt.	x	x	x					
	Rich	x	x						
MD6	Lean	x	x	x	x	x			
	Opt.	x	x	x	x				
	Rich	x							
MD7	Lean	x	x	x	x	x			
	Opt.	x	x	x	x	x	x	x	x
	Rich	x	x	x	x				
MD8	Lean	x	x	x	x	x	x	x	x
	Opt.	x	x	x	x	x	x	x	x
	Rich	x	x	x	x	x	x	x	x
MD9	Lean	x	x	x	x	x	x	x	x
	Opt.	x	x	x	x	x	x	x	x
	Rich	x	x	x	x	x	x	x	x

Note: The cell with x indicates the mixture has rut depth less than 0.5 inch under an equivalent number of ESALs.

### 6.10 Statistical Analyses

Depth of rutting is related to loading conditions, environmental conditions and mixture properties. In the APT tests, loading and environmental conditions were constant. Therefore, a statistical analysis was performed using SAS software to determine the significant relationships between amount of rutting and mixture physical properties presented in previous sections.

In the statistical analyses, the dependent variable is taken as total rut depth (Y). The independent variables included in the analysis are aggregate type (AT), percent crushed coarse aggregate (CA), percent natural sand (NS), and relative asphalt content (AC). Relative asphalt content is calculated by subtracting the target optimum asphalt content from extracted asphalt content. Due to the incomplete experimental design for all combinations of factors investigated, the statistical analyses were performed among four sub-blocks of the experimental design that were complete for some combinations of the factors. Initially, quadratic terms were included in the analyses. It was found that these quadratic terms were not significant. Therefore, linear models were assumed in the subsequent analyses.

#### 6.10.1 40% Crushed Gravel Mixtures

Forty percent crushed gravel mixtures were analyzed with two independent variables, percent natural sand (NS) and relative asphalt content (AC). The following linear model was assumed in the analysis.

$$Y_{ij} = \mu + NS_i + AC_j + NS \times AC_{ij} + \varepsilon_{ij} \dots\dots\dots(6.6)$$

Where:

$Y_{ij}$  = response variable, total rut depth at 5000 load repetitions

- $\mu$  = overall mean  
 $NS_i$  = effect of percent natural sand  
 $AC_j$  = effect of relative asphalt content  
 $NS \times AC_{ij}$  = effect of main factor interaction  
 $\varepsilon_{ij}$  = experimental error  
 $i = 1, 2, 3; \quad j = 1, 2, 3$

Table 6.22 ANOVA Results for 40% Crushed Gravel Mixtures

Source of Variation	df	SS	MS	F	Pr>F
NS	1	0.105	0.105	2.226	0.1928
AC	1	0.308	0.308	6.64	0.0496
NS×AC	1	0.005	0.005	0.11	0.7521
Error	5	0.232	0.046		

An ANOVA was performed and the results are summarized in Table 6.22. The main effect, relative asphalt content, is significant. This suggests rut depth is significant for different asphalt contents. The main effect, percent natural sand, and interaction effect are not significant, which means that the rut depths are not significantly affected by percent natural sand in the 40% gravel mixtures.

A regression equation was developed for a relationship between rut depth and percent natural sand and asphalt content.

$$Y = 0.766 - 0.157NS + 0.52AC + 0.067NS \times AC \dots\dots\dots(6.7)$$

Note: NS is coded in the equation. 1=100%, 0 = 50%, and -1 = 0%

The coefficient of determination ( $R^2$ ) for this equation is 0.65 and the equation is statistically significant. It is noted that 0.5% increase in asphalt content of the 40% crushed gravel mixtures will result in about 0.25 inch increase in total rut depth.

Figure 6.25 is a response surface for relative asphalt content, percent natural sand and total rut depth along with a 0.5" rut contour line. As can be seen from this figure, the rut depth decreases when relative asphalt content decreases at any level of natural sand percentage. The effect of natural sand is not significant in this plot. It appears that rut depth decreases when percent natural sand increases at low relative asphalt content. This trend disappears at high relative asphalt content. As noted previously, mixture #4 was produced from a drum mix plant. Significant variability, particularly for low volumes of material, is associated with this type of plant. As a result, the effects of natural sand are not clear.

#### 6.10.2 70% Crushed Gravel Mixtures

A similar analysis was conducted for 70% crushed gravel mixtures. The two independent variables included in the analysis were the percent natural sand (NS) and relative asphalt content (AC). The following linear model was assumed in the analysis.

$$Y_{ij} = \mu + NS_i + AC_j + NS \times AC_{ij} + \varepsilon_{ij} \dots\dots\dots(6.8)$$

Where:

- $Y_{ij}$  = response variable, total rut depth at 5000 load repetitions
- $\mu$  = overall mean
- $NS_i$  = effect of percent natural sand.
- $AC_j$  = effect of relative asphalt content
- $NS \times AC_{ij}$  = effect of main factor interaction



## 40% Crushed Gravel

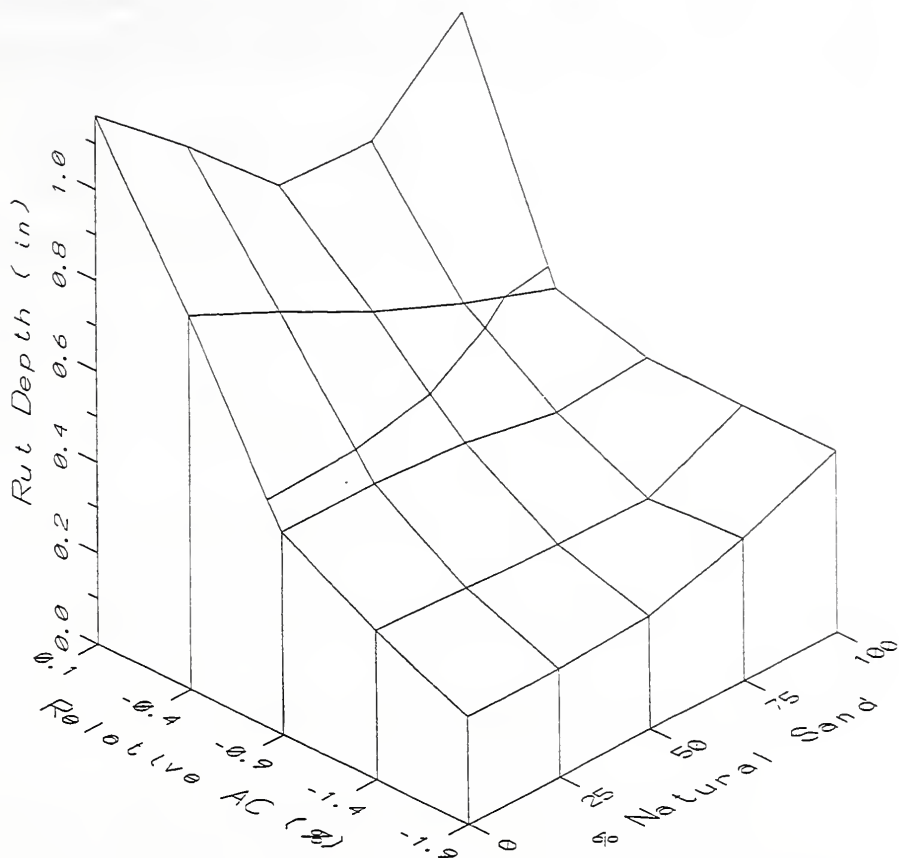


Figure 6.25 Response Surface of 40% Crushed Gravel Mixtures.

$$\varepsilon_{ij} = \text{experimental error}$$

$$i = 1, 2, 3 \quad j = 1, 2, 3$$

Table 6.23 ANOVA Results for 70% Crushed Gravel Mixtures

Source of Variation	df	SS	MS	F	Pr>F
NS	1	0.076	0.076	11.86	0.0184
AC	1	0.040	0.040	6.29	0.0539
NS×AC	1	0.002	0.002	0.27	0.6240
Error	5	0.032	0.002		

The ANOVA results are summarized in Table 6.23. Both main effects, percent natural sand and relative asphalt content, are significant. The significance of the main effects suggests that the rut depths are affected by percent natural sand and asphalt content in gravel mixtures designed with 70% crushed level.

A regression equation was developed and is briefly discussed below.

$$Y = 0.691 + 0.126NS + 0.170AC + 0.039NS \times AC \dots\dots\dots(6.9)$$

Note: NS is coded in the equation. 1=100%, 0 = 50%, and -1 = 0%

The coefficient of determination ( $R^2$ ) for this equation is 0.81 and the equation is statistically significant. It is noted that 0.5% increase in asphalt content will result in about 0.09 inch increase in total rut depth. Compared with the corresponding 0.25 inch increase for 40% crushed gravel mixtures, it is concluded that the rutting is more sensitive to asphalt content in 40% crushed gravel mixtures than in 70% crushed gravel mixtures. It is

also noted that 50% increase in natural sand will result in about 0.13 inch increase in total rut depth of the 70% crushed gravel mixtures.

Figure 6.26 is a response surface plot of percent natural sand, asphalt content, and total rut depth along with 0.5" and 0.6" rut contours. As can be seen, in general, rut depth increases with increase of percent natural sand and relative asphalt content.

### 6.10.3 100% Natural Sand Gravel Mixtures

An analysis was made for 100% natural sand gravel mixtures, Two independent variables were included in the analysis, percent crushed coarse aggregate (CA) and relative asphalt content (AC). The following linear model was assumed in the analysis.

$$Y_{ij} = \mu + CA_i + AC_j + CA \times AC_{ij} + \varepsilon_{ij} \dots\dots\dots(6.10)$$

Where:

$Y_{ij}$  = response variable, total rut depth at 5000 load repetitions

$\mu$  = overall mean

$CA_i$  = effect of percent crushed coarse aggregate

$AC_j$  = effect of relative asphalt content

$CA \times AC_{ij}$  = effect of main factor interaction

$\varepsilon_{ij}$  = experimental error

$i = 1,2,3$        $j = 1,2,3$

## 70% Crushed Gravel

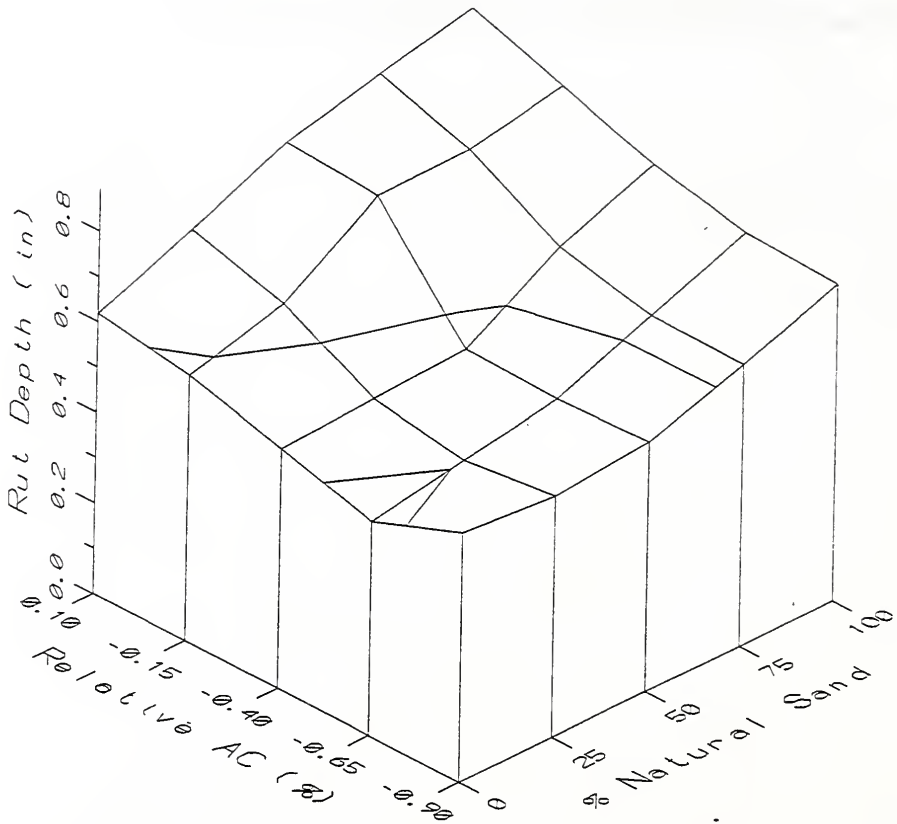


Figure 6.26 Response Surface of 70% Crushed Gravel Mixtures.

An ANOVA was performed and the results are summarized in Table 6.24. The main effects, percent crushed coarse aggregate and relative asphalt content, are not significant. This means that the rut depths are not significantly affected by percent crushed coarse aggregate and asphalt content in gravel mixtures designed with 100% natural sand.

Table 6.24 ANOVA Results for 100% Natural Sand Gravel Mixtures

Source of Variation	df	SS	MS	F	Pr>F
CA	1	0.0142	0.0142	0.26	0.6385
AC	1	0.0084	0.0084	0.15	0.7155
CA×AC	1	0.0004	0.0004	0.01	0.9331
Error	4	0.2197	0.0551		

#### 6.10.4 95% Crushed Gravel, Slag, and Limestone Mixtures

For 95% crushed gravel, slag, and limestone mixtures, two independent variables were included in the ANOVA analysis, aggregate type (AT) and relative asphalt content (AC). The following linear model was assumed in the analysis of rut depth.

$$Y_{ij} = \mu + AT_i + AC_j + AT \times AC_{ij} + \epsilon_{ij} \dots \dots \dots (6.11)$$

Where:

$Y_{ij}$  = response variable, total rut depth at 5000 load repetitions

$\mu$  = overall mean

$AT_i$  = effect of aggregate type.

$AC_j$  = effect of relative asphalt content

$AT \times AC_{ij}$  = effect of main factor interaction

$\epsilon_{ij}$  = experimental error

$i = 1, 2, 3$        $j = 1, 2, 3$

Results of the ANOVA are summarized in Table 6.25. The main effects, aggregate type and relative asphalt content, are significant. The significance of main effects means that the rut depth is significantly affected by aggregate type and asphalt content. The effect of interaction is not significant.

Table 6.25 ANOVA Results for 95% Crushed Gravel, Slag, and Limestone Mixtures

Source of Variation	df	SS	MS	F	Pr>F
AT	2	0.0214	0.0107	31.37	0.0309
AC	1	0.0045	0.0045	13.08	0.0687
AT×AC	2	0.0005	0.0002	0.69	0.5912
Error	2	0.0007	0.0003		

Figures 27 through 31 show the total rut depths for all mixtures at 800, 2000, 3500, and 5000 load repetitions respectively. It is clear that rutting of slag and limestone mixtures is much less than all gravel mixtures. The slag and limestone mixtures are also much less sensitive to asphalt content variation.

### 6.11 WTD Test Results

All gravel mixtures, MD-1 through MD-7, and the limestone mixture, MD-9, were tested in the WTD. The mixture numbering system relative to the percentage of coarse crushed aggregate and sands is given in Table 5.1. Stockpile characteristics and percentages are given in Table 5.4. Details and a summary of the Marshall mix designs are in Appendix A and Table 6.1, respectively. As previously described INDOT criteria was applied in conducting the Marshall mix designs. The viscosity-temperature chart for the AC-20 asphalt used in the mixtures is shown in Figure 5.2.

Slabs tested in the WTD were 12 in wide, 24 in long and 3 in thick. The bulk specific gravity, maximum specific gravity and air voids for all slabs are given in Table

6.26. Results for the WTD tests are summarized in Table 6.27. Three dimensional plots for the WTD creep slope and number of passes to stripping inflection point Vs percent crushed aggregate and percent natural sand are shown in Figures 6.32 and 6.33, respectively.

#### 6.12 Additional APT Tests

Two gravel mixtures, MD-4 and MD-7, were retested in the APT. These mixtures were selected for retesting after evaluation of the original APT tests and subsequent WTD tests. An additional, larger quantity of each aggregate stockpile was provided by participating members of the Indiana Mineral Aggregates Association. The additional aggregate was provided to enhance the plant calibration.

Test section mixture target and actual asphalt contents and gradations are given in Tables 6.28 and 6.29, respectively. The gradations are plotted in Figures 6.34 and 6.35. As constructed maximum and bulk specific gravities and air voids are given in Tables 6.30 and 6.31, respectively. Rutting Vs. asphalt content for 5000 passes is shown in Figure 6.36. The individual modes of rutting and the combined “stringline” rutting are given in both tabular and plotted form in Appendix C.

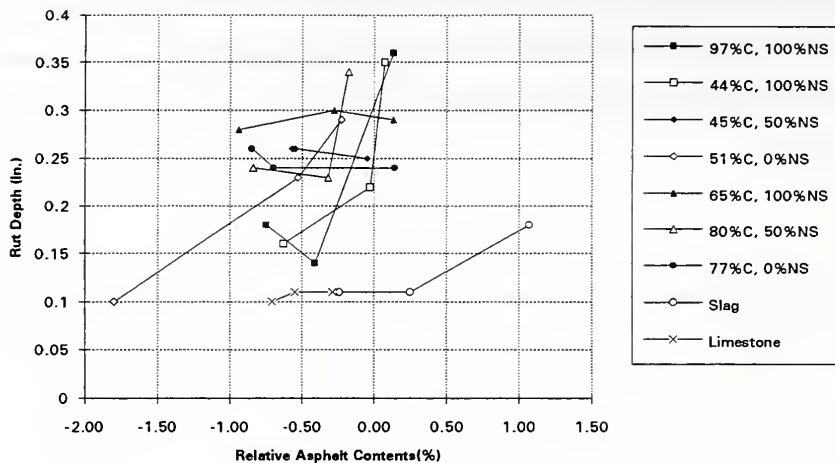


Figure 6.27 Rut Depth vs. Relative Asphalt Contents (@800 Loading Cycles)

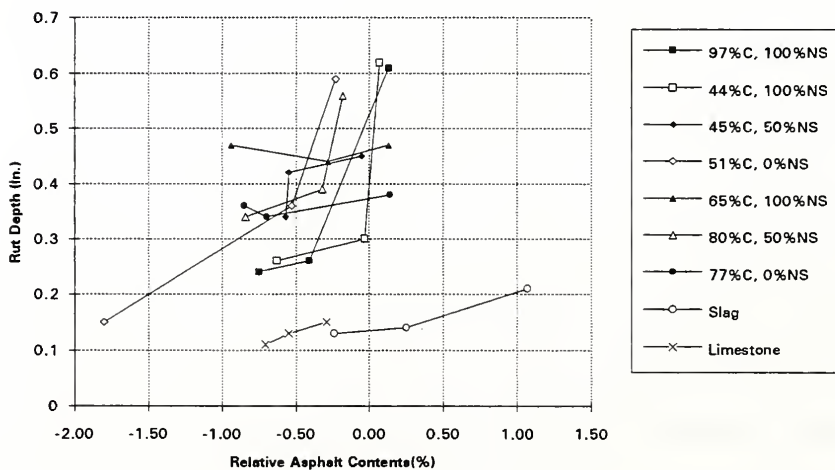


Figure 6.28 Rut Depth vs. Relative Asphalt Contents (@2000 Loading Cycles)



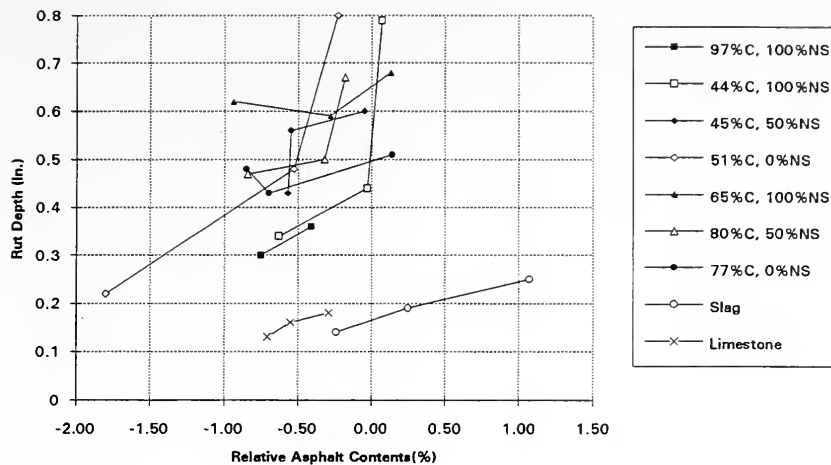


Figure 6.29 Rut Depth vs. Relative Asphalt Contents (@3500 Loading Cycles)

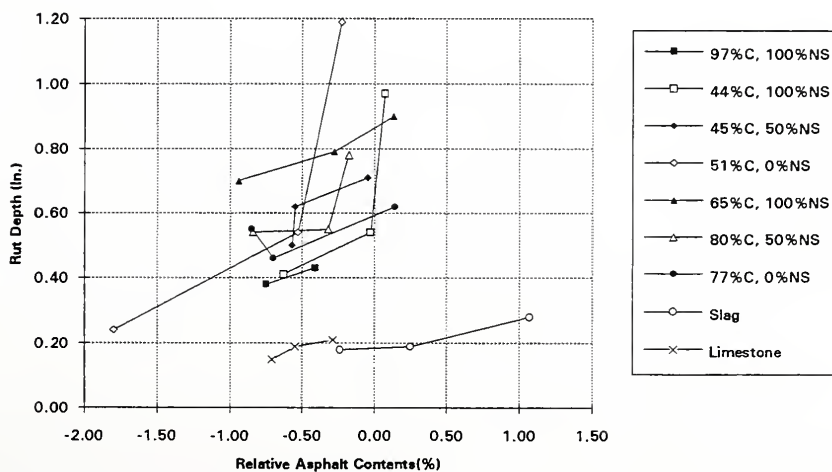


Figure 6.30 Rut Depth vs. Relative Asphalt Contents (@5000 Loading Cycles)



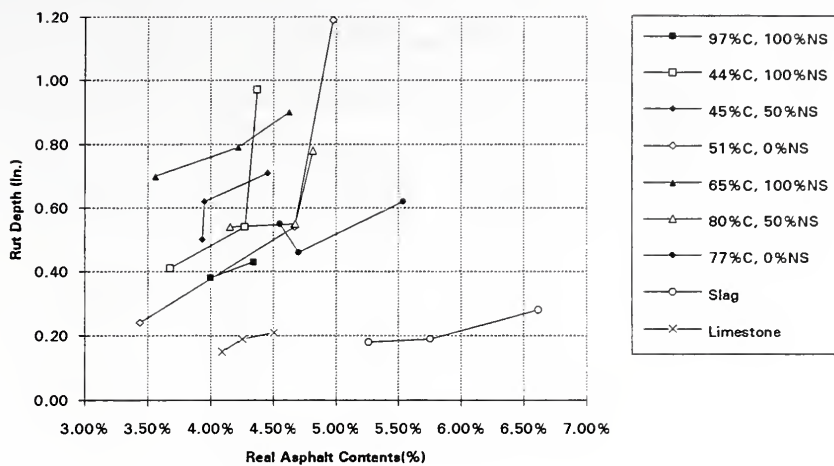


Figure 6.31 Rut Depth vs. Real Extracted Asphalt Contents (@5000 Loading Cycles)



Table 6.26 Summary of WTD Sample Physical Properties

Mix	Asphalt Content	BSG (pcf)	MSG (pcf)	Air Voids (%)
	Lean	139.80	155.02	9.82
MD1	Opt.	145.05	156.66	7.41
	Rich	145.24	158.39	8.30
	Lean	147.91	153.74	3.79
MD2	Opt.	146.26	155.63	6.02
	Rich	146.00	156.43	6.67
	Lean	144.46	157.59	8.33
MD3	Opt.	149.16	157.22	5.13
	Rich	146.79	156.49	6.20
	Lean	144.92	156.07	7.15
MD4	Opt.	144.00	156.41	7.94
	Rich	146.79	156.57	6.24
	Lean	146.79	156.35	6.11
MD5	Opt.	144.62	157.86	8.39
	Rich	144.74	157.77	8.26
	Lean	144.58	156.52	7.63
MD6	Opt.	145.45	156.36	6.98
	Rich	146.89	156.69	6.25
	Lean	143.16	154.93	7.60
MD7	Opt.	143.16	154.93	7.60
	Rich	143.16	154.93	7.60
	Lean	142.87	160.61	11.05
MD9	Opt.	144.60	160.78	10.06
	Rich	146.61	161.36	9.14



Table 6.27 Summary of WTD Tests

Mix	Asphalt Content	Creep Slope	No. of Passes to Stripping Inflection Points	Rut Depth at Stripping Inflection Points
	Lean	0.0044	2201	12.21
MD1	Opt.	0.0015	10264	18.31
	Rich	0.0017	7062	12.57
	Lean	0.0033	2399	10.21
MD2	Opt.	0.0024	2498	8.92
	Rich	0.0028	3891	9.60
	Lean	0.0012	5072	7.24
MD3	Opt.	0.0058	2481	17.33
	Rich	0.0011	10164	14.39
	Lean	0.0032	2586	10.03
MD4	Opt.	0.0018	1776	4.39
	Rich	0.0017	5394	13.09
	Lean	0.0010	3969	4.54
MD5	Opt.	0.0050	993	5.43
	Rich	0.0010	9495	10.98
	Lean	0.0008	14067	12.24
MD6	Opt.	0.0008	3932	6.05
	Rich	0.0009	10229	12.83
	Lean	0.0009	10818	13.14
MD7	Opt.	0.0017	6374	12.64
	Rich	0.0015	7474	13.38
	Lean	0.0012	13812	17.75
MD9	Opt.	0.0006	18615	14.54
	Rich	0.0005	16542	9.28





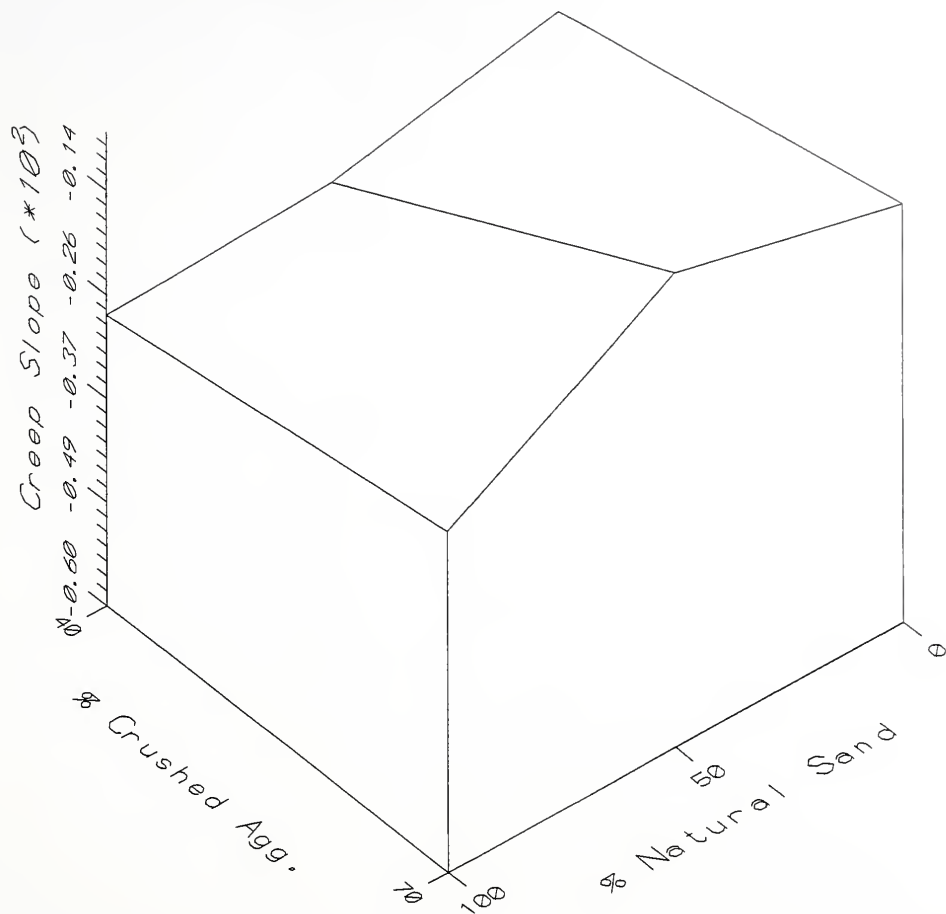


Figure 6.32 WTD Creep Slope vs. Percent Coarse Crushed Aggregate and Percent Natural Sand



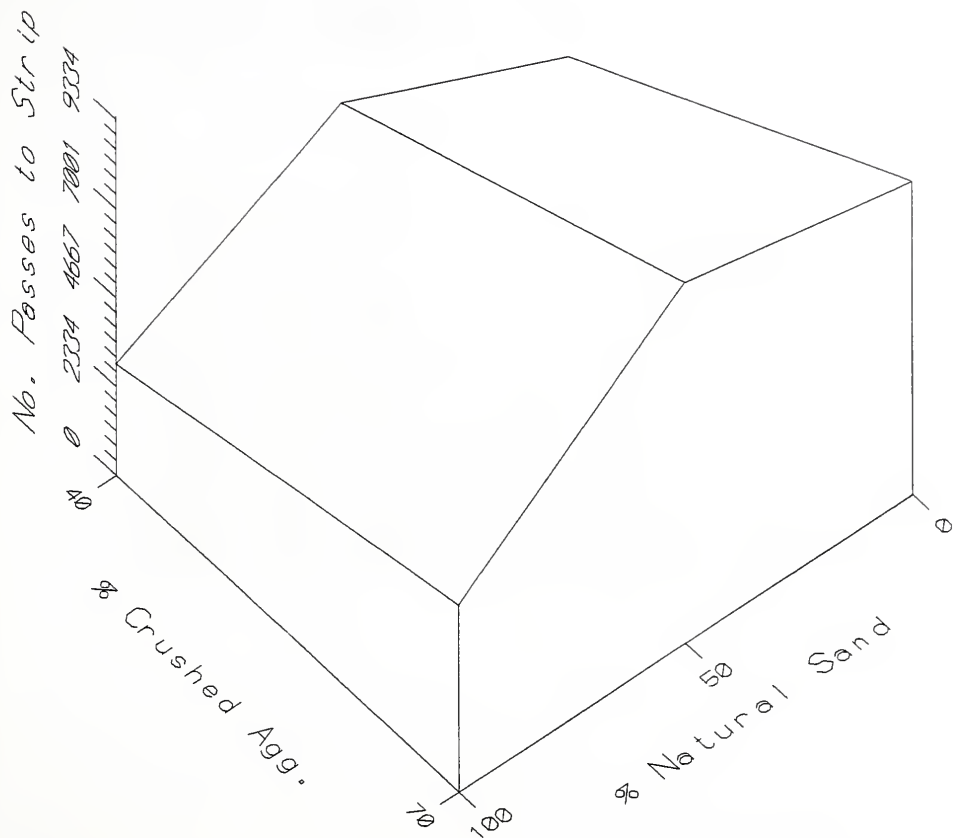


Figure 6.33 WTD Number of Passes to Stripping Inflection Point vs. Percent Coarse Crushed Aggregate and Percent Natural Sand



Table 6.28 Repeated APT Test Section Extracted Asphalt Content

Mix	Asphalt Content	Average Extracted	Target
MD4	Lean	4.2%	4.3%
	Optimum	5.0%	4.8%
	Rich	5.6%	5.3%
MD7	Lean	3.6%	4.4%
	Optimum	5.5%	4.9%
	Rich	4.5%	5.4%

Table 6.29 Repeated APT Test Section Graditions

Sieve Size	MD4			MD7		
	Lean	Opti.	Rich	Lean	Opti.	Rich
1"	100.0%	100.0%	100.0%	100.0%	100.0%	100.0%
3/4"	98.6%	97.6%	96.8%	96.7%	95.3%	97.0%
1/2"	83.1%	78.6%	78.7%	82.6%	73.9%	76.0%
3/8"	71.7%	67.8%	66.0%	72.5%	61.5%	61.2%
#4	43.0%	40.0%	40.2%	42.5%	31.4%	29.7%
#8	23.0%	23.0%	21.7%	27.7%	20.4%	19.9%
#16	13.4%	14.7%	13.3%	17.8%	14.1%	13.5%
#30	9.3%	10.6%	9.0%	12.4%	10.0%	9.5%
#50	6.6%	7.1%	5.6%	8.4%	7.2%	6.5%
#100	4.3%	4.4%	3.2%	5.3%	4.9%	4.0%
#200	2.4%	2.6%	2.0%	3.0%	3.2%	2.4%



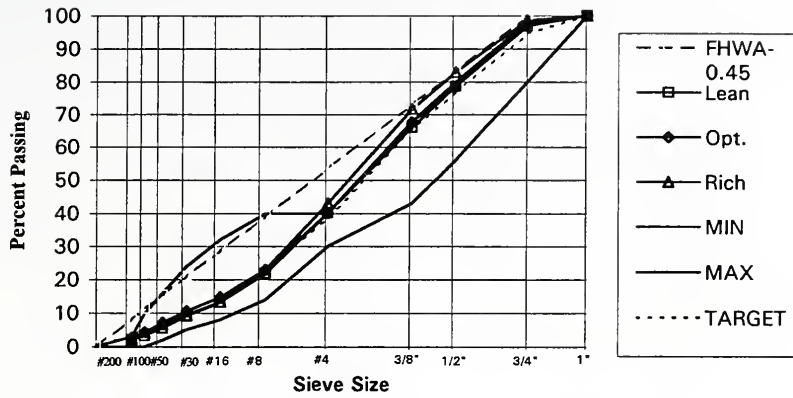


Figure 6.34 Gradation Curves for Repeated Mix #4

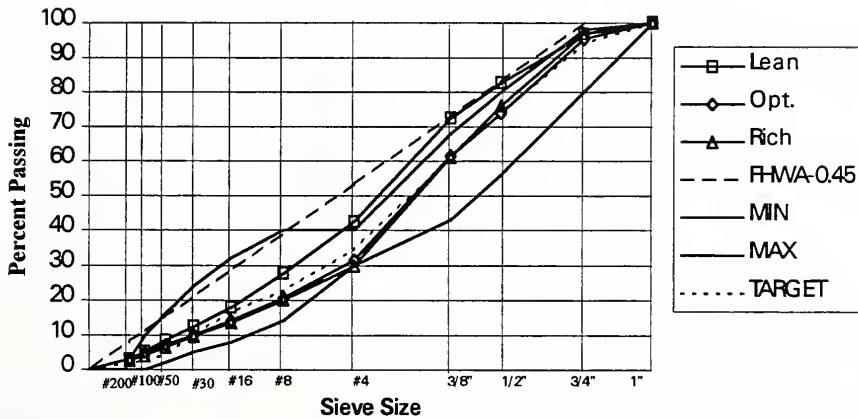


Figure 6.35 Gradation Curves for Repeated Mix #7





Table 6.30 Repeated APT Test Section BSG

Mix	Asphalt	MSG	In Wheel Path	Out of Wheel Path
MD4	Lean	2.517	2.276	2.294
	Optimum	2.492	2.290	2.277
	Rich	2.487	2.226	2.243
MD7	Lean	2.546	2.326	2.305
	Optimum	2.522	2.299	2.262
	Rich	2.516	2.333	2.274

Table 6.31 Repeated APT Test Section Air Voids

Mix	Asphalt Content	In Wheel Path	Out of Wheel Path
MD4	Lean	9.6	8.9
	Optimum	8.1	8.6
	Rich	10.5	9.8
MD7	Lean	8.6	9.5
	Optimum	8.8	10.3
	Rich	7.3	9.6



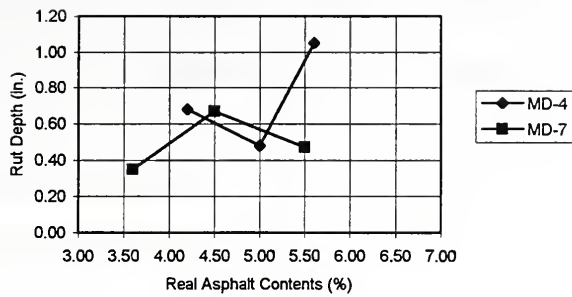


Figure 6.36 Rut Depth vs. Real Extracted Asphalt Contents (@5000 Loading Cycles)



### 6.13 Summary

Data collected from the APT provides significant information on rutting potential of asphalt mixtures with varying percent coarse crushed aggregate, percent natural sand, and asphalt content. Supporting laboratory tests were presented to provide background on the mixtures that were tested. Mixture properties included results of Marshall mix design, air voids, extracted asphalt content, penetration and viscosity of extracted asphalt, gradation of aggregates, percentage of crushed faces and flat & elongated particles, Gyratory stability index, and Gyratory shear strength.

Statistical analysis was performed to correlated actual rut depths to measurements of mixture physical properties. The dependent variable is total rut depth (Y) at 5000 load repetitions. The independent variables included in the analysis were aggregate type (AT), percent crushed coarse aggregate (CA), percent natural sand (NS), and relative asphalt content (AC). Relative asphalt content was used in the analysis to minimize the effect of variation of optimum asphalt content from mixture to mixture.

Results of Marshall mix design show that an optimum asphalt content increases with increase of crushed level and decrease of natural sand. Marshall stability increases with increase of crushed percent in 100% natural sand gravel mixtures. The Marshall stability of 40% crushed gravel mixtures is below INDOT's minimum stability requirement. Effects of percent natural sand on Marshall stability are not consistent at the different levels of crushed gravel.

Air voids analysis of the pavement test sections shows that the air voids are significantly different at three different locations on a test lane. The air voids between the wheel path are the highest and air voids in the wheel path are the lowest. The overall average difference of air voids in and out of the wheel paths is 1.0%. This difference corresponds to 0.03 in. of densification for a 3 in. asphalt overlay.

The increase or decrease of penetration and viscosity, respectively, of extracted asphalt are significant. The percent retained penetration ranged from 33.8% to 54.9% with an average of 44.1%. The viscosity ratios ranged from 1.47 to 2.17 with an average of 1.78. There is an increase of the viscosity ratio with increase of air voids in mixtures.

Aggregate type is significant. Slag and limestone mixtures have much lower rutting potential than gravel mixtures. For 100 percent natural sand, percent crushed coarse aggregate in gravel mixtures was not significant, i.e., the data does not show an obvious trend of rut depth with crushed levels.

Percent natural sand was not significant in the 40% crushed gravel mixtures but was significant in the 70% crushed gravel mixtures. It is also noted that a 50% increase in natural sand will result in about 0.13 inch increase in total rut depth of the 70% crushed gravel mixtures.

Relative asphalt content is significant. It is noted that 0.5% increase in asphalt content will result in about 0.25 inch increase in total rut depth of 40% crushed gravel mixtures and about 0.09 inch increase in total rut depth of 70% crushed gravel mixtures. Forty percent crushed gravel mixtures are more sensitive to asphalt content than 70%

crushed gravel mixtures. The slag and limestone mixtures also are much less sensitive to asphalt content variation.





## CHAPTER 7

### FINITE ELEMENT ANALYSIS

Finite element analysis is a numerical procedure that can be applied effectively to analysis of many physical and mathematical phenomena. Engineering applications of the finite element method include the study and analysis of solid mechanics, fluid mechanics, heat transfer, ground water seepage, and many other areas.

A typical finite element analysis involves mesh generation, material property definition, load simulation, and computation and solution. The geometric model consists of discrete elements that are connected at their common nodes. These elements are shaped and sized to reasonably represent the physical problem's geometry. The connected nodes form a mesh within the boundaries of that geometry. A set of material properties is associated with the elements. Also, there are constraints, such as boundary conditions, that must be included in the model. Environmental properties and initial conditions may also be required. A load model includes definition of load type, magnitude, position and direction, depending on the finite element model capabilities. According to material and load types, an appropriate analysis procedure should be selected, such as static or dynamic analysis procedures.

In this research the finite element program, ABAQUS [ABAQUS, 1994], was selected to study asphalt pavement rutting resulting from accelerated pavement tests. ABAQUS is a general purpose finite element program that has been used to analyze many civil engineering structural and soil mass problems.

Input requirements for ABAQUS include model data that defines nodes, elements, element properties, material definitions and so on. History data is also required that defines what happens to the model, such as the sequence of loading for which the model's response is sought.

In this chapter, the application of ABAQUS to analysis of asphalt pavement rutting is presented. Sensitivity of model parameters will be discussed. Back-calculation of model parameters related to APT rutting phenomenon will be conducted. Also regression analyses were conducted to investigate the relationship between backcalculated model parameters and asphalt mixture physical properties.

### 7.1 Features of the Finite Element Model

In finite element analysis, the structure and other auxiliary conditions have to be correctly modeled to obtain reasonable response results

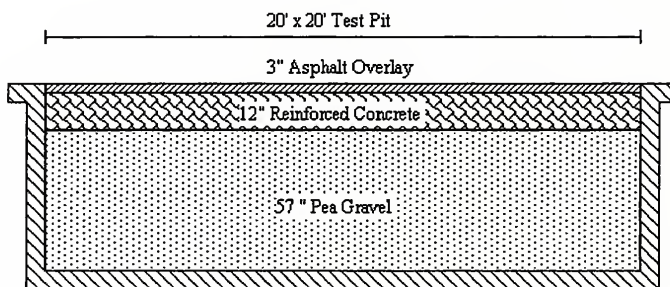


Figure 7.1 Cross Section of APT Test Pit

In the analysis of the APT tests a three-dimensional finite element mesh was created to represent the 3 in. asphalt overlay mixtures of a rigid base. The basic APT test pit cross section of is shown in Figure 7.1. The test pit is 20 ft. wide by 20 ft. long by 72 in. deep. The pavement section built in the test pit include 57 inches of pea gravel, 12 inches of reinforced concrete slab and a 3 in. asphalt overlay. Traffic applied to the test sections resulted in both densification and plastic flow of the asphalt overlay. No permanent deformation occurred in the 12" concrete slab or 57" pea gravel layer.

#### 7.1.1 Material Models

Asphalt concrete is a time, temperature, and stress dependent material. Perl, et al [1983] showed that an asphalt mixture subjected to repeated loading exhibits elastic, plastic, visco-elastic, and viscoplastic responses. The elastic properties do not contribute to permanent deformation and are therefore modeled by modulus of elasticity and Poisson's Ratio. Plastic properties contribute to permanent deformation which is cumulative under repeated loading. A creep model was used to characterize the permanent deformation properties of the asphalt mixtures. The constitutive equations for the creep model in ABAQUS are:

$$\dot{\epsilon} = A \sigma^n t^m \dots\dots\dots(7.1)$$

Where:

$\dot{\epsilon}$  = creep strain rate

$\sigma$  = the uniaxial equivalent deviatoric stress

$t$  = the total time

$A, m, n$  = parameters related to material properties

The above function is defined as a power law equation and its use assumes that viscoplastic strain is the sole contributor to permanent deformation. An instantaneous plastic strain is neglected in this model. Creep test results conducted by Lai, et al [1973] and Perl, et al [1983] resulted in the following creep models:

$$(1) \text{ Lai: } \dot{\epsilon}_p = (0.7580\sigma - 0.004078\sigma^2) \times 10^{-5} t^{-0.75} \dots\dots\dots(7.2)$$

$$(2) \text{ Perl: } \dot{\epsilon}_p = (0.2882\sigma - 0.000879\sigma^2) \times 10^{-5} t^{-0.78} \dots\dots\dots(7.3)$$

They regressed polynomial functions of stress in their analysis. Since a stress power law is used in ABAQUS to define the creep model, regression analyses were used to convert the polynomial functions of stress to the stress power law form. The corresponding creep models in the stress power law form are listed below for Lai and Perl's models respectively.

$$(1) \text{ Lai: } \dot{\epsilon}_p = 1.03 \times 10^{-5} \sigma^{0.8477} t^{-0.75} \dots\dots\dots(7.4)$$

$$(1) \text{ Perl: } \dot{\epsilon}_p = 0.47116 \times 10^{-5} \sigma^{0.8159} t^{-0.78} \dots\dots\dots(7.5)$$

Figure 7.2 shows the fitted power law curves along with the data points from the original polynomial functions. It is noted that the stress at which the creep test was conducted ranges from 10 psi to 50 psi in Lai's experiment and from 14.5 psi to 116 psi in Perl's experiment. Tire pressure during the APT tests was 90 psi. This applied stress is with the range of tests conducted by Perl. Therefore, the stress function based on Perl's equation was considered more appropriate for this study.

### 7.1.2 Boundary conditions

Boundary conditions have a significant influence on model predicted response. There are two potential boundary conditions for the asphalt overlay that need to be considered.

(1) Bottom of the asphalt layer. An asphalt tack coat was applied on the rough concrete surface before the asphalt overlay was constructed. This tack coat provided substantial bonding effect. The bonding made it difficult to remove cores that were cut after completion of traffic tests. Therefore, the contact between the bottom of asphalt layer and the concrete surface was modeled as a bonded contact. As a result, translations

of the nodes on the bottom of the asphalt layer are constrained, i.e., they remain bonded to the concrete surface, being unable to separate from or slide along the surface.

(2) Edges of the asphalt layer. The asphalt overlay edges are surrounded by asphalt mixture. Expansion of the asphalt overlay under repeated load would create a passive pressure between the edges and adjacent mixture. An elastic foundation was used to model the horizontal passive pressure.

### 7.1.3 Element Types

An available element library is listed in the ABAQUS user's manual [ABAQUS, 1994]. In this analysis, pavement structures were modeled using first-order three-dimensional stress-displacement elements (8 node brick) designated as C3D8 in ABAQUS.

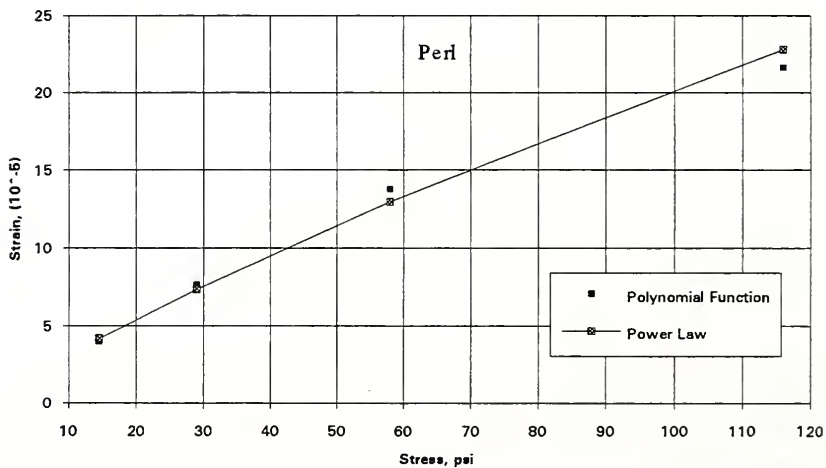
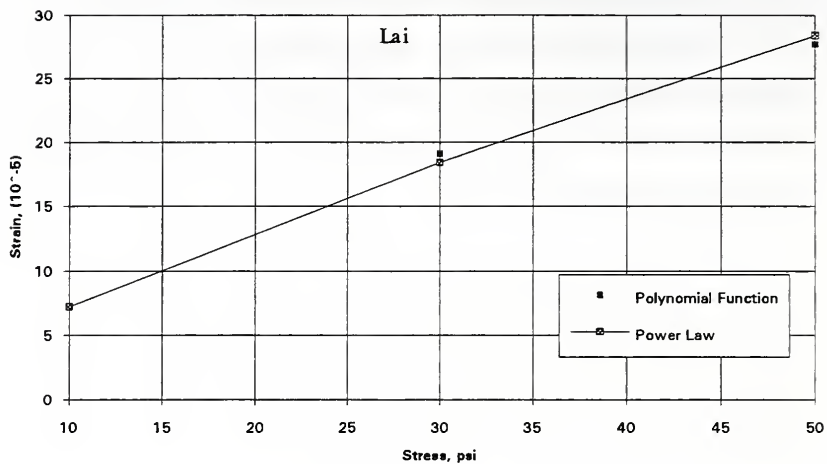


Figure 7.2 Fitted Curves of Material Models

#### 7.1.4 Load Models

The test sections were subjected to a 9000 lb. force on a dual wheel truck tire assemble which was moved across the test sections at 5 mph. An actual tire print is shown in Figure 5.3. The contact areas were modeled as two rectangle areas shown in Figure 7.3. Width of the contact area was taken to be equal to the measured tire width, 7.8 inches. Length of the contact area was determined to be 6.4 inches based on a contact area of 50 square inches. The 50 square inch area was obtained by dividing a single wheel load of 4500 lb by the 90 psi tire pressure.

Initially, a step load function was used in the analysis to simulate the moving wheel load. The duration of the step load function was 0.0727 second which corresponds to a speed of 5 mph in the APT. The step load function was applied at the beginning of the mesh and moved to the next set of elements in the wheel path. When the loaded area reached the edge of the mesh, a single load pass was completed and the loaded area was started from the beginning point again and so on. This sequence simulated the one way APT traffic. However, this load analysis required significant computer running time because approximately 20 hours were needed to apply 20 load applications. Approximately 200 days would be needed to run a complete simulation of 5000 load applications.

As a result of the extended running time, a technique was used to approximate the loading. The approximation involved applying the load to a single set of elements in the middle of the sections with a single step function. The total loading time in the single step was taken to be 364 seconds which is equal to the total cumulative loading time for 5000 load applications at 5 mph. This approximation is reasonable for the calculation of permanent deformation[Huang,1993].

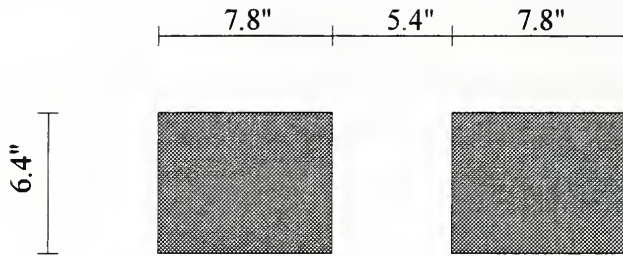


Figure 7.3 Modeled Contact Areas

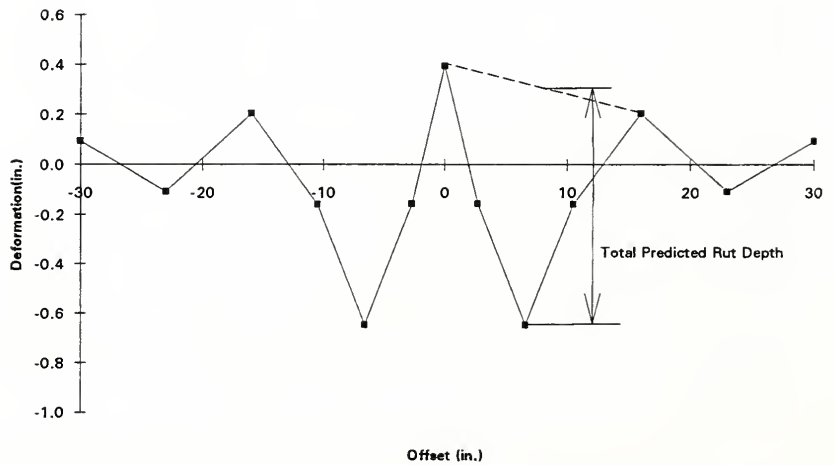


Figure 7.4 Deformed Cross Section from ABAQUS



### 7.1.5 Model Responses

In this analysis the response predicted by ABAQUS is rut depth. Figure 7.4 shows a transverse profile predicted by ABAQUS and the total rut depth previously defined for rutting in APT tests. The pattern of predicted rutting is similar to the measured rutting which consisted of longitudinal depressions in the wheel paths accompanied by upheavals to the sides.

### 7.1.6 Model Geometry

As previously discussed, the pavement structures in the test pit were modeled as asphalt overlays of a rigid surface. In the finite element analysis a finite element mesh had to be created to represent the overlay continuum. Four factors control the finite element mesh geometry:

1. Pavement geometry, which control the general size of the mesh.
2. Load configuration, such as dimensions and spacing of contact areas.
3. Degree of detail, i.e., locations where response parameters will be predicted.
4. Desired accuracy

In general, mesh dimensions have to be small enough to allow detailed analysis of the pavement section. However, small mesh dimensions increase the number of elements and cause an increase of memory and computational time. On the other hand, a coarse mesh will not allow detailed analysis. A compromise is to use a fine mesh where a detailed analysis is desired and a coarse mesh elsewhere

The five foot APT test lane was modeled full width. Mesh dimensions in the vertical direction were selected to match the asphalt layer thickness. The length and number of layers in a model have significant effect on predicted rut depth. Therefore, a sensitivity study was conducted varying the length and number of layers. This approach was used to identify the minimum length and number of layers for the model so that predicted response would not be affected by the model geometry.

The following properties were assumed in the model sensitivity studies:

(1) Elastic properties:

$$\text{Modulus of Elasticity} = 450,000 \text{ psi}$$

$$\text{Poisson's Ratio} = 0.3$$

(2) Creep model parameters

$$A = 4.0 \times 10^{-5}$$

$$n = 0.8$$

$$m = -0.75$$

The assumed modulus of elasticity was obtained from results of tests conducted by Huang and White (1994). Complex modulus tests in their study were conducted at 1, 4, and 8 Hz frequencies and at temperature of 20, 30, and 40°C respectively. It was decided to use the modulus of elasticity determined at 8 Hz and 40°C since such testing conditions were very close to the 5 mph speed and 38°C temperature during the APT traffic.

Parameters for the creep model were assumed based on the discussion in section 7.1.1, recognizing that different mixtures and testing temperature were used in the APT in comparison with those in Lai's and Perl's experiment. Use of these values for the creep model parameters resulted in prediction of one-half inch of total rutting which is about the average total rut depth developed in the APT tests.

An evaluation of section length was conducted first. The length was evaluated over a range of from 19.2 inches to 83.2 inches. Figure 7.5 shows the effect of length on predicted rut depth. It was found that the predicted rut depth approaches an asymptotic value as the length is increased. For models with length more than 44.8 inches, no significant change in predicted rut depth was found. As a result, a length of 57.6 inches was used for subsequent analysis.

After selecting the length, an evaluation was conducted to investigate the effects of number of layers on predicted rut depth. With other conditions being the same, analyses

were made varying the number of layers from 1 to 6 in modeling the 3" asphalt overlay. Figure 7.6 shows the effects of number of layers on the total predicted rut depth. The predicted rut depth approached an asymptotic value with increasing number of layers. There was no significant change in total rut depth for models with three or more layers. As a result, three layers were selected to model the 3" asphalt overlay.

Figure 7.7 shows the mesh plan view with dimensions. Figure 7.8 shows the mesh cross section view with boundary conditions. The view of the three dimensional mesh used in subsequent analyses is shown in Figure 7.9. The finite element mesh includes 162 elements with 280 nodes.

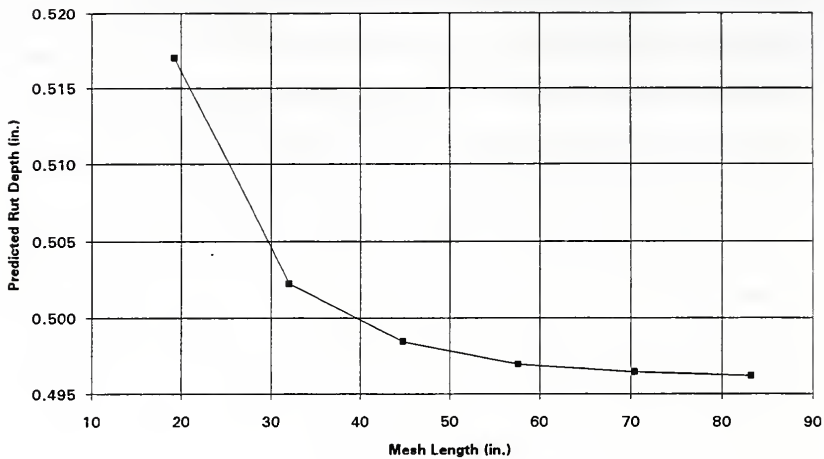


Figure 7.5 Effects of Mesh Length on Predicted Rut Depth.

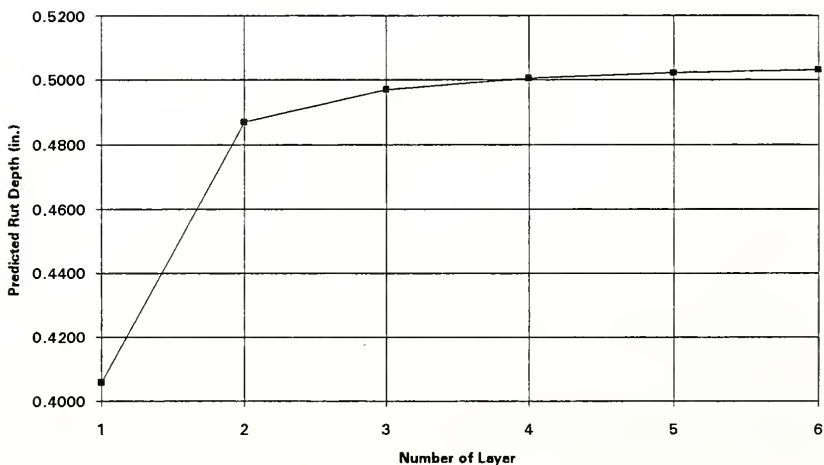


Figure 7.6 Effects of Layer Number on Predicted Rut Depth.

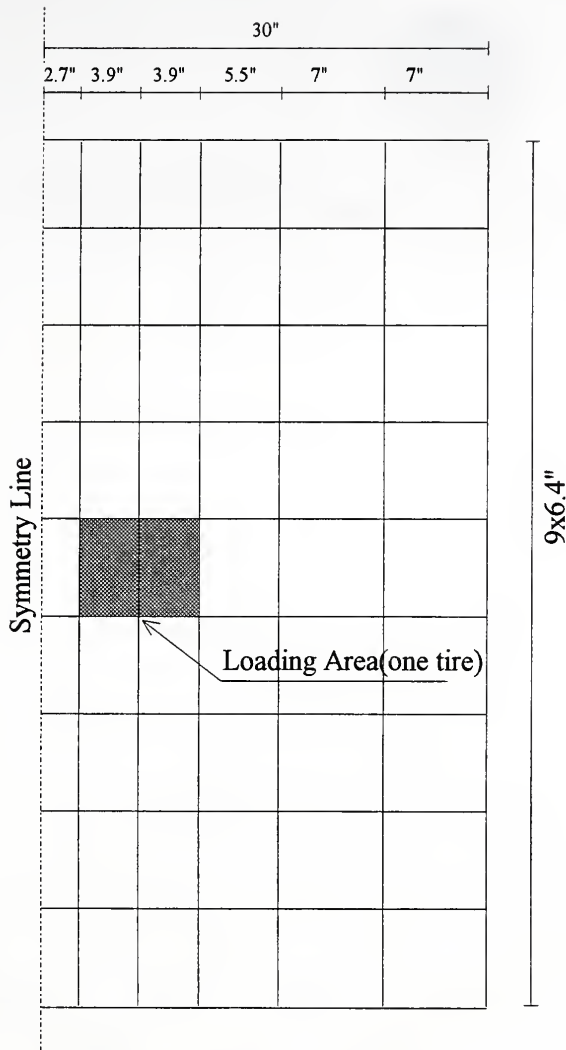


Figure 7.7 Plan View of Finite Element Mesh.



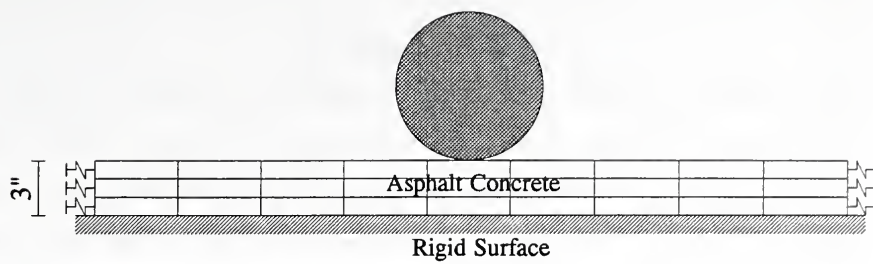


Figure 7.8 Side View of Finite Element Mesh.

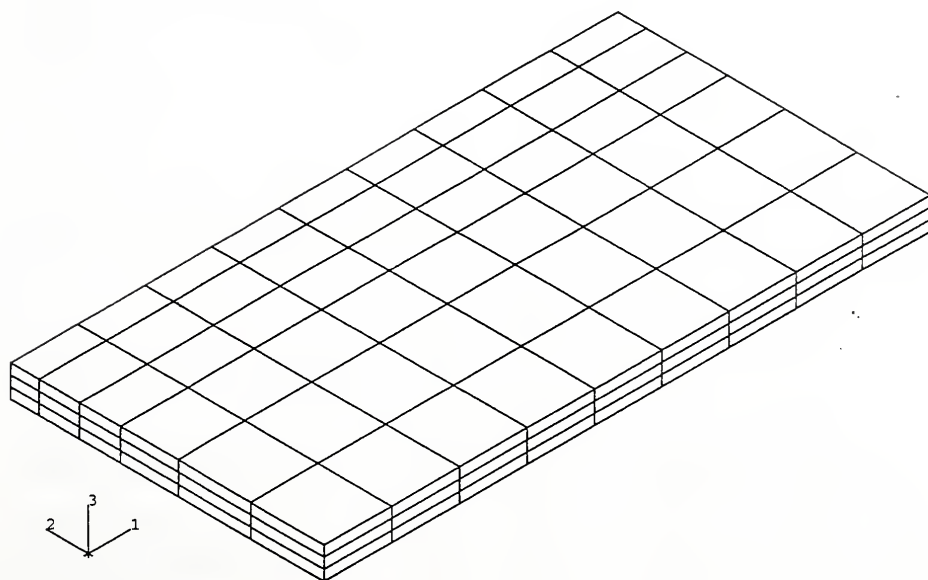


Figure 7.9 3-D View of Finite Element Mesh.





## 7.2 Sensitivity Analysis

Effects of model input parameters on predicted rut depth are evaluated in this section. Table 7.1 lists a total of nine possible factors which may affect the predicted rut depth. Three reasonable levels were included for each factor in the sensitivity analysis. The bold numbers in Table 7.1 are control values used in model calibration. The total number of combinations is large. Therefore, each factor level was only run with the control values.

Results of sensitivity analysis show that the predicted rut depth is not sensitive to the ranges of modulus of elasticity, Poisson's ratio and elastic foundation stiffness. This is expected because these three factors define the material elastic properties and are not related to permanent deformations. The other six factors listed in Table 7.1 have significant effect on predicted rut depths or the shape of creep curves as shown in Figure 7.10 to 7.15.

Table 7.1 Factor Levels for Sensitivity Analysis

Factors		Levels		
		Low	Medium	High
Material Parameter in Creep Model	A	$1.0 \times 10^{-4}$	<b><math>4.0 \times 10^{-4}</math></b>	$7.0 \times 10^{-4}$
	n	<b>0.8</b>	1.05	1.3
	m	-0.25	-0.5	<b>-0.75</b>
Modulus of Elasticity, psi	E	300,000	<b>450,000</b>	600,00
Poisson's Ratio	$\mu$	<b>0.3</b>	0.35	0.4
Foundation Stiffness, pci	K	250	<b>500</b>	750
Loading Speed, mph	S	<b>5</b>	10	20
Total Load, lb.	P	4500	<b>9000</b>	13500
Overlay Thickness, in.	T	1	<b>3</b>	5

As can be seen from Figure 7.10, with other factors constant, on a log-log scale parameter  $A$  changes the intercept of the creep curve without changing the slope. The predicted rut depth increases linearly with increased value of parameter  $A$ .

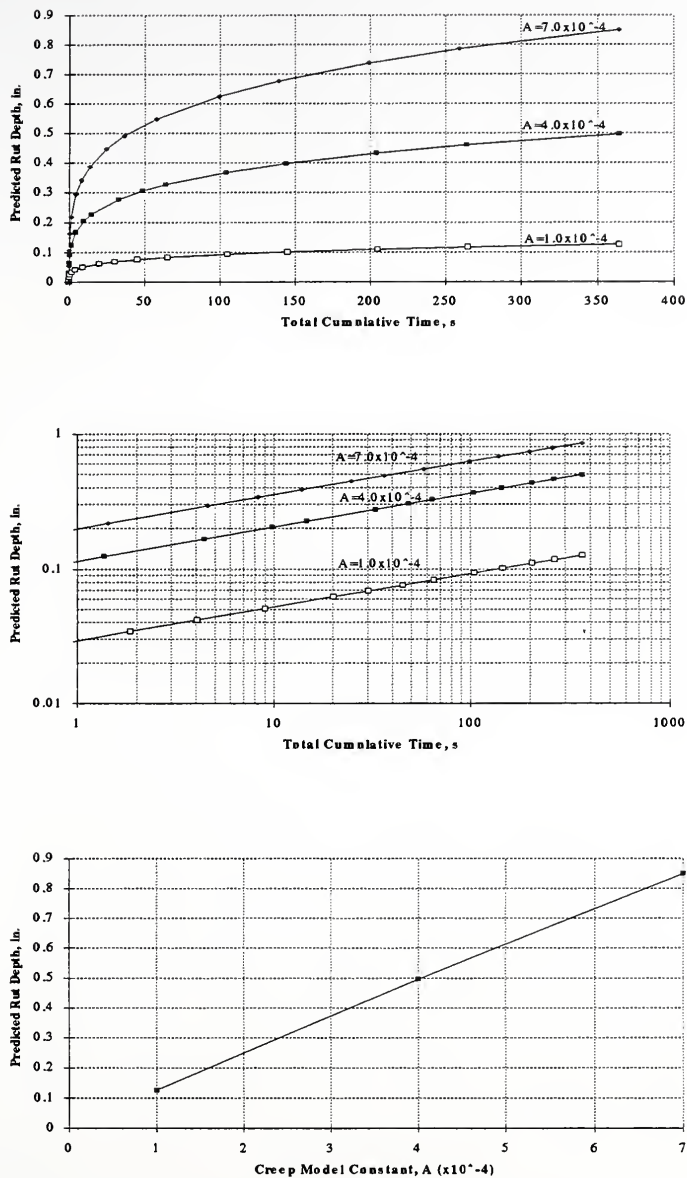
Figure 7.11 shows that the parameter  $m$  in the creep model defines the slope of the creep curves on a log-log scale. As the  $m$  value decreases, the slope decreases and total rut depth decreases.

Parameter  $n$  defines the stress function in the power law equation. As shown in Figure 7.12, with stress being the same, parameter  $n$  changes the intercept of creep curves on a log-log scale. Rut depth increases as the  $n$  value increases.

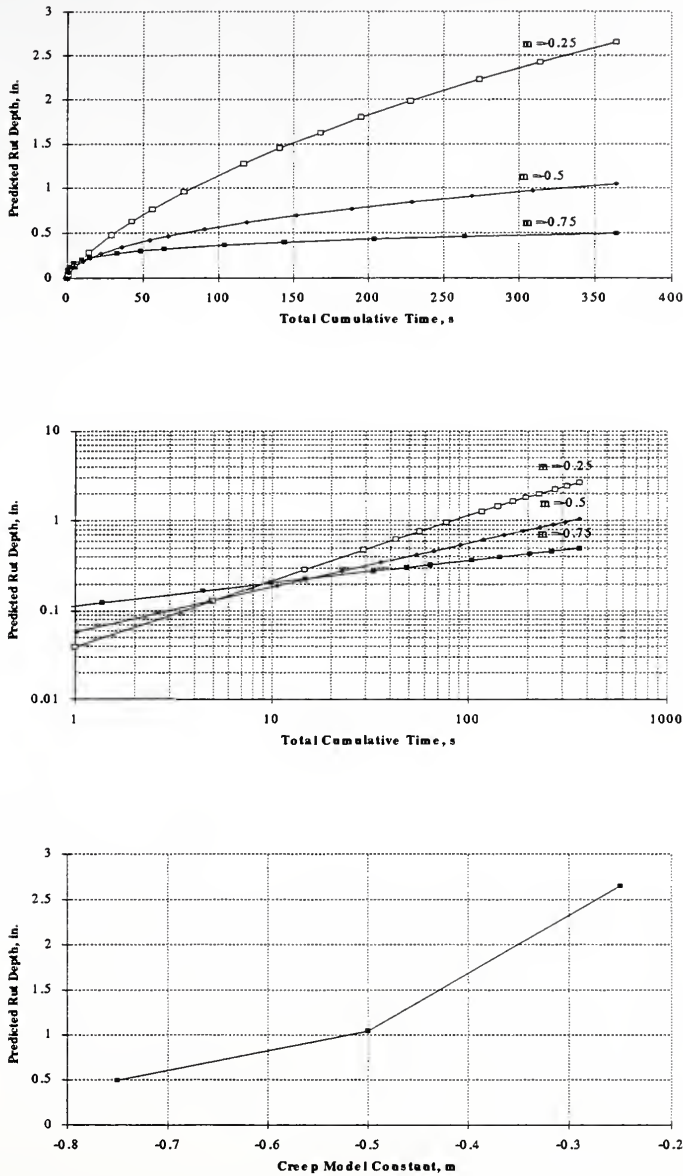
As shown in Figure 7.13, when the loading speed increases, the total loading duration on an element decreases. Therefore, the total rut depth decreases.

Figure 7.14 shows the effect of pavement thickness on total rut depth. When the thickness increases, the total rut depth increases. The 5" overlay would have a total rut depth 55% more than a 3" overlay. The 3" overlay would have a total rut depth four times more than a 1 in. overlay. But the increase in rate of rut depth decreases as overlay thickness increases.

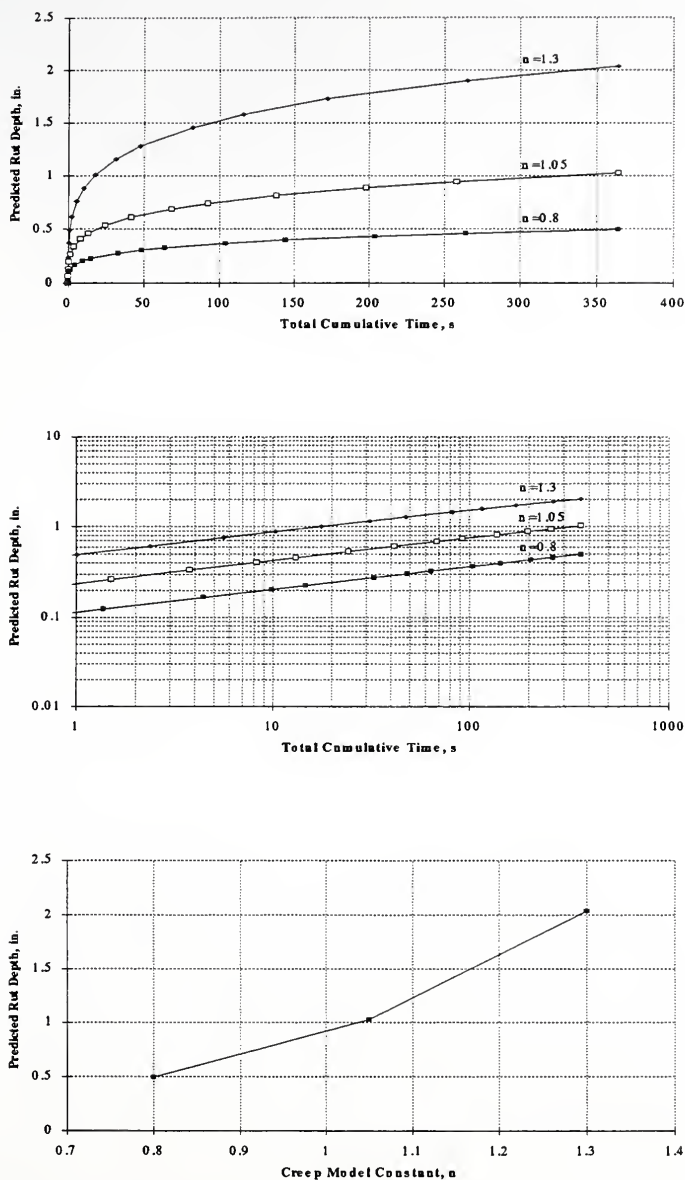
Figure 7.15 illustrates the relationship between total load/stress and rut depth. As can be seen, with other factor levels being constant, the rut depth increases as total load/stress increases. Whether the relationship is linear or non-linear depends on the parameter  $n$ . The relationship is linear when  $n$  is equal to 1.0. Otherwise, the relationship is non linear.

Figure 7.10 Effects of Creep Model Constant,  $A$



Figure 7.11 Effects of Creep Model Constant,  $m$



Figure 7.12 Effects of Creep Model Constant,  $n$





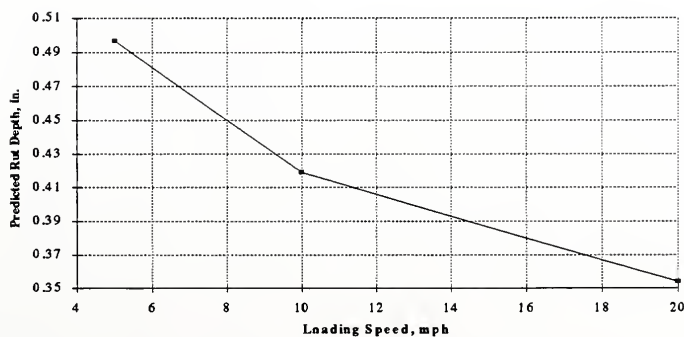
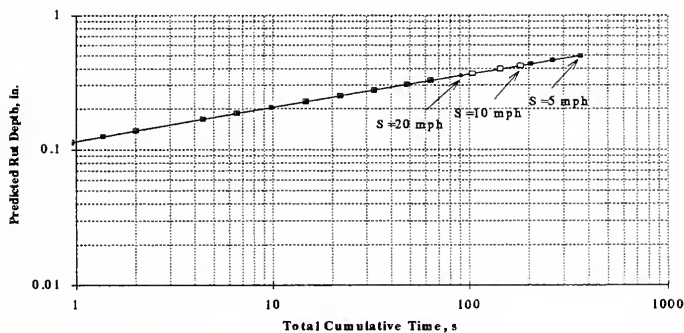
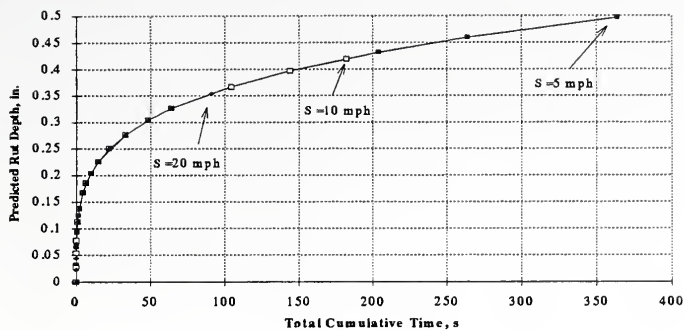


Figure 7.13 Effects of Loading Speed



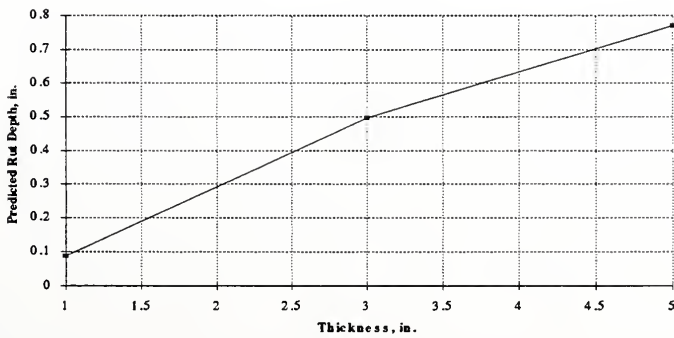
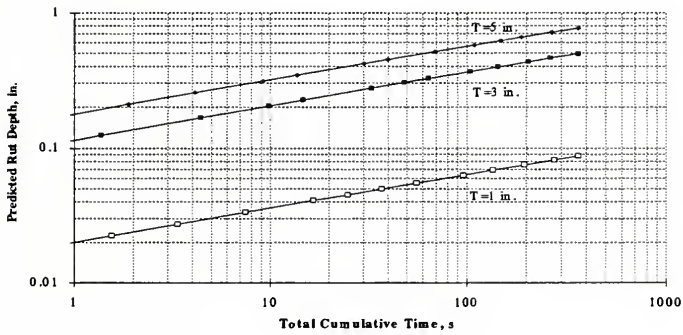
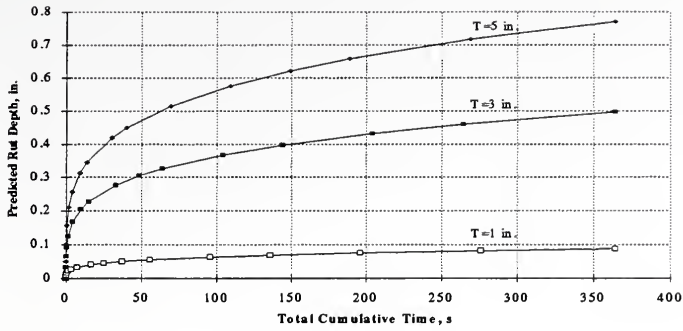


Figure 7.14 Effects of Thickness



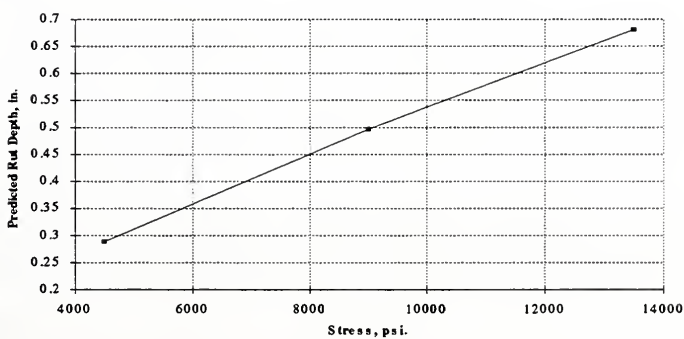
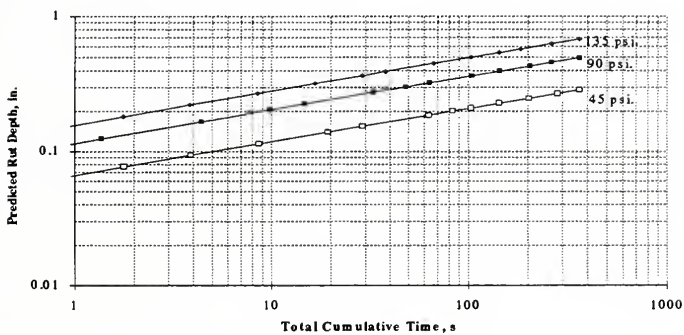
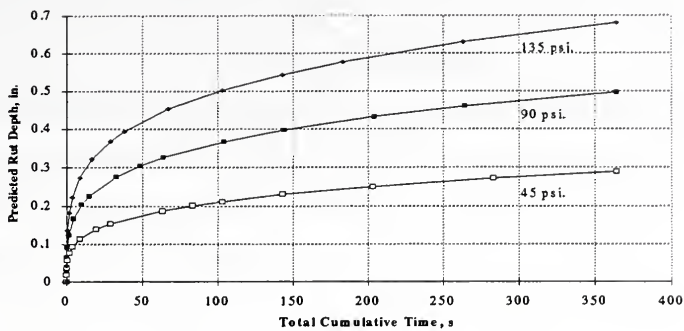


Figure 7.15 Effects of Load



### 7.3 Backcalculation

Irrecoverable creep strain accumulates under repeated loading and contributes to a large portion of asphalt concrete rutting. Based on the sensitivity study, the creep model is capable of capturing permanent deformation responses of asphalt mixtures. The parameter  $A$ ,  $m$ , and  $n$  in the creep model are material related. Each mixture has a unique set of  $A$ ,  $m$ , and  $n$  which define the creep behavior of the mixture. Measured rut depth data were used to backcalculate the creep model parameters. In the backcalculation procedure, creep model parameters were estimated by trial and error. The total predicted rut depth was compared with the measured rut depths at different cumulative times. The parameters were estimated when a good fit was obtained.

Since APT tests were conducted at only 90 psi tire pressure, the stress function in the creep model could not be estimated. Based on Perl's model, parameter  $n$  was fixed at 0.8 throughout the backcalculation. Parameter  $m$  was estimated first by matching the slope of predicted creep curves with the slope of measured rut curves. After the parameter  $m$  was determined, the  $A$  value was estimated by matching the intercept of the predicted creep curves with the intercept of measured rut curves.

A total of nine mixtures were selected for backcalculation of material parameters in the creep model. Table 7.2 lists the physical properties of each mixture and backcalculated material parameters. Figures 7.16 through 7.24 show the fitted curve and rutting data from the APT.

Figure 7.25 shows the effects of aggregate type on parameter  $m$ . As can be seen, the parameter  $m$  for slag and limestone is smaller (more negative) than that for the gravel mixtures.

Table 7.2. Backcalculated Material Constants

No.	Mixture Physical Property										Model Parameter		
	Aggr. Type	% NS	%C	%AC	% Relative AC	% #4	F.M.	Air Voids	VMA(%)	VFA(%)	A $\times 10^{-4}$	n	m
1	Gravel	100	43	3.7	-0.6	43.3	3.57	9.72	15.5	37.1	1.80	0.8	-0.558
2	Gravel	100	48	4.3	0.0	46.1	3.72	9.5	16.5	42.6	1.65	0.8	-0.444
3	Gravel	100	40	4.4	0.1	46.7	3.66	10.04	17.7	43.4	3.73	0.8	-0.510
4	Gravel	100	71	4.2	-0.3	29.1	2.96	7.21	14.6	50.6	3.00	0.8	-0.540
5	Gravel	50	82	4.7	-0.3	30.6	3.17	8.33	15.5	46.3	3.20	0.8	-0.630
6	Gravel	0	78	4.7	-0.7	29.7	3.41	9.93	17.4	43.0	2.60	0.8	-0.610
7	Gravel	100	96	4.3	-0.4	30.9	3.36	8.85	16.0	44.8	1.70	0.8	-0.534
8	Slag	100	100	5.8	0.3	33.9	2.96	9.85	18.2	45.8	1.54	0.8	-0.724
9	Limestone	100	100	4.3	-0.5	38.6	3.28	8.55	16.5	48.3	1.47	0.8	-0.800



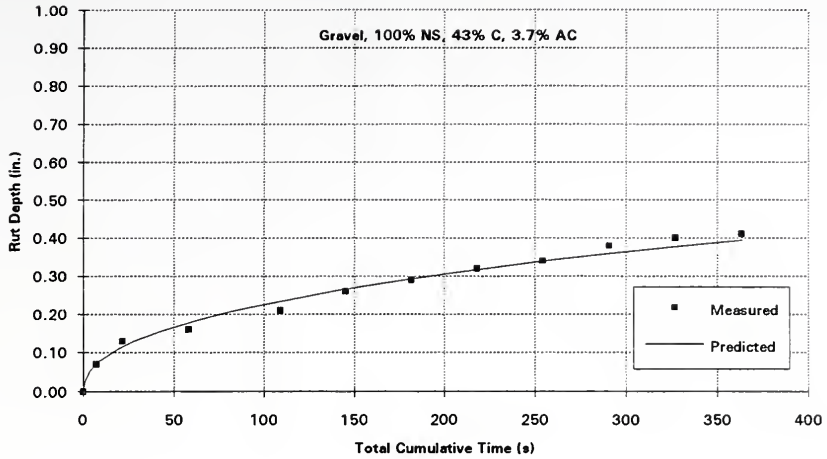


Figure 7.16 Fitted Curves (#2 Mixture, Lean Lane)

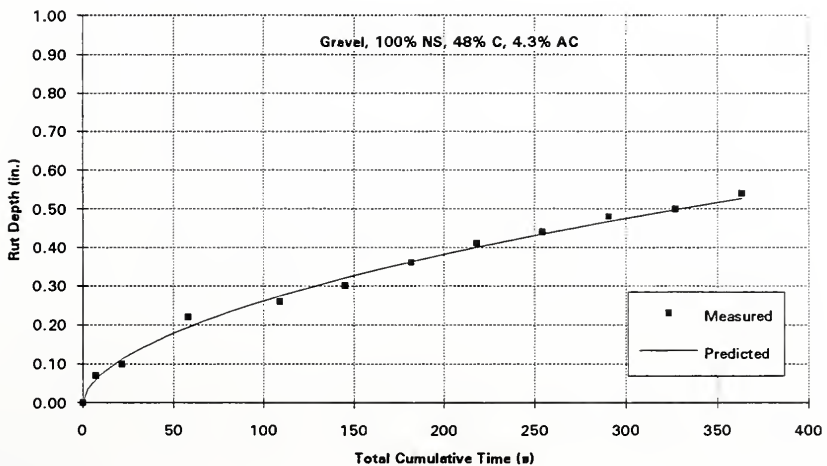


Figure 7.17 Fitted Curves (#2 Mixture, Optimum Lane)



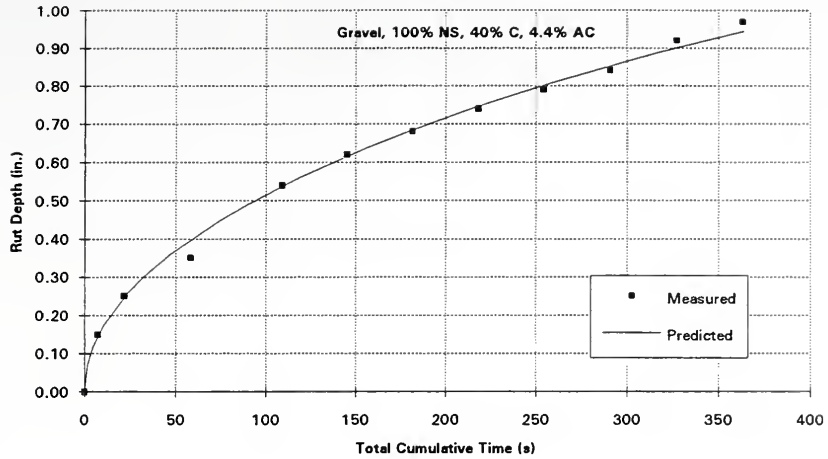


Figure 7.18 Fitted Curves (#2 Mixture, Rich Lane)

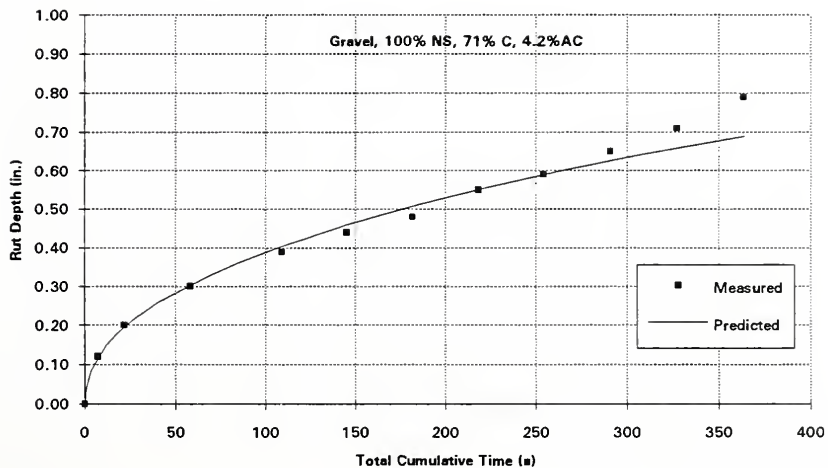


Figure 7.19 Fitted Curves (#5 Mixture, Optimum Lane)



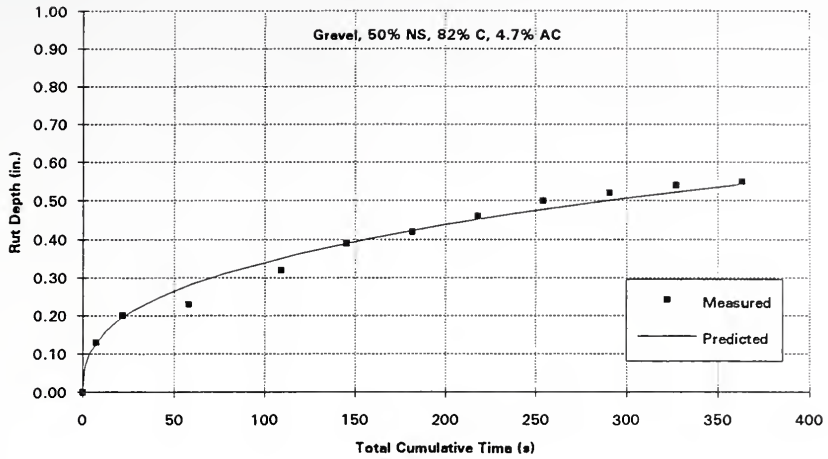


Figure 7.20 Fitted Curves (#6 Mixture, Optimum Lane)

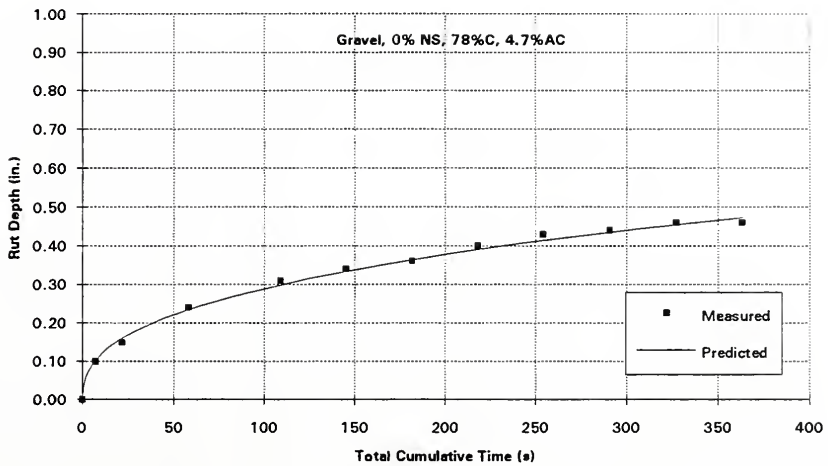


Figure 7.21 Fitted Curves (#7 Mixture, Optimum Lane)



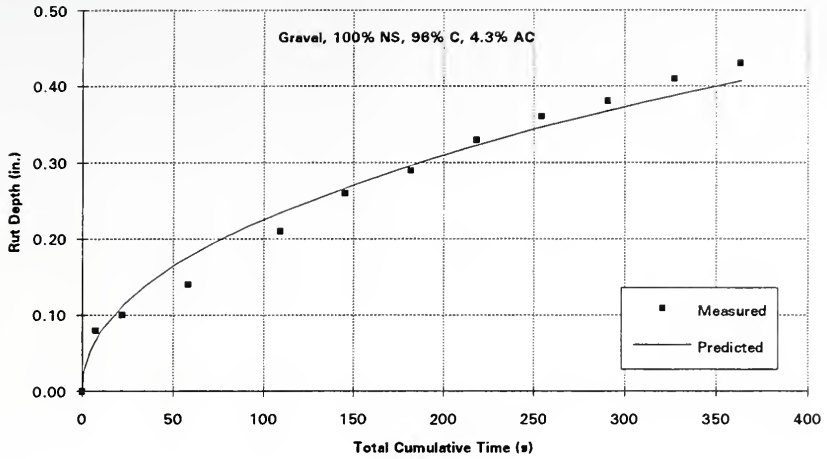


Figure 7.22 Fitted Curves (#1 Mixture, Optimum Lane)

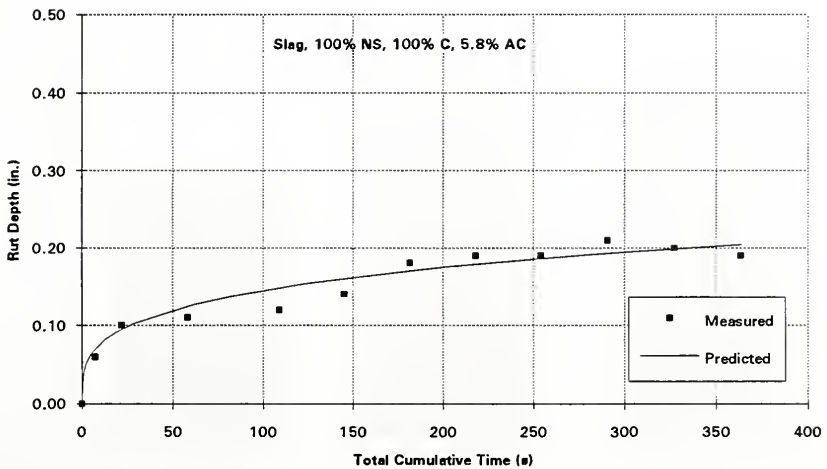


Figure 7.23 Fitted Curves (#8 Mixture, Optimum Lane)





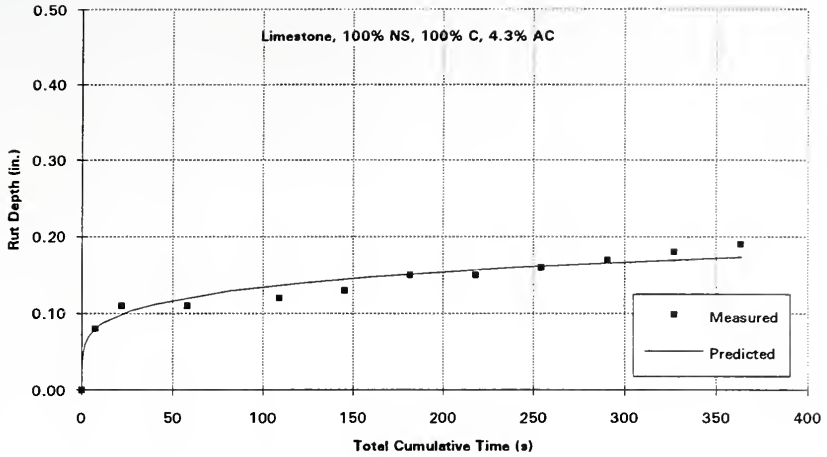


Figure 7.24 Fitted Curves (#9 Mixture, Optimum Lane)

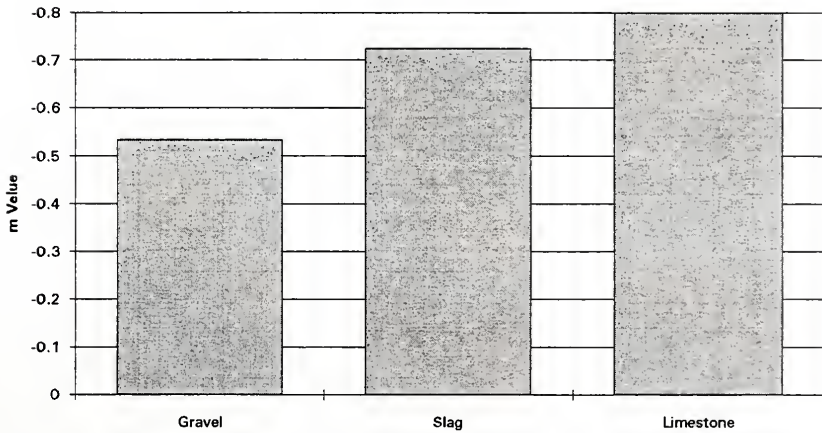


Figure 7.25 Effects of Aggregate Type on  $m$



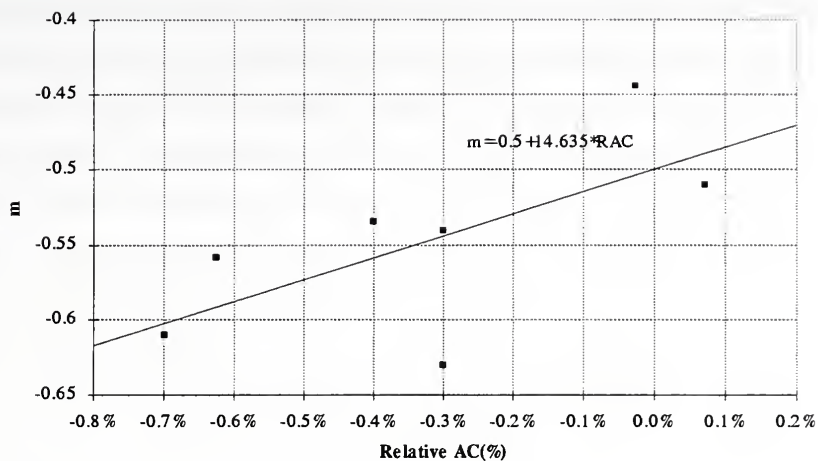


Figure 7.26 Effects of Relative Asphalt Content on  $m$  (Gravel Mixtures)

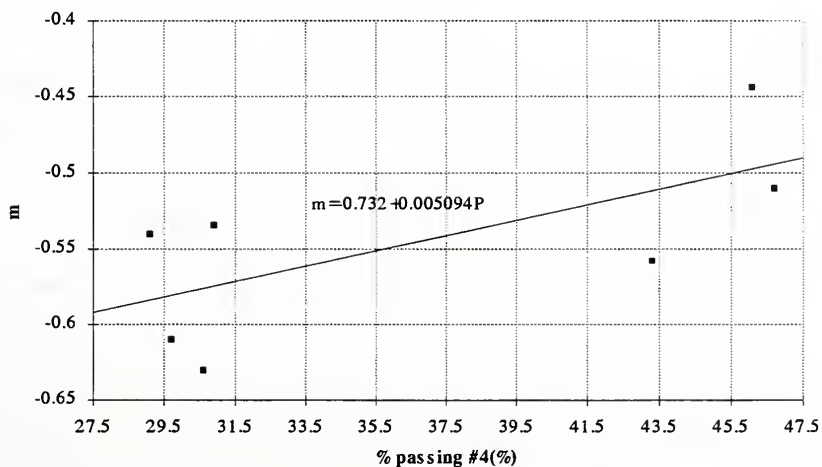


Figure 7.27 Effects of Percent Passing #4 Sieve on  $m$  (Gravel Mixtures)



Regression analyses were conducted to correlate the backcalculated parameters  $m$  and  $A$  of gravel mixtures with mixture physical properties. It is found that parameter  $m$  is strongly related to the relative asphalt content and percentage passing #4 sieve. Figure 7.26 shows the effects of relative asphalt content on parameter  $m$  along with the regression equation. The coefficient of determination ( $R^2$ ) for the equation is 0.45. The P-values are 0.0001 for intercept and 0.0822 for slope, respectively. Figure 7.27 shows the effects of percent passing the #4 sieve on parameter  $m$  along with the regression equation. The coefficient of determination ( $R^2$ ) for the equation is 0.44. The P-values are 0.0002 for intercept and 0.0856 for slope, respectively. Both regression equations are significant at  $\alpha = 0.1$ . It is clear from the figures that parameter  $m$  increases with increase of relative asphalt content and/or percent passing the #4 sieve.

Parameter  $A$  does not appear to be influenced by any mixture physical properties listed in Table 7.2. However, this is not unexpected since parameter  $A$  could not be uniquely backcalculated from the available testing data.

#### 7.4 Summary

A finite element program, ABAQUS, was used to model the APT pavement structure and predict permanent deformation. The APT loading was approximated. A creep model was used to characterize the pavement material behavior. Based on rut-depth data from the APT tests, material parameters in the creep model were backcalculated. Regression analyses were conducted to correlate these material parameters with mixture physical properties.

Good agreement was obtained between predicted rutting and measured rutting from APT traffic through a reasonable approximation of loading and careful consideration of model geometry, boundary conditions, and material properties. The finite element model is capable of capturing the permanent deformation response of asphalt layer and can be used to predict asphalt pavement permanent deformation.

Results of the sensitivity studies show that the predicted rut depth is not sensitive to the input values of modulus of elasticity, Poisson's ratio and elastic foundation stiffness. The predicted rut depth is very sensitive to the parameters in the creep model. Other factors such as loading speed, tire pressure, and pavement thickness also have significant influence on the predicted rut depth.

No estimate of the stress function in the creep model could be obtained based on tests with a single tire pressure. Parameter  $n$  was fixed at 0.8 while material parameters  $m$  and  $A$  were backcalculated by matching the slope and intercept of predicted rut curves with those of measured rut curves.

The backcalculated material parameter  $m$  is strongly related to aggregate type, percent passing #4 sieve and relative asphalt content in mixtures. The parameter  $m$  of slag and limestone mixtures is smaller than that for gravel mixture. Regression analyses show that parameter  $m$  increases with increase of relative asphalt content and/or percent passing the #4 sieve.

## CHAPTER 8

### CONCLUSIONS AND RECOMMENDATIONS

The objectives of this research were to address effects of various constituents of asphalt mixtures on pavement rutting utilizing accelerated pavement testing. Factors included in this study are aggregate type, percentage of crushed gravel, percentage of natural vs. crushed sand and asphalt content. Using these factors and selected levels, 27 test sections were tested.

Statistical analyses were performed to correlate actual rut depths to measurements of mixture physical properties. The dependent variable is total rut depth (Y) at 5000 load repetitions and the independent variables included in the analysis were aggregate type (AT), percent crushed coarse aggregate (CA), percent natural sand (NS), and relative asphalt content (AC). Relative asphalt content was used in the analysis to minimize the effect of variation of optimum asphalt content from mixture to mixture.

A finite element program, ABAQUS, was used to model the pavement structure and predict permanent deformation. An approximation was used to simulate the APT loading conditions. A creep model was used to characterize the actual pavement material behavior. Based on the rut-depth development data from the APT, material parameters in the creep model were backcalculated. Regression analyses were conducted to correlate these material parameters with mixture physical properties.

After test air voids analysis of APT test sections shows that the air voids between the wheel path are the highest and air voids in the wheel path are the lowest. The overall average difference of air voids in and out of the wheel paths is 1.0%. This difference corresponds to 0.03 in. of densification for a 3 in. asphalt overlay.

Penetration and viscosity tests of extracted asphalt reveal that the percent retained penetrations range from 33.8% to 54.9% with an average of 44.1%. Viscosity ratios

range from 1.47 to 2.17 with an average of 1.78. The viscosity ratio increases with increase of air voids in mixtures.

Aggregate type is significant. Slag and limestone mixture rutting is less than all gravel mixtures. Percent of coarse crushed particles in gravel mixtures was not significant.

Percent natural sand is not significant in the 40% crushed gravel mixtures but is significant in 70% crushed gravel mixtures. Insensitivity of the 40% crushed gravel mixtures to amount of natural and crushed sand is likely to be the result of the low percent of crushed faces or problems with achieving the target mix design. A 50% increase in natural sand results in 0.13 inch increase in total rut depth of 70% crushed gravel mixtures.

Relative asphalt content is significant. A 0.5% increase in asphalt content will result in 0.25 inch increase in total rut depth of 40% crushed gravel mixtures and about 0.09 inch increase in total rut depth of 70% crushed gravel mixtures. Rut depth is more sensitive to asphalt content in the 40% crushed gravel mixtures than in the 70% crushed gravel mixtures. Slag and limestone mixtures also are less sensitive to asphalt content.

Rutting in the APT was correctly modeled through a reasonable approximation of loading and careful consideration of model geometry, boundary conditions, and material models. Results of sensitivity studies show the predicted rut depth is not sensitive to modulus of elasticity, Poisson's ratio and elastic foundation stiffness. The predicted rut depth is sensitive to the creep model parameters. Other factors such as loading speed, tire pressure, and pavement thickness also have significant influence on the predicted rut depth. In particular, as a result of the analysis, the speed factor to convert results from the APT 5 mph to other speeds was determined. For example the number of loads at 5 mph can be multiplied by 12 to 13 to predict the number of loads to produce the same amount of rutting at 60 mph. This factor is valid for the gravel mixtures.

No estimate could be made of the stress function in the creep model because only a single tire pressure was used in APT tests. The parameter  $n$  was fixed at 0.8 while



material parameters  $m$  and  $A$  were backcalculated by matching the slope and intercept of predicted rut curves with those of measured rut curves. It is recommended that tests with varying stress levels be conducted in future research so that the parameters  $A$  and  $n$  can be uniquely backcalculated.

The backcalculated material parameter  $m$  is strongly related to aggregate type, percent passing #4 sieve and relative asphalt content. The parameter  $m$  of slag and limestone mixtures is smaller than that for gravel mixtures. Regression analyses show that  $m$  increases with an increase of relative asphalt content and/or percent passing #4 sieve.

Laboratory wheel track (WTD) tests confirm the prototype scale APT test results. WTD tests show that there is a decrease in rutting/stripping potential from increasing the coarse crushed aggregate from 40% to 70%. Decreasing the amount of natural sand from 100% to 50% is even more significant in reducing the rutting/stripping potential.

APT retests of mixtures MD 4 and MD 7 confirm the difficulty of closely matching target mix design gradations and asphalt contents. The retests indicate that mixture performance is related to asphalt content and density (or air voids). For example, lower asphalt content and/or higher density are associated with lower rutting. Conversely, higher asphalt content and/or lower density are associated with higher rutting.

The following recommendations are made:

1. The Accelerated Pavement Tester (APT) proved to be very effective in evaluating rutting potential of asphalt mixtures. Several years of inservice rutting performance can be compressed into a few days of testing. As a result, the APT can and should be utilized to evaluate rutting performance of Superpave mixtures being utilized in Indiana.
2. There is no reason for the APT to be idle. As long as mixtures are being produced for existing construction projects there is opportunity to divert one or two truck loads for APT testing. This includes both Superpave and non-Superpave projects.

3. The finite element model is capable of capturing the permanent deformation response of asphalt layers and can be used to predict permanent deformation.
4. Additional tests should be conducted over a range of temperatures and tire pressures. These tests would define the effect of temperature and tire pressure on rutting performance of asphalt mixtures as well as define the temperatures and stress functions in the theoretical rutting model.
5. The type of coarse crushed aggregate has a significant effect on rutting. Rutting of limestone and slag mixtures is much less than gravel mixtures with 95 percent one crushed face, all with 100 percent natural sand. The past requirements on limiting gravel on high volume roads is valid from a rutting perspective.
6. High percentages of natural sand increased rutting potential of gravel mixtures. Even for non-Superpave mixtures the sand fraction should be 50 percent or less natural sand.
7. Future tests should be planned that complete the matrix with tests of limestone, slag and 95 percent coarse crushed gravel. This would include these coarse aggregate and zero and 50 percent natural sand, respectively.
8. Tests were conducted at asphalt contents of optimum and  $\pm 0.5$  percent of optimum. Asphalt content proved to be very significant with respect to rutting. Similar tests should be conducted to validate Superpave optimum asphalt content criteria.
9. The PURWheel laboratory wheel track tester in large part mirrored the APT results. The PURWheel should be utilized to screen materials to be tested in the APT. Subsequent use of the APT will be more efficient and cost effective.

## LIST OF REFERENCES



## LIST OF REFERENCES

1. "AASHTO Interim Guide for the Structural Design of Flexible Pavements" (1972), American Association of State Highway and Transportation Officials, Washington, D.C.
2. "ABAQUS, Theory Manual" (1994), Version 5.4, Hibbitt, Karlsson and Sorensen, Inc.
3. "ABAQUS / Standard, User's Manual" (1994), Version 5.4, Volume I & II, Hibbitt, Karlsson and Sorensen, Inc.
4. "ABAQUS / Standard, Example Problems Manual" (1994), Version 5.4, Volume I & II, Hibbitt, Karlsson and Sorensen, Inc.
5. "ASTM (1991), "Annual Book of ASTM Standards," American Society for Testing Materials, Vol. 04.03, Philadelphia, PA.
6. Brown, E.R. (1990), "Density of Asphalt Concrete - How much is Needed?," Transportation Research Record 1282, TRB, National Research Council, Washington, D.C. 1990 ,pp. 27-32.
7. Brown, E. R., McRae, J. L., and Crawley, A. B. (1989), " Effect of Aggregates on Performance of Bituminous Concrete, " Implication of Aggregates in the Design, Construction and Performance of Flexible Pavements, ASTM STP 1016, H. G. Schreuders and C. R. Marek, Eds., American Society for Testing and Materials, Philadelphia, pp. 34-62.
8. Brown, E. R., and Bassett, Charles E. (1990), " Effects of Maximum Aggregate Size on Rutting Potential and other Properties of Asphalt-Aggregate Mixtures," Transportation Research Record 1259, TRB, National Research Council, Washington, D.C., pp. 107-119.
9. Carpenter, S.H. and Enockson, L. (1987), " Field Analysis of Rutting in Overlays of Concrete Interstate Pavements in Illinois," Transportation Research Record 1136, TRB, National Research Council, Washington, D.C., pp. 46-56.
10. Claessen, A. I. M., Edwards, J. M., Sommer, P. and Uge, P. (1977), "Asphalt Pavement Design - The Shell Method," Proceedings, Fourth International Conference, Structural Design of Asphalt Pavements, Ann Arbor, MI, pp. 39-74.
11. Coree, B. J. and White, T. D. (1989), "The Synthesis of Mixture Strength Parameters Applied to the Determination of AASHTO Layer Coefficients Distributions,"

- Proceedings, Association of Asphalt Paving Technologists, Nashville, TN, pp. 109-141.
12. Dawley, C.B., Hogewiede, B.L., and Anderson, K.O. (1990), "Mitigation of Instability Rutting of Asphalt Concrete Pavements in Lethbridge, Alberta, Canada," Proceedings, The Association of Asphalt Paving Technologists, Vol. 59, pp. 481-508.
  13. Decker, D. S., and Goodrich, J. L. (1989), "Asphalt Cement Properties Related to Pavement Performance," Proceedings, The Association of Asphalt Paving Technologists, Vol. 58, pp. 503-518.
  14. Dukatz, E. L. Jr. (1989), "Aggregate Properties Related to Pavement Performance," Proceedings, The Association of Asphalt Paving Technologists, Vol. 58, pp.492-501.
  15. Eisenmann, J. and Hilmer, A. (1987), "Influence of Wheel Load and Inflation Pressure on the Rutting Effect at Asphalt-Pavements - Experiments and Theoretical Investigations," Proceedings, Sixth International Conference on the Structural Design of Asphalt Pavements, Vol. I, Ann Arbor, MI, pp. 392-403.
  16. Evans, J.V., and Ott, L.E. (1986), "The Influence of Material Properties and Pavement Composition on Permanent Deformation by Flow," Proceedings, The Association of Asphalt Paving Technologists, Vol. 55, pp.353-399.
  17. Ford, Miller C.(1988), "Pavement Densification Related to Asphalt Mix Characteristics," Transportation Research Record 1178, TRB, National Research Council, Washington, D.C., pp. 9-15.
  18. Hofstra, A., and Klomp, A. J. G. (1972), "Permanent Deformation of Flexible Pavements Under Simulated Road Traffic Conditions", Proceedings, Third International Conference on the Structural Design of Asphalt Pavements, Ann Arbor, MI, pp. 613-621.
  19. Hofstra, A., and Valkering, C. P. (1972), "The Modulus of Asphalt Layers at High Temperatures: Comparison of Laboratory Measurements Under Simulated Traffic Conditions with Theory", Proceedings, Third International Conference on the Structural Design of Asphalt Pavements, Ann Arbor, MI, pp. 430-443.
  20. Huang, H. and White, T.D. (1994), "Concrete Pavement Crack and Seat Performance and Overlay Design.", Draft Final Report, Joint Highway Research Project, FHWA/IN/JHRP-94/12, Purdue University.
  21. Huang, Y.H.(1993), "Pavement Analysis and Design", Prentice Hall, Inc., Englewood Cliffs, New Jersey 07632.

22. Kalcheff, I. V., and Tunnicliff, D. G. (1982), " Effects of Crushed Stone Aggregate Size and Shape on Properties of Asphalt Concrete, " Proceedings, The Association of Asphalt Paving Technologists, Vol. 51, pp. 453-479.
23. Lai, J.S. and Anderson, D. (1973), "Irrecoverable and Recoverable Nonlinear Viscoelastic Properties of Asphalt Concrete", Transportation Research Record 468, National Research Council, Washington, D.C. ,pp.73-88.
24. Lundy, J.R., Hicks, R.G., and McHattie, R. (1989), "Evaluation of Percent Fracture and Gradation on the Behavior of Asphalt Concrete Mixtures," Implication of Aggregates in the Design, Construction and Performance of Flexible Pavements, ASTM STP 1016, H. G. Schreuders and C. R. Marek, Eds., American Society for Testing and Materials, Philadelphia, pp. 120-143.
25. Marks, V. J., Monroe, R. W., and Adams, J. F. (1983), " Effect of Crushed Particles in Asphalt Mixtures, " Transportation Research Record 1259, TRB, National Research Council, Washington, D.C. 1990 ,pp. 91-106.
26. McRae, J.L. (1993), " Gyrotory Testing Machine Technical Manual", Engineering Developments Co., Inc., Vicksberg, Mississippi 39181.
27. Monismith, C. L., Epps, J. A., and Finn, F. N. (1985), " Improved Asphalt Mix Design, " Proceedings, The Association of Asphalt Paving Technologists, Vol. 54, pp. 347-392.
28. Perl, Mordechi, Uzan, Jacob, and Sides, Arie (1983), "Visco-Elasto-Plastic Constitutive Law for a Bituminous Mixture Under Repeated Loading," Transportation Research Record 911, National Research Council, Washington, D.C. ,pp.21-27.
29. Roberts, F.L., et al (1991), "Hot Mix Asphalt Materials, Mixture Design, and Construction," First Edition, NAPA Education Foundation, Lanham, Maryland.
30. Santucci, L.E., Allen, D.D., Coats, R.L. (1985), "The Effects of Moisture and Compaction on the Quality of Asphalt Pavements," Proceedings, The Association of Asphalt Paving Technologists, Vol. 54, pp. 168-208.
31. SAS, (1991), "SAS System for Linear Models" SAS Institute, Inc., SAS Campus Drive, Cary, North Carolina 27513.
32. "Shell Pavement Design Manual" (1978), Shell Petroleum Company Limited, London.
33. Sousa, J. and Weissman, S. (1994), " Modeling Permanent Deformation of Asphalt-Aggregate Mixes," Preprint for The Association of Asphalt Paving Technologists

34. White, T. D., Albers, J. M. and Haddock, J. E., Sr.(1992), "Limiting Design Parameters for a Pavement Accelerated Testing System", ASCE Journal of Transportation Engineering, Vol. 118, No. 6, pp. 787-804.
35. Yoder, E. J., and Witczak, M. W. (1975), "Principles of Pavement Design", 2nd Ed., John Wiley and Sons, Inc., New York.



## APPENDICES



Appendix A Marshall Mix Design Data



Table A.1 MD #1 Marshall Data (Gravel, 95% Crushed and 100% Natural Sand)

%ASP	Core#	Avg.Ht.	BSG	MaxSG	Stability	Flow
4.0	A	2.614	2.333	2.553	1922	9
4.0	B	2.625	2.320	2.535	1593	12
4.0	C	2.716	2.333	2.562	1911	10
4.5	A	2.633	2.340	2.495	1497	8
4.5	B	2.732	2.329	2.522	1482	13
4.5	C	2.755	2.355	2.546	2079	13
5.0	A	2.649	2.382	2.505	2216	12
5.0	B	2.661	2.366	2.518	2123	12
5.0	C	2.602	2.387	2.473	2360	12
5.5	A	2.673	2.399	2.490	1763	12
5.5	B	2.696	2.373	2.489	1960	18
5.5	C	2.692	2.409	2.500	2000	13
6.0	A	2.783	2.404	2.460	2153	17
6.0	B	2.665	2.403	2.467	2513	20
6.0	C	2.720	2.411	2.457	2698	15
6.5	A	2.669	2.359	2.479	1302	16
6.5	B	2.641	2.384	2.461	2092	16
6.5	C	2.736	2.396	2.473	1615	19
Summary						
%ASP	Stability	Flow	AirVoids	Density	VMA	VFA
4.0	1591	10.3	8.68	144.94	14.74	41.12
4.5	1446	11.3	7.13	145.72	14.73	51.58
5.0	1978	12.0	4.83	148.01	13.84	65.13
5.5	1643	14.3	3.98	148.98	13.73	70.99
6.0	2096	17.3	2.25	149.74	13.75	83.62
6.5	1449	17.0	3.23	148.83	14.73	78.08



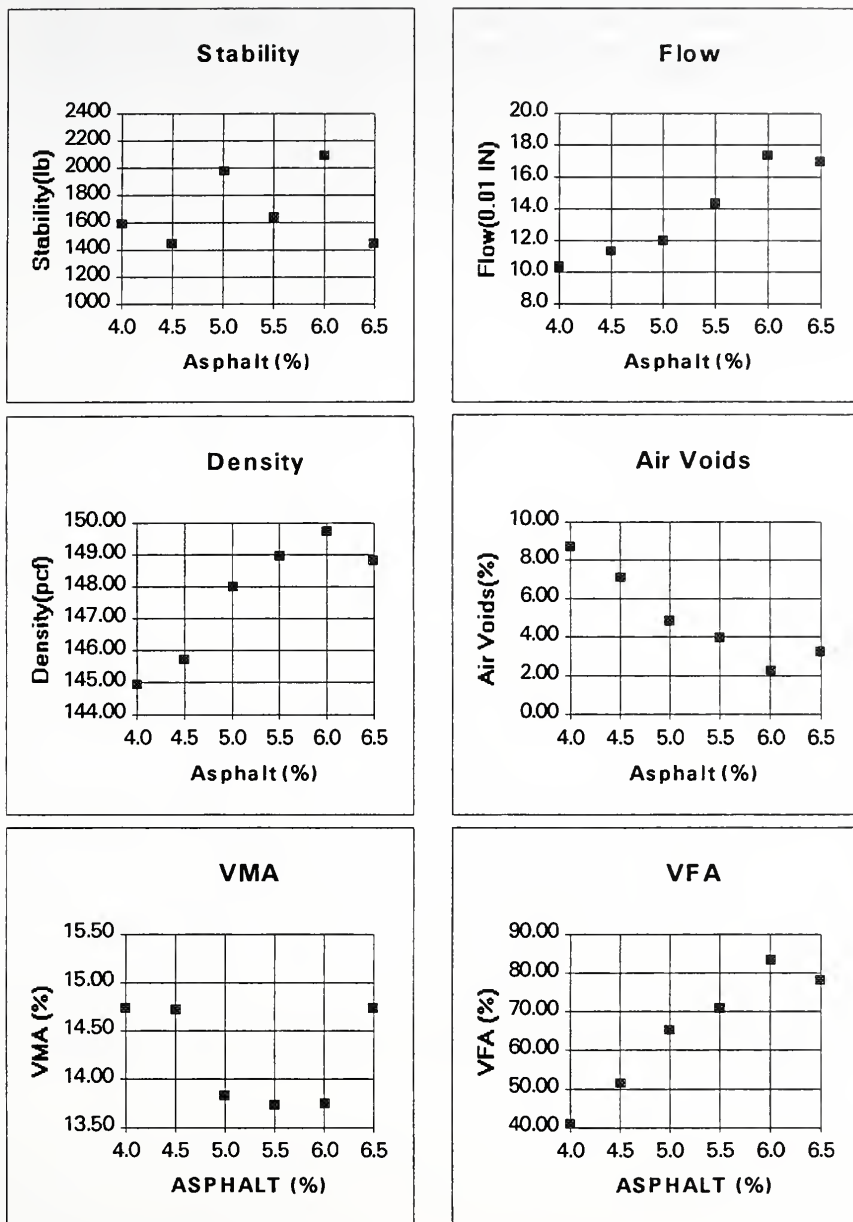


Figure A.1 MD #1 Marshall Plots (Gravel, 95% Crushed and 100% Natural Sand)





Table A.2 MD #2 Marshall Data (Gravel, 40% Crushed and 100% Natural Sand)

%ASP	Core#	Avg.Ht.	BSG	MaxSG	Stability	Flow
4.0	A	2.835	2.313		475	
4.0	B	2.771	2.342		775	9.5
4.0	C	2.698	2.327		950	10.5
4.5	A	2.762	2.344		925	12
4.5	B	2.828	2.350		1230	10.5
4.5	C	2.707	2.373		1100	10.3
5.0	A	2.711	2.362	2.476	1085	11.5
5.0	B	2.847	2.339	2.470	1120	10
5.0	C	2.697	2.372	2.461	785	11
5.5	A	2.799	2.343		640	11.8
5.5	B	2.688	2.378		1090	11.5
5.5	C	2.644	2.375		750	9.5
6.0	A	2.698	2.401		875	13
6.0	B	2.852	2.350		590	12.2
6.0	C	2.753	2.378		1150	11.7
Summary						
%ASP	Stability	Flow	AirVoids	Density	VMA	VFA
4.0	631	10.0	6.93	144.86	14.33	51.66
4.5	921	10.9	5.09	146.60	13.75	63.00
5.0	854	10.8	4.51	146.73	14.13	68.07
5.5	733	10.9	3.24	147.21	14.30	77.34
6.0	751	12.3	2.06	147.89	14.36	85.62



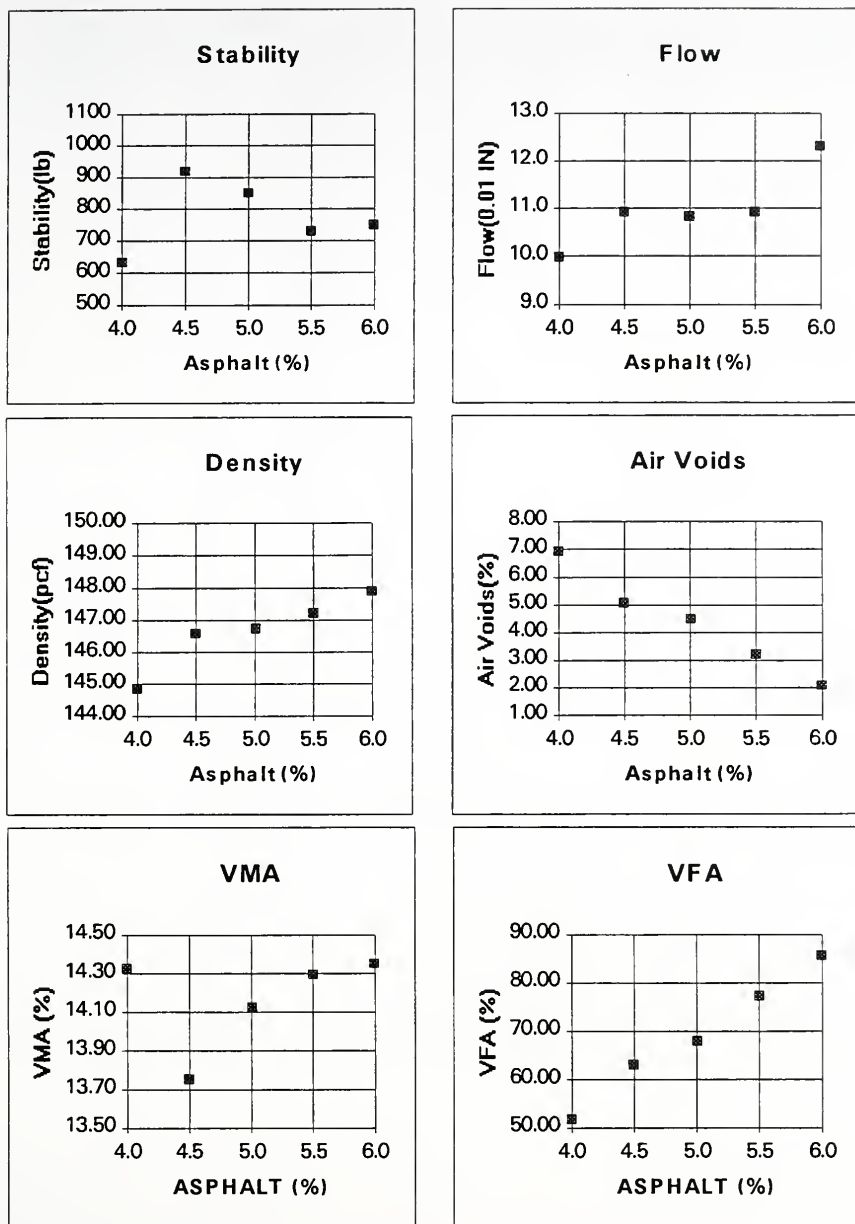


Figure A.2 MD #2 Marshall Plots (Gravel, 40% Crushed and 100% Natural Sand)



Table A.3 MD #3 Marshall Data (Gravel, 40% Crushed and 50% Natural Sand)

%ASP	Core#	Avg.Ht.	BSG	MaxSG	Stability	Flow
4.0	A	2.684	2.323		1750	9
4.0	B	2.751	2.355		1600	9
4.0	C	2.870	2.357		1600	9.5
4.5	A	2.834	2.370		1670	9
4.5	B	2.662	2.388		1450	9
4.5	C	2.802	2.364		1775	9
5.0	A	2.853	2.340	2.524	950	9
5.0	B	2.843	2.400	2.500	1550	9
5.0	C	2.893	2.384	2.498	1100	9
5.5	A	2.901	2.333		960	10
5.5	B	2.880	2.402		1150	8.5
5.5	C	2.880	2.389		1325	9
6.0	A	2.871	2.409		1650	10
6.0	B	2.851	2.384		900	9.5
6.0	C	2.853	2.411		1150	9
Summary						
%ASP	Stability	Flow	AirVoids	Density	VMA	VFA
4.0	1410	9.2	7.74	145.89	13.75	43.70
4.5	1387	9.0	5.86	147.71	13.13	55.40
5.0	977	9.0	5.30	147.79	13.54	60.88
5.5	924	9.2	4.34	147.79	14.00	69.01
6.0	1006	9.5	2.51	149.46	13.48	81.37



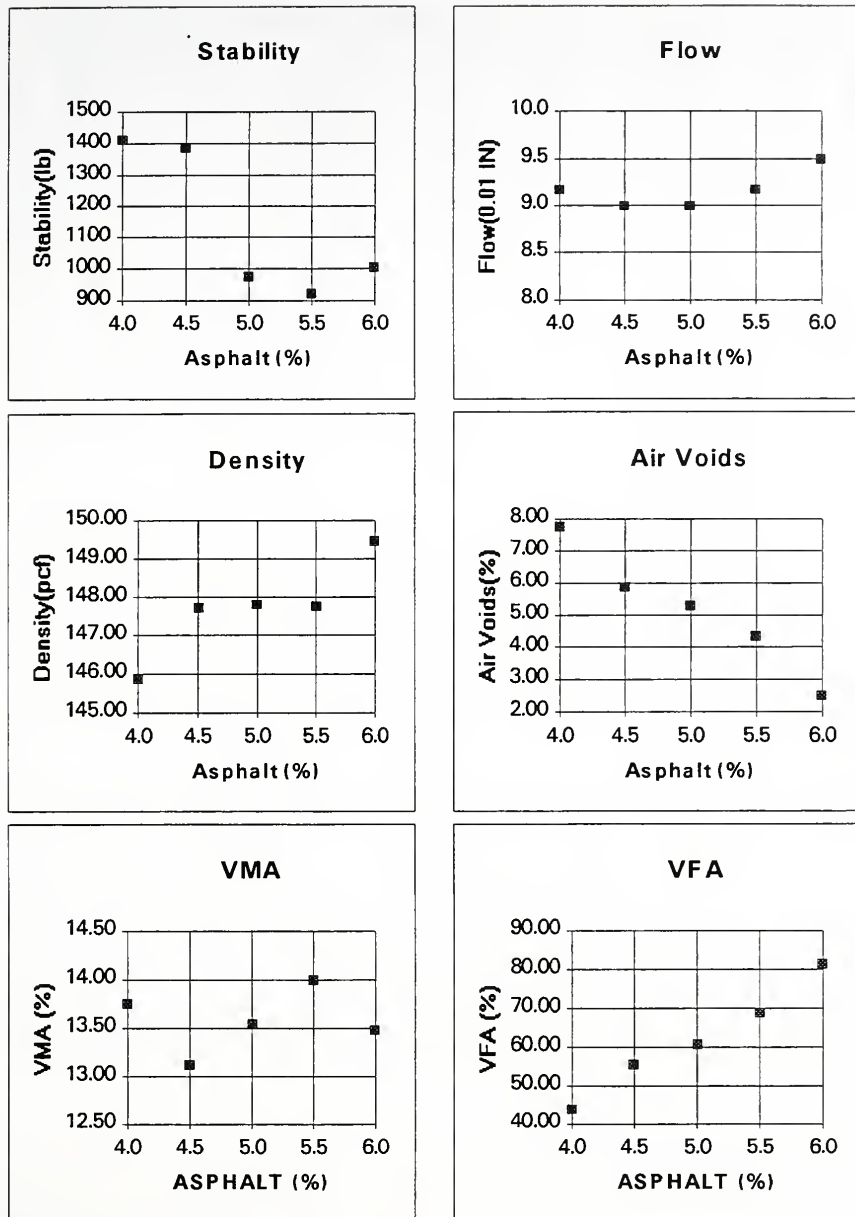


Figure A.3 MD #3 Marshall Plots (Gravel, 40% Crushed and 50% Natural Sand)





Table A.4 MD #4 Marshall Data (Gravel, 40% Crushed and 0% Natural Sand)

%ASP	Core#	Avg.Ht.	BSG	MaxSG	Stability	Flow
4.0	A	2.605	2.286	2.563	900	10.5
4.0	B	2.548	2.335	2.552	1675	7.7
4.0	C	2.573	2.340	2.543	1590	8.1
4.5	A	2.480	2.362		1350	10.2
4.5	B	2.508	2.341		1100	11.1
4.5	C	2.555	2.334		1175	11
5.0	A	2.487	2.363	2.521	1325	10.4
5.0	B	2.444	2.368	2.503	1100	10.7
5.0	C	2.475	2.347	2.520	1025	11.9
5.5	A	2.794				
5.5	B	2.527	2.382		1140	11
5.5	C	2.536	2.321		875	13
6.0	A	2.519	2.375	2.495	1080	10.5
6.0	B	2.565	2.366	2.476	1000	11.7
6.0	C	2.515	2.367	2.478	825	11.3
Summary						
%ASP	Stability	Flow	AirVoids	Density	VMA	VFA
4.0	1332	8.8	9.11	144.40	14.57	37.47
4.5	1201	10.8	7.22	146.01	14.06	48.66
5.0	1176	11.0	6.18	146.85	14.02	55.92
5.5	987	12.0	5.53	146.37	14.75	62.50
6.0	949	11.2	4.56	147.48	14.56	68.69



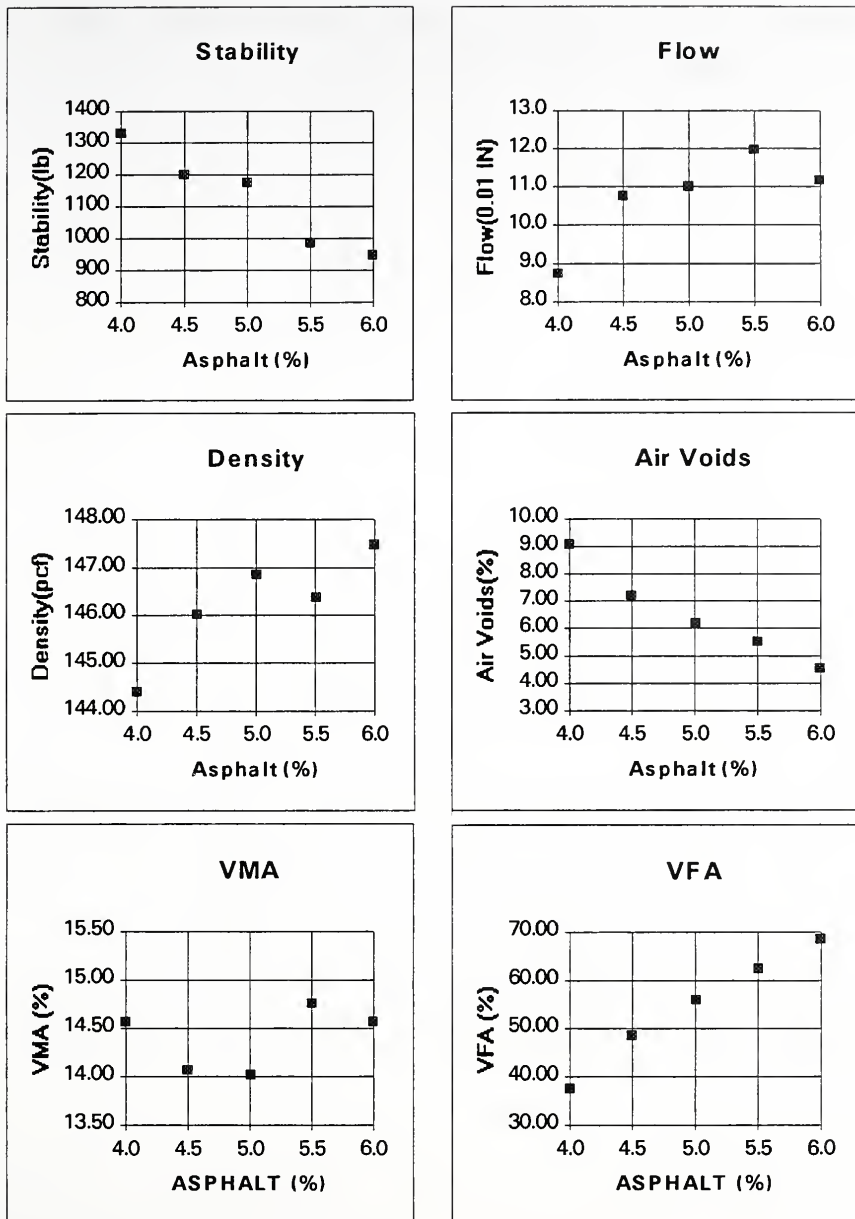


Figure A.4 MD #4 Marshall Plots (Gravel, 40% Crushed and 0% Natural Sand)



Table A.5 MD #5 Marshall Data (Gravel, 70% Crushed and 100% Natural Sand)

%ASP	Core#	Avg.Ht.	BSG	MaxSG	Stability	Flow
4.0	A	2.586	2.352	2.539	1770	8
4.0	B	2.635	2.371	2.539	2175	8.2
4.0	C	2.630	2.343	2.526	1530	8.2
4.5	A	2.620	2.369		1650	10.4
4.5	B	2.622	2.389		1640	9.8
4.5	C	2.497	2.372		1540	9.4
5.0	A	2.542	2.380	2.525	1600	11
5.0	B	2.629	2.373	2.496	1230	9.4
5.0	C	2.595	2.382	2.502	1600	10
5.5	A	2.584	2.384		1110	13
5.5	B	2.454	2.380		970	12.4
5.5	C	2.447	2.416		1330	9
6.0	A	2.471	2.387	2.497	1000	11.2
6.0	B	2.541	2.388	2.473	1540	12
6.0	C	2.572	2.366	2.472	1040	10.6
Summary						
%ASP	Stability	Flow	AirVoids	Density	VMA	VFA
4.0	1702	8.1	7.08	146.59	13.30	46.75
4.5	1533	9.9	5.93	147.93	12.97	54.32
5.0	1400	10.1	5.14	148.03	13.36	61.50
5.5	1141	11.5	3.83	148.96	13.28	71.15
6.0	1167	11.3	4.05	148.16	14.20	71.46



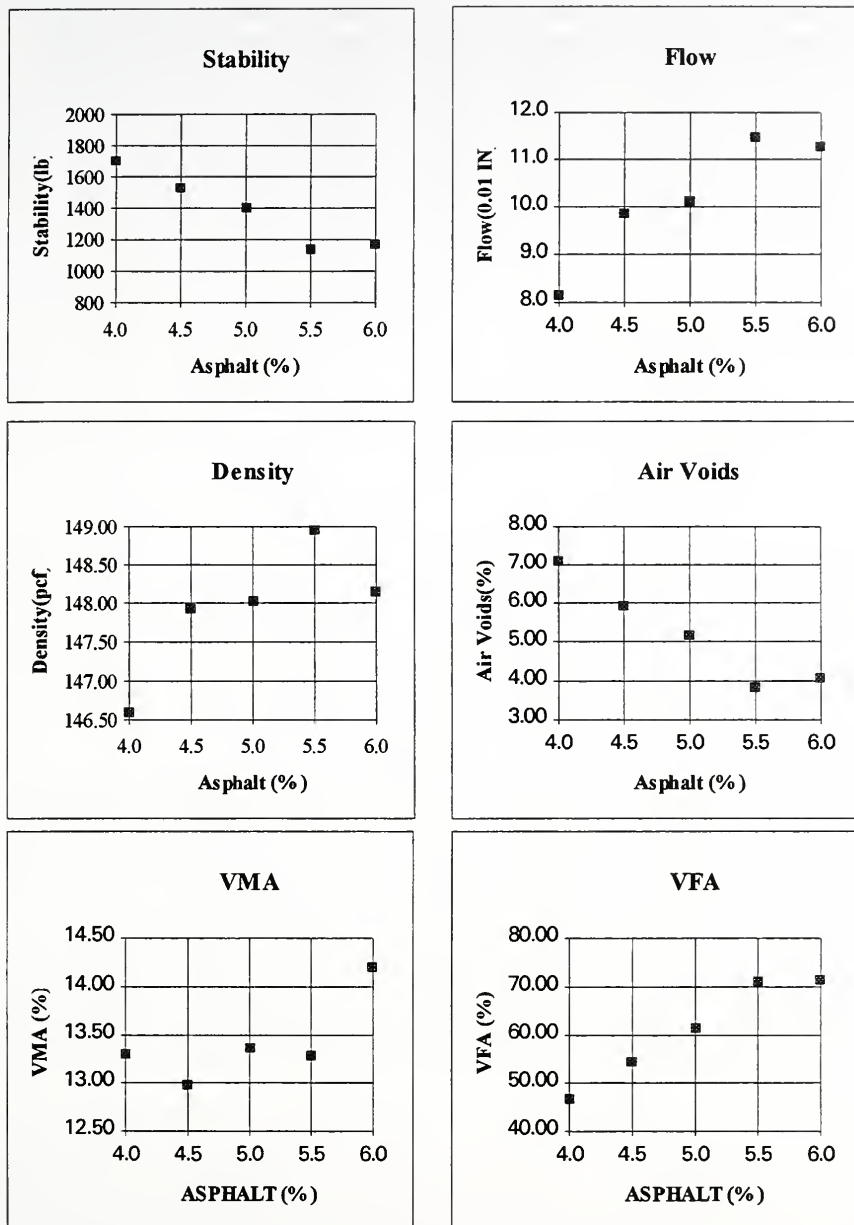


Figure A.5 MD #5 Marshall Plots (Gravel, 70% Crushed and 100% Natural Sand)





Table A.6 MD #6 Marshall Data (Gravel, 70% Crushed and 50% Natural Sand)

%ASP	Core#	Avg.Ht.	BSG	MaxSG	Stability	Flow
4.0	A	2.663	2.340	2.560	2350	11.5
4.0	B	2.645	2.328	2.554	2220	11.3
4.0	C	2.651	2.341	2.552	2225	11.2
4.5	A	2.634	2.349		1900	13.5
4.5	B	2.662	2.361		2175	15.4
4.5	C	2.667	2.363		2310	12.8
5.0	A	2.648	2.348	2.508	1975	16.6
5.0	B	2.629	2.388	2.508	2000	11.8
5.0	C	2.672	2.345	2.509	1925	17.3
5.5	A	2.595	2.335		1800	17.1
5.5	B	2.652	2.385		2150	15
5.5	C	2.605	2.346		1925	16.1
6.0	A	2.581	2.380	2.484	1700	13.4
6.0	B	2.625	2.381	2.469	1700	15.2
6.0	C	2.615	2.370	2.485	1950	14
Summary						
%ASP	Stability	Flow	AirVoids	Density	VMA	VFA
4.0	2076	11.3	8.57	145.41	13.93	38.49
4.5	1942	13.9	6.94	146.73	13.61	49.01
5.0	1803	15.2	5.91	146.90	13.96	57.68
5.5	1827	16.1	5.60	146.60	14.59	61.60
6.0	1670	14.2	4.15	147.93	14.27	70.92



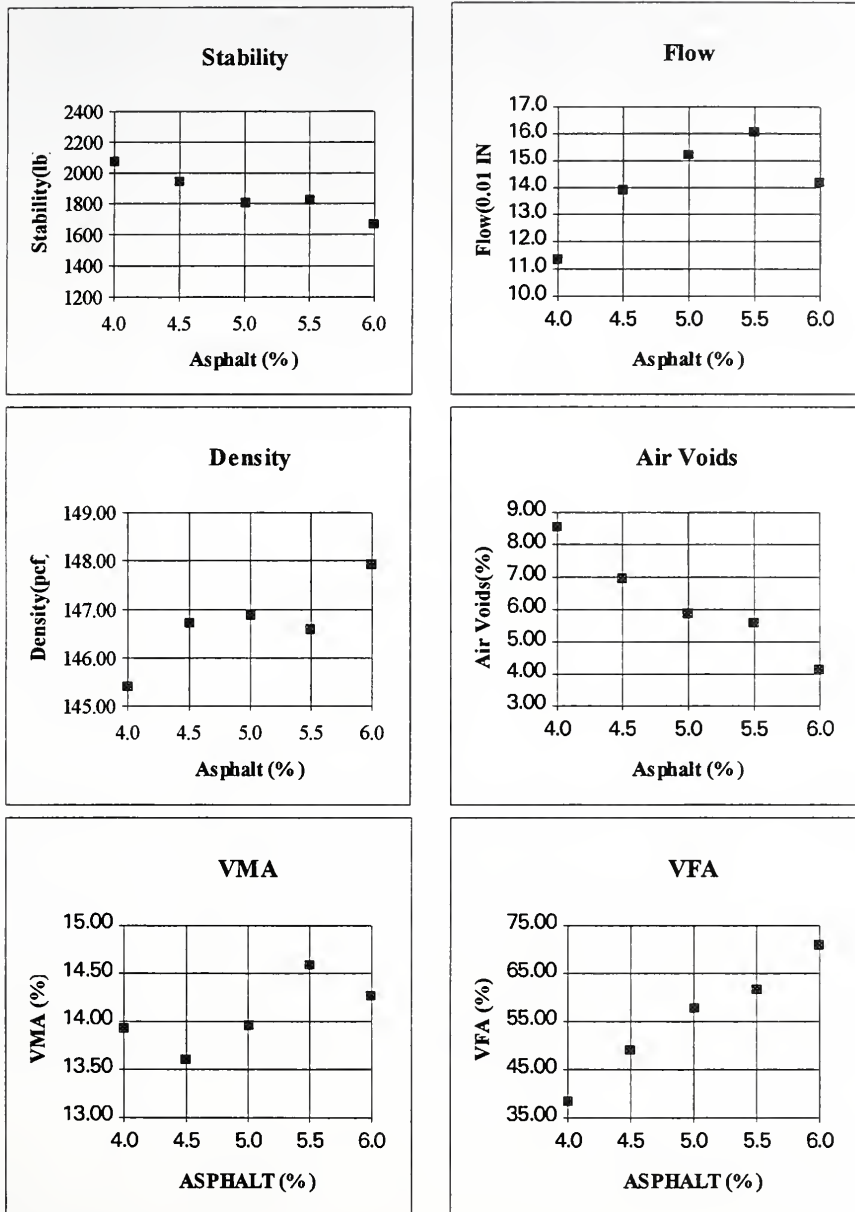


Figure A.6 MD #6 Marshall Plots (Gravel, 70% Crushed and 50% Natural Sand)



Table A.7 MD #7 Marshall Data (Gravel, 70% Crushed and 0% Natural Sand)

%ASP	Core#	Avg.Ht.	BSG	MaxSG	Stability	Flow
4.0	A	2.681	2.302	2.564	2670	13.4
4.0	B	2.683	2.329	2.556	2600	13.9
4.0	C	2.667	2.329	2.549	2280	12
4.5	A	2.646	2.342		2440	12.5
4.5	B	2.652	2.335		2525	15.3
4.5	C	2.648	2.323		2180	16.1
5.0	A	2.646	2.324	2.522	2050	17.9
5.0	B	2.640	2.331	2.501	2200	14.7
5.0	C	2.648	2.349	2.508	2350	16.5
5.5	A	2.633	2.365			
5.5	B	2.602	2.352		1790	17
5.5	C	2.669	2.345		2150	16.5
6.0	A	2.598	2.352	2.494	1920	19.2
6.0	B	2.622	2.346	2.474	1890	15.2
6.0	C	2.634	2.367	2.476	2090	13.9
Summary						
%ASP	Stability	Flow	AirVoids	Density	VMA	VFA
4.0	2247	13.1	9.23	144.42	14.46	36.13
4.5	2183	14.6	7.94	145.24	14.42	44.92
5.0	2024	16.4	7.01	145.30	14.83	52.75
5.5	1809	16.8	5.72	146.52	14.57	60.76
6.0	1835	16.1	5.09	146.58	14.99	66.06



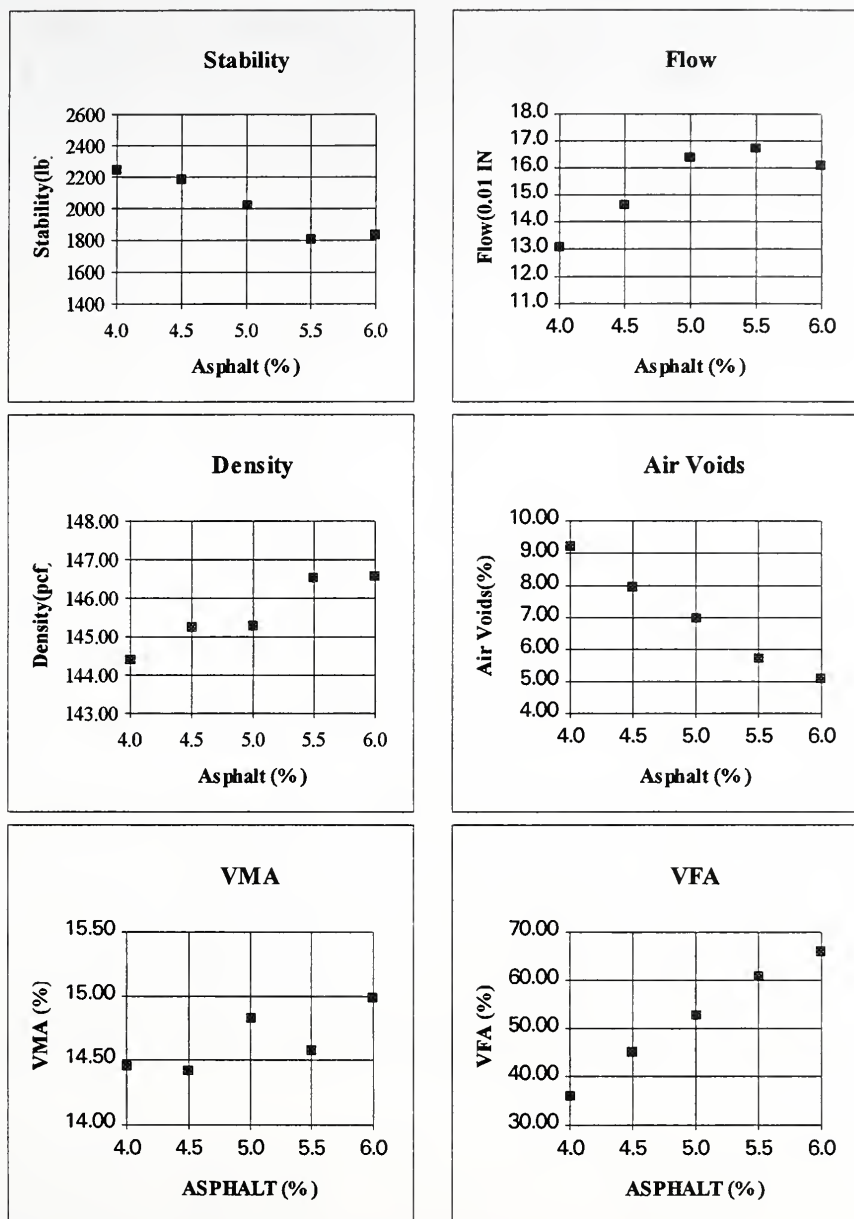


Figure A.7 MD #7 Marshall Plots (Gravel, 70% Crushed and 0% Natural Sand)





Table A.8 MD #8 Marshall Data (Slag, 100% Crushed and 100% Natural Sand)

%ASP	Core#	Avg.Ht.	BSG	MaxSG	Stability	Flow
5.0	A	2.426	2.201	2.426	4070	13.2
5.0	B	2.591	2.202	2.426	4500	14.5
5.0	C	2.589	2.223	2.426	5100	12.8
5.5	A	2.639	2.180		4000	15
5.5	B	2.651	2.191		4650	14.5
5.5	C	2.620	2.213		4850	14.3
6.0	A	2.619	2.204	2.374	4610	14.8
6.0	B	2.602	2.223	2.374	5060	14.5
6.0	C	2.626	2.218	2.374	4760	13.5
6.5	A	2.601	2.230		5050	13.7
6.5	B	2.590	2.234		4500	12.6
6.5	C	2.636	2.217		4450	16.3
7.0	A	2.612	2.241	2.352	4400	12.6
7.0	B	2.599	2.233	2.352	4330	15.9
7.0	C	2.599	2.233	2.352	4420	11.9
Summary						
%ASP	Stability	Flow	AirVoids	Density	VMA	VFA
5.0	4433	13.5	8.94	137.48	14.21	37.05
5.5	4141	14.6	8.56	136.60	15.21	43.69
6.0	4490	14.3	6.71	137.86	14.88	54.89
6.5	4357	14.2	5.92	138.60	14.88	60.18
7.0	4120	13.5	4.93	139.14	15.00	67.11



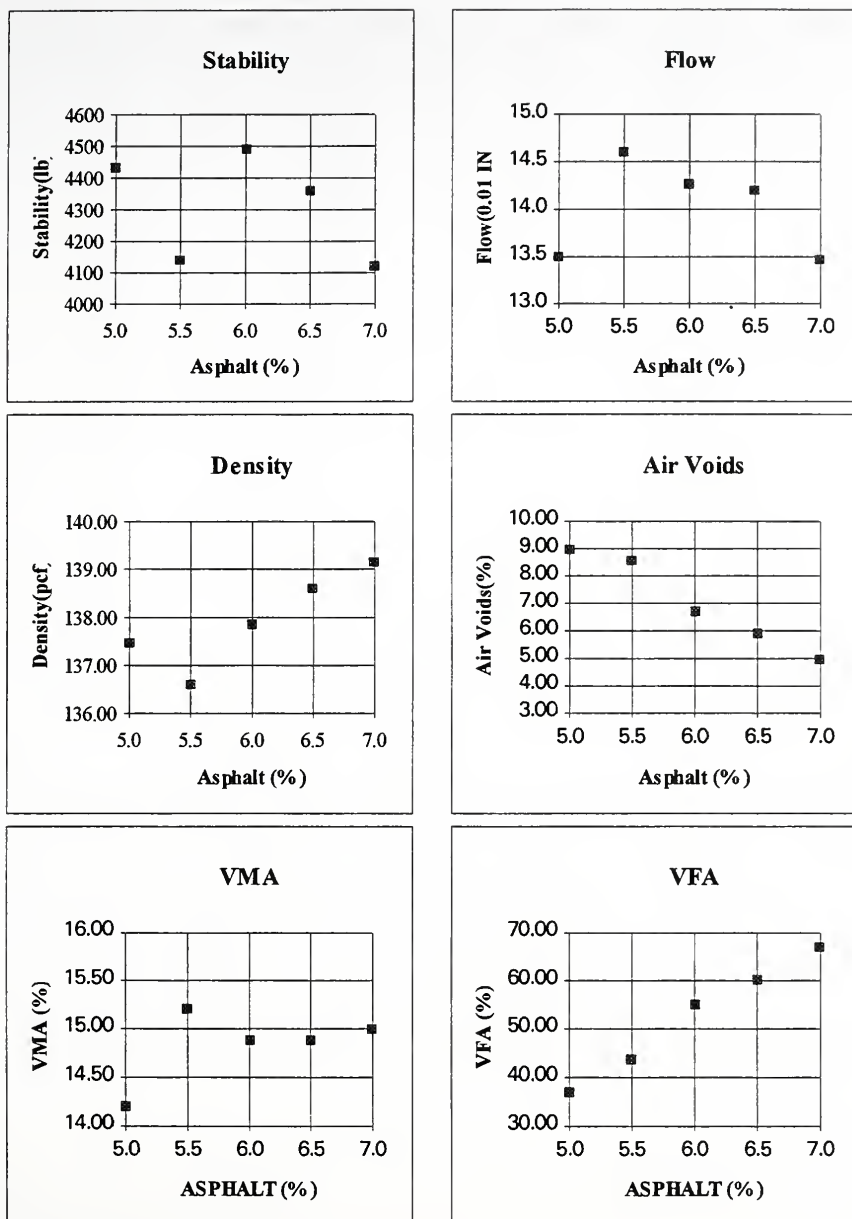


Figure A.8 MD #8 Marshall Plots (Slag, 100% Crushed and 100% Natural Sand)



Table A.9 MD #9 Marshall Data (Limestone, 100% Crushed and 100% Natural Sand)

%ASP	Core#	Avg.Ht.	BSG	MaxSG	Stability	Flow
4.0	A	2.603	2.429	2.612	2960	9.9
4.0	B	2.572	2.419	2.607	2880	12.4
4.0	C	2.567	2.413	2.608	2750	11
4.5	A	2.583	2.419		2380	11.5
4.5	B	2.588	2.421		2250	13.1
4.5	C	2.563	2.414		2500	11.9
5.0	A	2.586	2.424	2.574	2340	10.6
5.0	B	2.590	2.419	2.576	1950	12.6
5.0	C	2.631	2.441	2.569	1980	11.7
5.5	A	2.546	2.440		2550	10.8
5.5	B	2.604	2.411		2600	12.8
5.5	C	2.508	2.454		2310	10.4
6.0	A	2.521	2.451	2.544	2530	11.3
6.0	B	2.564	2.421	2.547	2280	12.1
6.0	C	2.507	2.426	2.557	1880	10.6
Summary						
%ASP	Stability	Flow	AirVoids	Density	VMA	VFA
4.0	2729	11.1	7.24	150.63	13.95	48.14
4.5	2259	12.2	6.89	150.51	14.47	52.34
5.0	1958	11.6	5.63	151.13	14.57	61.38
5.5	2409	11.3	4.76	151.55	14.78	67.77
6.0	2191	11.3	4.57	151.41	15.30	70.16



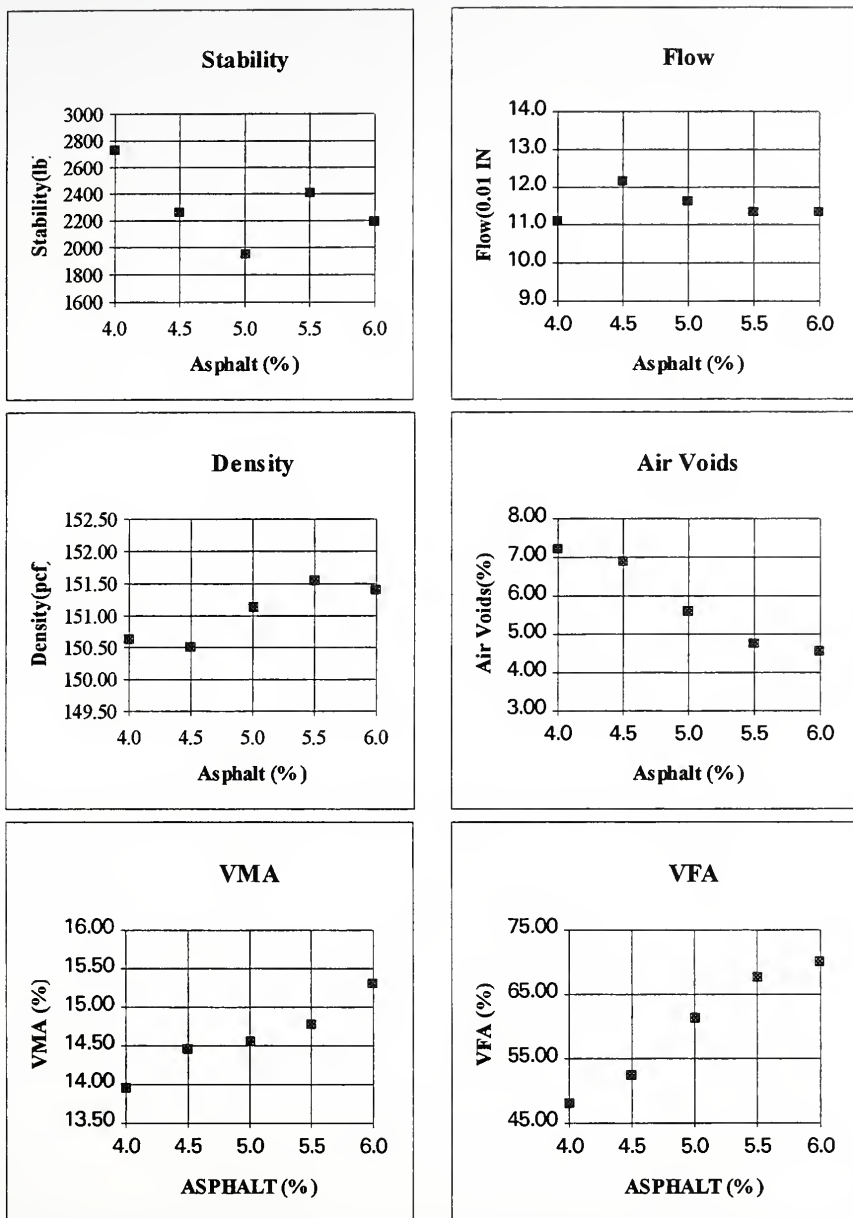


Figure A.9 MD #9 Marshall Plots (Limestone, 100% Crushed and 100% Natural Sand)





Appendix B Mix Rutting Development



Table B.1 Rutting Data of MD#1, MD#2, and MD#3

Load Repetition	M D	Lean			Optimum			Rich		
		Plastic	Comp.	Total	Plastic	Comp.	Total	Plastic	Comp.	Total
0	1	0.00	0.00	0.00	0.00	0.00	0.00	0.00	0.00	0.00
100		0.05	0.05	0.10	0.03	0.05	0.08	0.04	0.08	0.12
300		0.10	0.07	0.17	0.03	0.07	0.10	0.14	0.12	0.26
800		0.10	0.08	0.18	0.04	0.10	0.14	0.18	0.18	0.36
1500		0.10	0.10	0.20	0.09	0.12	0.21	0.22	0.26	0.48
2000		0.13	0.11	0.24	0.10	0.16	0.26	0.33	0.28	0.61
2500		0.13	0.14	0.27	0.12	0.17	0.29	0.43	0.31	0.74
3000		0.14	0.14	0.28	0.14	0.19	0.33	0.47	0.38	0.85
3500		0.14	0.16	0.30	0.16	0.20	0.36			
4000		0.16	0.17	0.33	0.18	0.21	0.38			
4500		0.18	0.18	0.36	0.19	0.21	0.41			
5000		0.20	0.18	0.38	0.21	0.22	0.43			
0	2	0.00	0.00	0.00	0.00	0.00	0.00	0.00	0.00	0.00
100		0.03	0.04	0.07	0.03	0.04	0.07	0.05	0.10	0.15
300		0.05	0.08	0.13	0.04	0.06	0.10	0.09	0.16	0.25
800		0.06	0.10	0.16	0.10	0.12	0.22	0.12	0.23	0.35
1500		0.09	0.12	0.21	0.13	0.13	0.26	0.22	0.32	0.54
2000		0.12	0.14	0.26	0.16	0.14	0.30	0.26	0.36	0.62
2500		0.13	0.16	0.29	0.20	0.16	0.36	0.30	0.38	0.68
3000		0.16	0.16	0.32	0.23	0.18	0.41	0.36	0.38	0.74
3500		0.16	0.18	0.34	0.25	0.19	0.44	0.39	0.40	0.79
4000		0.19	0.19	0.38	0.28	0.20	0.48	0.40	0.44	0.84
4500		0.20	0.20	0.40	0.30	0.20	0.50	0.44	0.48	0.92
5000		0.20	0.21	0.41	0.32	0.22	0.54	0.48	0.49	0.97
0	3	0.00	0.00	0.00	0.00	0.00	0.00	0.00	0.00	0.00
100		0.03	0.06	0.09	0.05	0.04	0.09	0.02	0.10	0.12
300		0.06	0.10	0.16	0.10	0.11	0.21	0.04	0.13	0.17
800		0.10	0.16	0.26	0.14	0.12	0.26	0.09	0.16	0.25
1500		0.12	0.20	0.32	0.20	0.18	0.38	0.17	0.22	0.39
2000		0.12	0.22	0.34	0.22	0.20	0.42	0.21	0.24	0.45
2500		0.14	0.24	0.38	0.26	0.22	0.48	0.23	0.26	0.49
3364		0.17	0.25	0.42	0.28	0.26	0.54	0.27	0.28	0.55
3500		0.17	0.26	0.43	0.30	0.26	0.56	0.31	0.29	0.60
4000		0.18	0.28	0.46	0.33	0.27	0.60	0.34	0.31	0.65
4500		0.19	0.28	0.47	0.34	0.28	0.62	0.37	0.33	0.70
5000		0.20	0.30	0.50	0.34	0.28	0.62	0.38	0.33	0.71



Table B.2 Rutting Data of MD#4, MD#5, and MD#6

Load Repetition	M D	Lean			Optimum			Rich		
		Plastic	Comp.	Total	Plastic	Comp.	Total	Plastic	Comp.	Total
0	4	0.00	0.00	0.00	0.00	0.00	0.00	0.00	0.00	0.00
100		0.03	0.03	0.06	0.05	0.04	0.09	0.04	0.03	0.07
300		0.04	0.04	0.08	0.08	0.07	0.15	0.08	0.07	0.15
800		0.05	0.05	0.10	0.13	0.10	0.23	0.16	0.13	0.29
1500		0.07	0.06	0.13	0.17	0.13	0.30	0.30	0.18	0.48
2000		0.08	0.07	0.15	0.21	0.15	0.36	0.35	0.24	0.59
2500		0.09	0.07	0.16	0.25	0.17	0.42	0.41	0.26	0.67
3000		0.11	0.08	0.19	0.27	0.19	0.46	0.46	0.28	0.74
3500		0.12	0.10	0.22	0.28	0.20	0.48	0.50	0.30	0.80
4000		0.12	0.10	0.22	0.32	0.21	0.53	0.60	0.35	0.95
4500		0.13	0.11	0.24	0.33	0.20	0.53	0.65	0.40	1.05
5000		0.13	0.11	0.24	0.33	0.21	0.54	0.75	0.44	1.19
0	5	0.00	0.00	0.00	0.00	0.00	0.00	0.00	0.00	0.00
100		0.05	0.08	0.13	0.03	0.09	0.12	0.03	0.08	0.11
300		0.10	0.11	0.21	0.08	0.12	0.20	0.06	0.15	0.21
800		0.12	0.16	0.28	0.12	0.18	0.30	0.12	0.17	0.29
1500		0.22	0.20	0.42	0.18	0.21	0.39	0.16	0.20	0.36
2000		0.25	0.22	0.47	0.21	0.23	0.44	0.24	0.23	0.47
2500		0.27	0.23	0.50	0.24	0.24	0.48	0.30	0.25	0.55
3000		0.31	0.25	0.56	0.28	0.27	0.55	0.32	0.27	0.59
3500		0.36	0.26	0.62	0.31	0.28	0.59	0.38	0.30	0.68
4000		0.38	0.28	0.66	0.35	0.30	0.65	0.42	0.33	0.75
4500		0.40	0.28	0.68	0.40	0.31	0.71	0.49	0.35	0.84
5000		0.40	0.30	0.70	0.45	0.34	0.79	0.54	0.36	0.90
0	6	0.00	0.00	0.00	0.00	0.00	0.00	0.00	0.00	0.00
100		0.02	0.06	0.08	0.07	0.06	0.13	0.07	0.11	0.18
300		0.04	0.10	0.14	0.10	0.10	0.20	0.09	0.16	0.25
800		0.08	0.16	0.24	0.11	0.12	0.23	0.16	0.18	0.34
1500		0.12	0.18	0.30	0.16	0.16	0.32	0.24	0.25	0.49
2000		0.14	0.20	0.34	0.19	0.20	0.39	0.29	0.27	0.56
2500		0.16	0.23	0.39	0.21	0.21	0.42	0.30	0.27	0.57
3364		0.18	0.24	0.42	0.24	0.22	0.46	0.33	0.29	0.62
3500		0.21	0.26	0.47	0.28	0.22	0.50	0.37	0.30	0.67
4000		0.24	0.28	0.52	0.29	0.23	0.52	0.40	0.33	0.73
4500		0.24	0.28	0.52	0.30	0.24	0.54	0.43	0.35	0.78
5000		0.24	0.30	0.54	0.31	0.24	0.55	0.43	0.35	0.78



Table B.3 Rutting Data of MD#7, MD#8, and MD#9

Load Repetition	M D	Lean			Optimum			Rich		
		Plastic	Comp.	Total	Plastic	Comp.	Total	Plastic	Comp.	Total
0	7	0.00	0.00	0.00	0.00	0.00	0.00	0.00	0.00	0.00
100		0.04	0.08	0.12	0.02	0.08	0.10	0.03	0.08	0.11
300		0.08	0.11	0.19	0.03	0.12	0.15	0.05	0.10	0.15
800		0.11	0.15	0.26	0.08	0.16	0.24	0.12	0.12	0.24
1500		0.15	0.17	0.32	0.14	0.17	0.31	0.16	0.14	0.30
2000		0.19	0.17	0.36	0.17	0.17	0.34	0.20	0.18	0.38
2500		0.20	0.20	0.40	0.18	0.18	0.36	0.24	0.20	0.44
3000		0.25	0.21	0.46	0.21	0.19	0.40	0.26	0.22	0.48
3500		0.26	0.22	0.48	0.23	0.20	0.43	0.28	0.23	0.51
4000		0.28	0.23	0.51	0.23	0.21	0.44	0.30	0.24	0.54
4500		0.31	0.23	0.54	0.24	0.22	0.46	0.33	0.26	0.59
5000		0.32	0.23	0.55	0.24	0.22	0.46	0.35	0.27	0.62
0	8	0.00	0.00	0.00	0.00	0.00	0.00	0.00	0.00	0.00
100		0.00	0.05	0.05	0.00	0.06	0.06	0.06	0.08	0.14
300		0.00	0.06	0.06	0.00	0.10	0.10	0.08	0.08	0.16
800		0.01	0.10	0.11	0.00	0.11	0.11	0.08	0.10	0.18
1500		0.02	0.11	0.13	0.01	0.11	0.12	0.08	0.11	0.19
2000		0.02	0.11	0.13	0.02	0.12	0.14	0.08	0.13	0.21
2500		0.02	0.12	0.14	0.02	0.16	0.18	0.08	0.15	0.23
3000		0.03	0.11	0.14	0.02	0.17	0.19	0.10	0.15	0.25
3500		0.03	0.11	0.14	0.03	0.16	0.19	0.10	0.15	0.25
4000		0.05	0.12	0.17	0.04	0.17	0.21	0.11	0.15	0.26
4500		0.04	0.13	0.17	0.03	0.17	0.20	0.11	0.16	0.27
5000		0.05	0.13	0.18	0.04	0.15	0.19	0.11	0.17	0.28
0	9	0.00	0.00	0.00	0.00	0.00	0.00	0.00	0.00	0.00
100		0.00	0.06	0.06	0.00	0.08	0.08	0.00	0.08	0.08
300		0.00	0.07	0.07	0.01	0.10	0.11	0.00	0.10	0.10
800		0.02	0.08	0.10	0.01	0.10	0.11	0.01	0.10	0.11
1500		0.02	0.09	0.11	0.02	0.10	0.12	0.02	0.11	0.13
2000		0.03	0.08	0.11	0.03	0.10	0.13	0.04	0.11	0.15
2500		0.02	0.10	0.12	0.04	0.11	0.15	0.05	0.11	0.16
3364		0.02	0.10	0.12	0.04	0.11	0.15	0.06	0.11	0.17
3500		0.03	0.10	0.13	0.05	0.11	0.16	0.07	0.11	0.18
4000		0.04	0.10	0.14	0.06	0.11	0.17	0.09	0.11	0.20
4500		0.05	0.10	0.15	0.07	0.11	0.18	0.10	0.11	0.21
5000		0.05	0.10	0.15	0.08	0.11	0.19	0.10	0.11	0.21





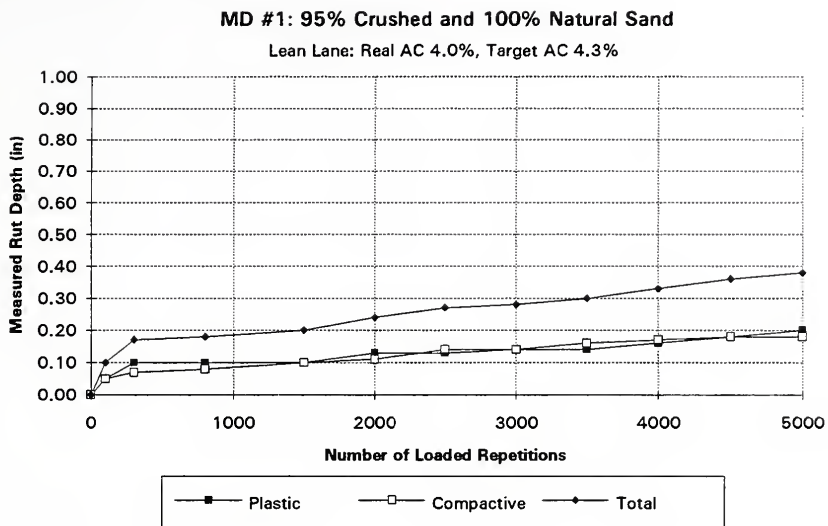


Figure B.1 Rutting of MD#1, Lean Lane



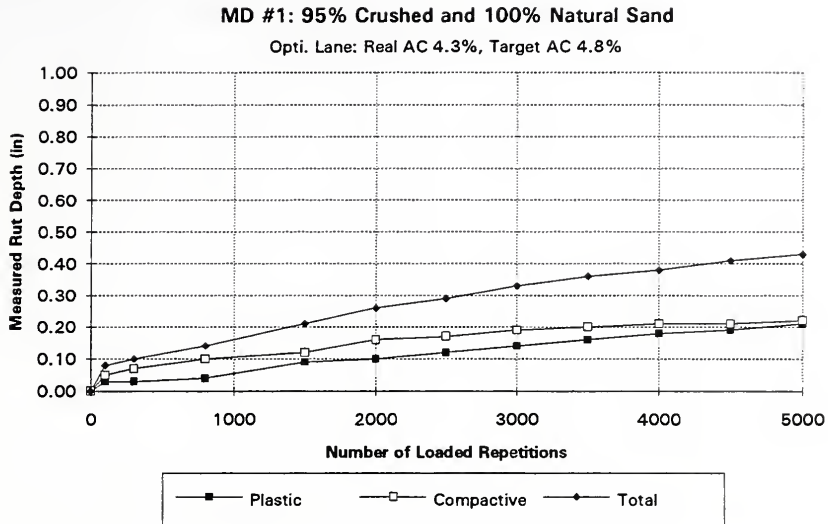


Figure B.2 Rutting of MD#1, Opti. Lane



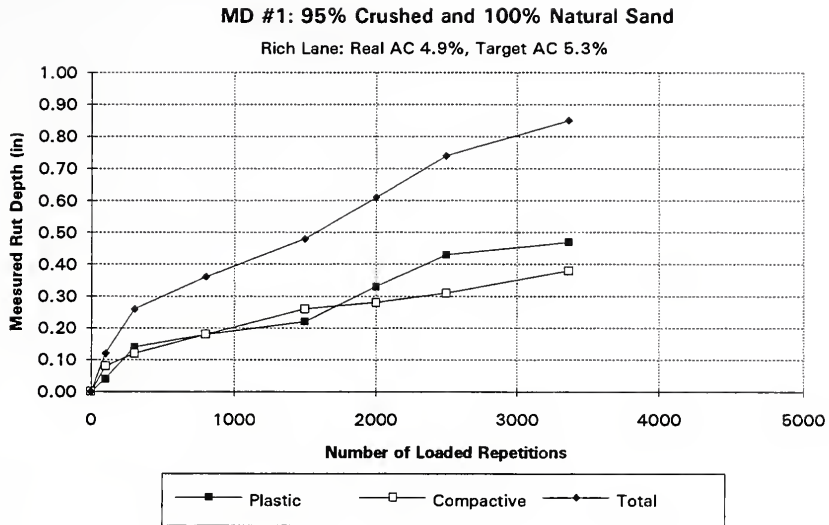


Figure B.3 Rutting of MD#1, Rich Lane



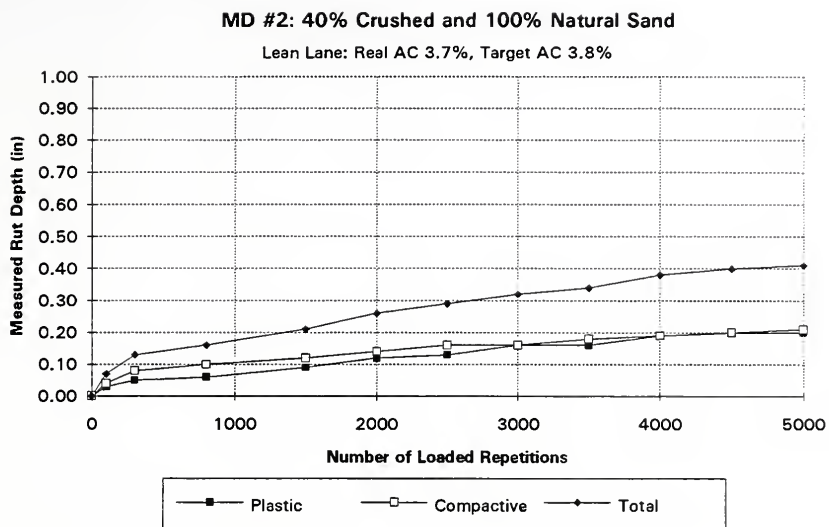


Figure B.4 Rutting of MD#2, Lean Lane





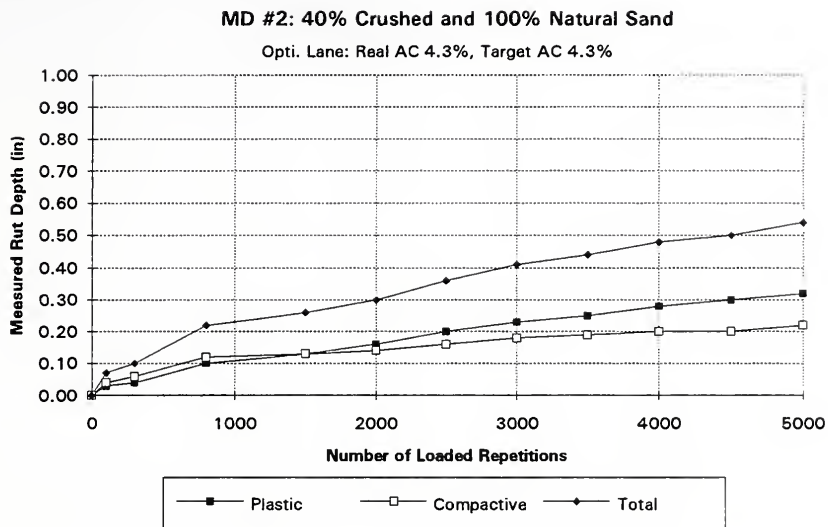


Figure B.5 Rutting of MD#2, Opti. Lane



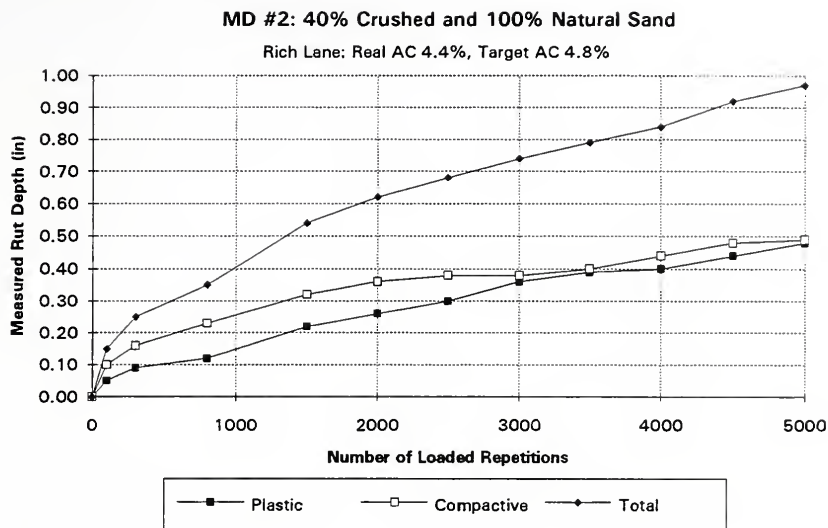


Figure B.6 Rutting of MD#2, Rich Lane



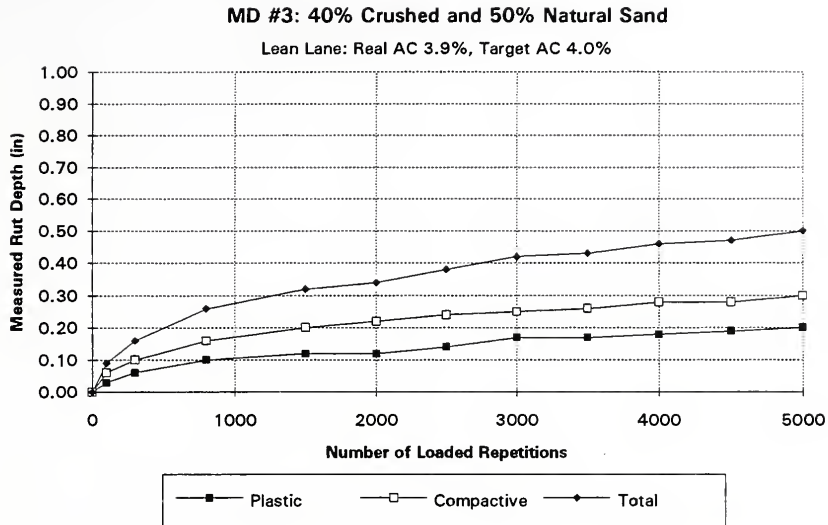


Figure B.7 Rutting of MD#3, Lean Lane



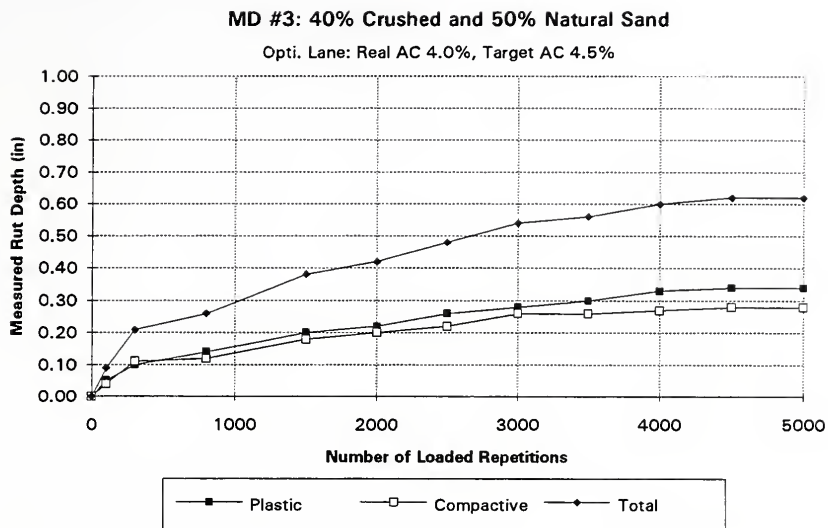


Figure B.8 Rutting of MD#3, Opti. Lane





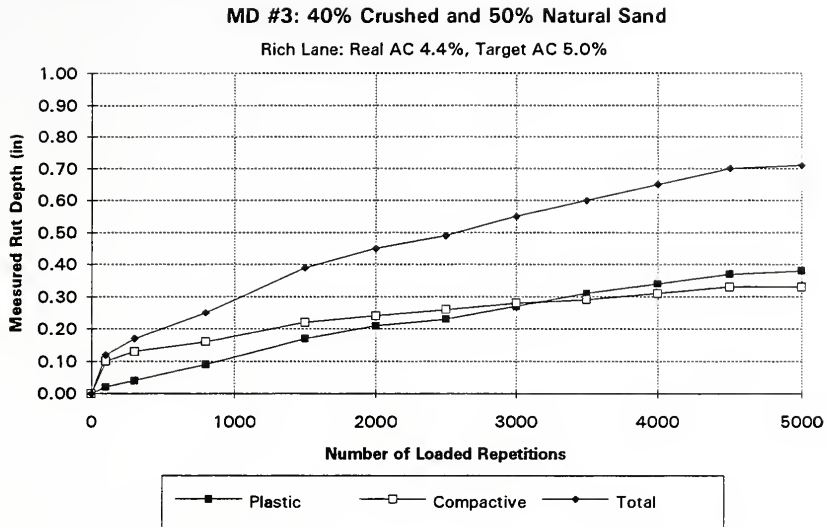


Figure B.9 Rutting of MD#3, Rich Lane



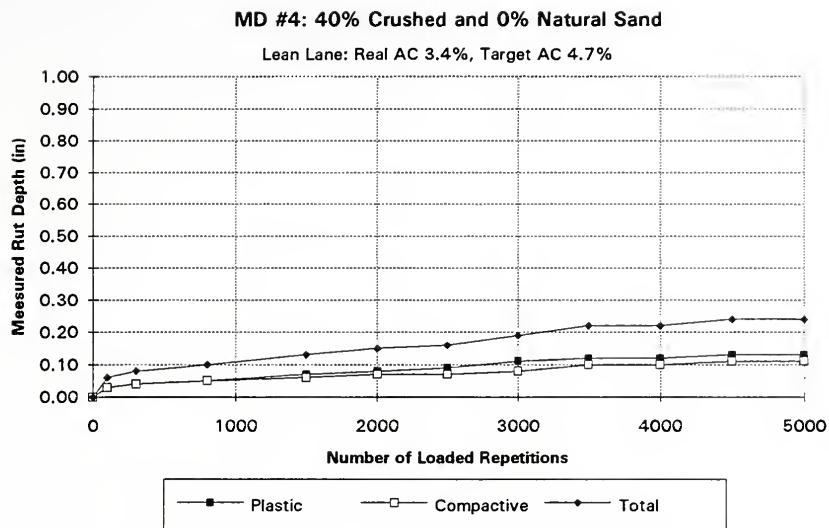


Figure B.10 Rutting of MD#4, Lean Lane



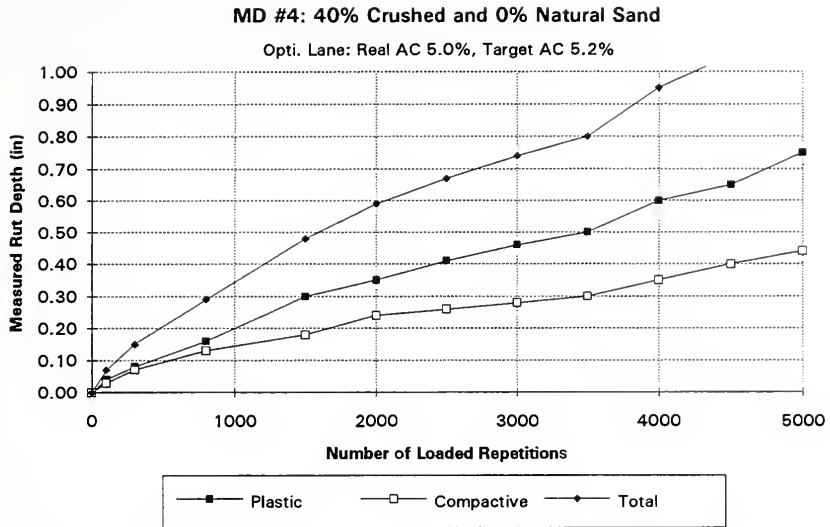


Figure B.11 Rutting of MD#4, Opti. Lane



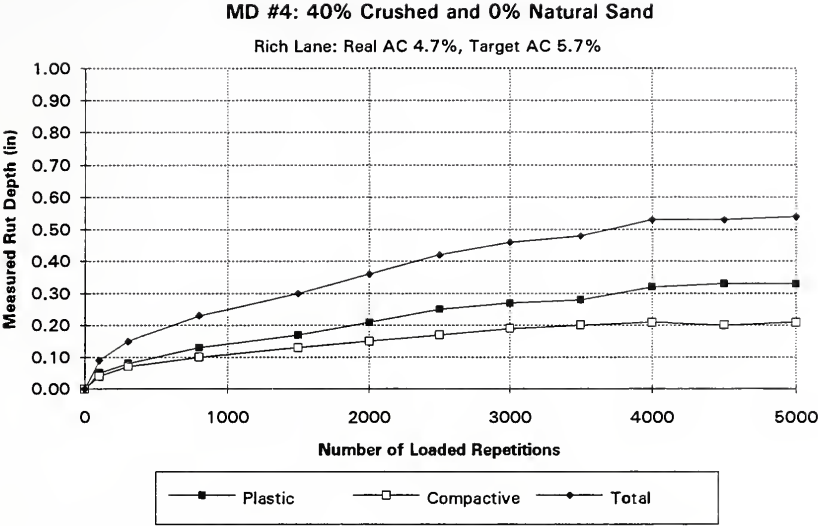


Figure B.12 Rutting of MD#4, Rich Lane





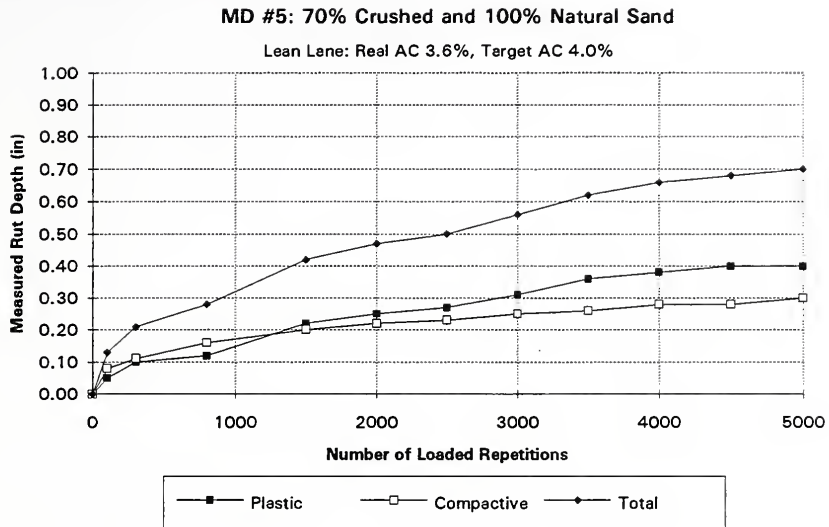


Figure B.13 Rutting of MD#5, Lean Lane



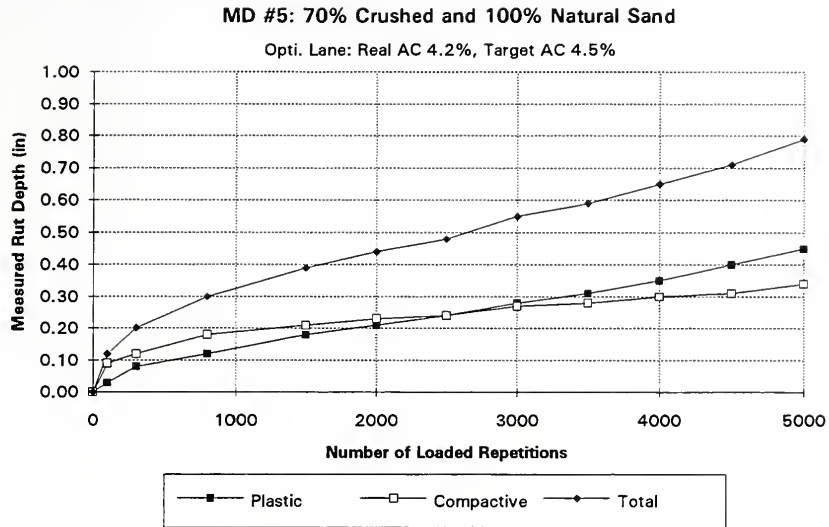


Figure B.14 Rutting of MD#5, Opti. Lane



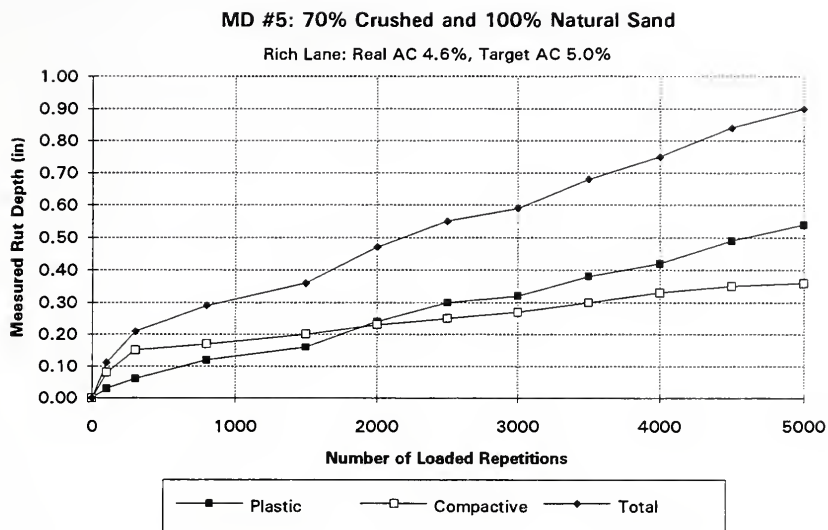


Figure B.15 Rutting of MD#5, Rich Lane



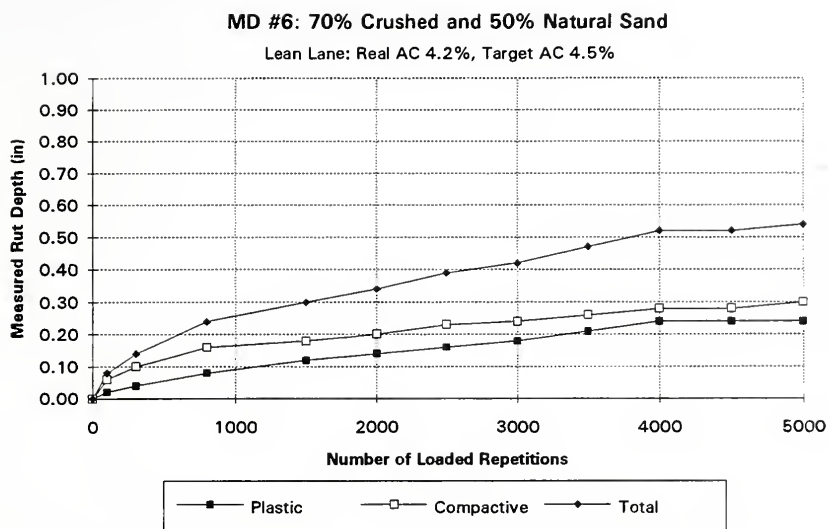


Figure B.16 Rutting of MD#6, Lean Lane





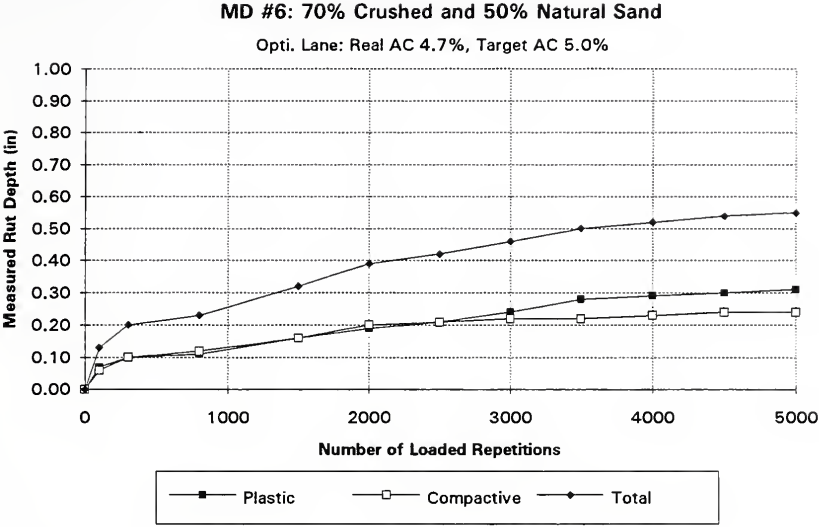


Figure B.17 Rutting of MD#6, Opti.Lane



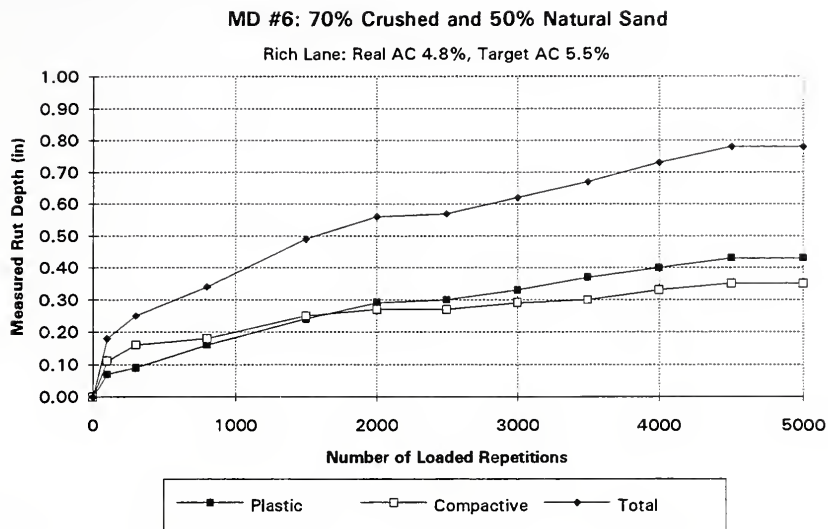


Figure B.18 Rutting of MD#6, Rich Lane



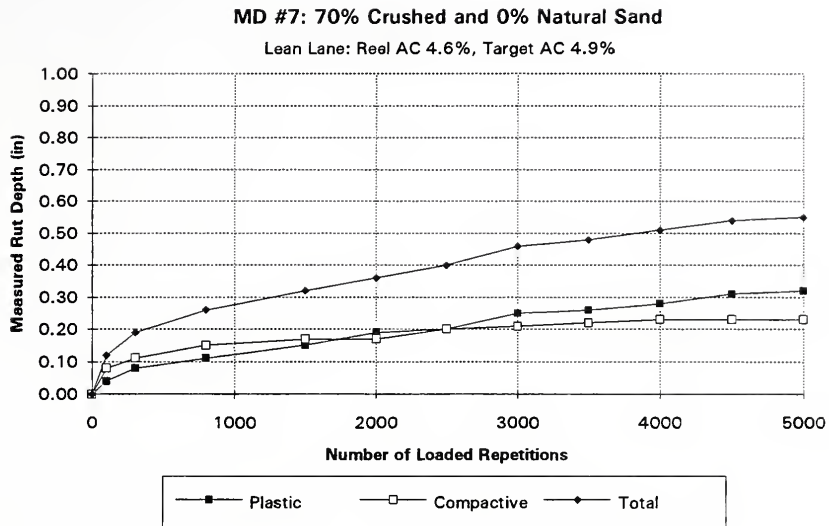


Figure B.19 Rutting of MD#7, Lean Lane



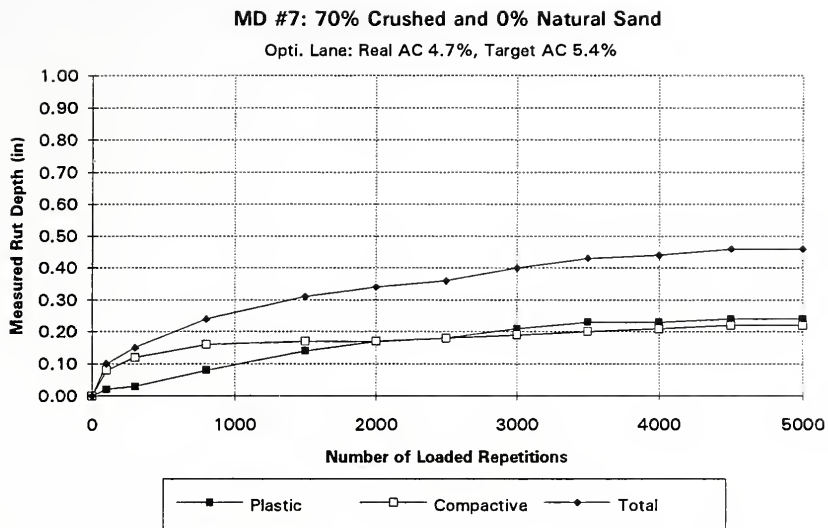


Figure B.20 Rutting of MD#7, Opti. Lane





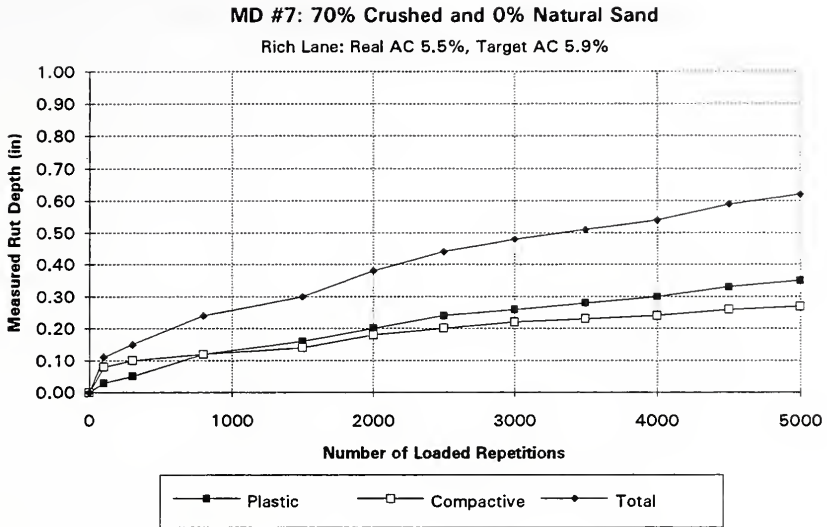


Figure B.21 Rutting of MD#7, Rich Lane



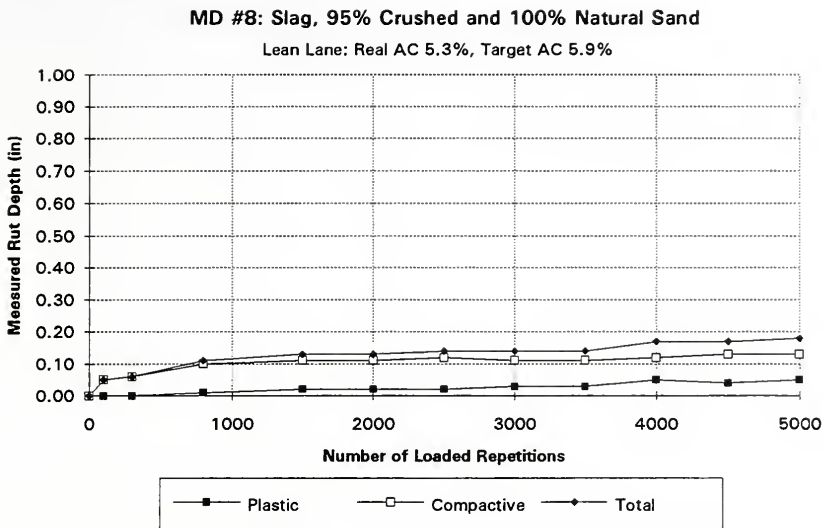


Figure B.22 Rutting of MD#8, Lean Lane



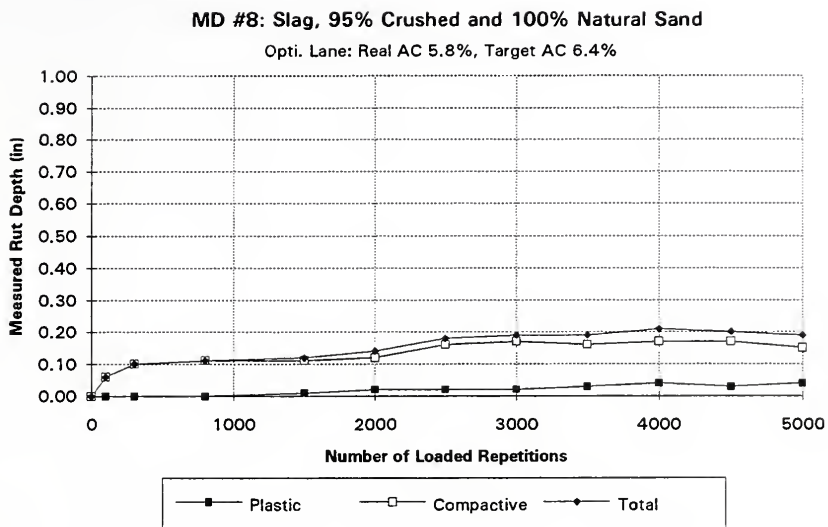


Figure B.23 Rutting of MD#8, Opti. Lane



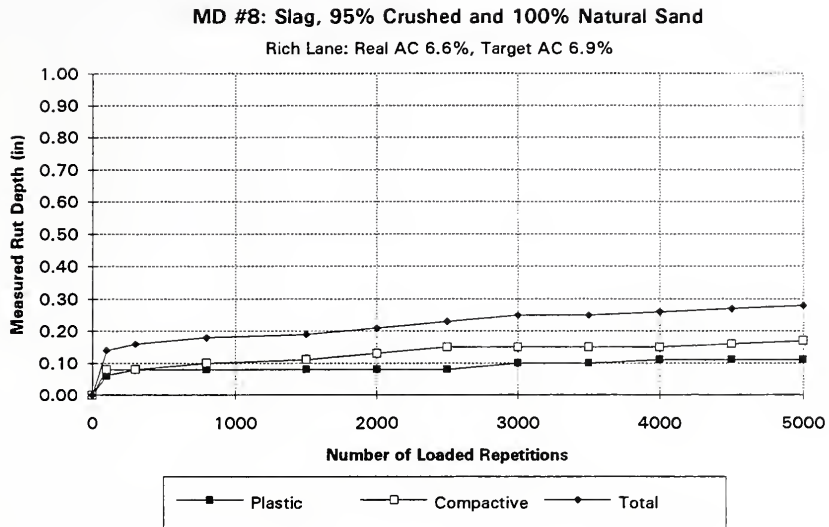


Figure B.24 Rutting of MD#8, Rich Lane





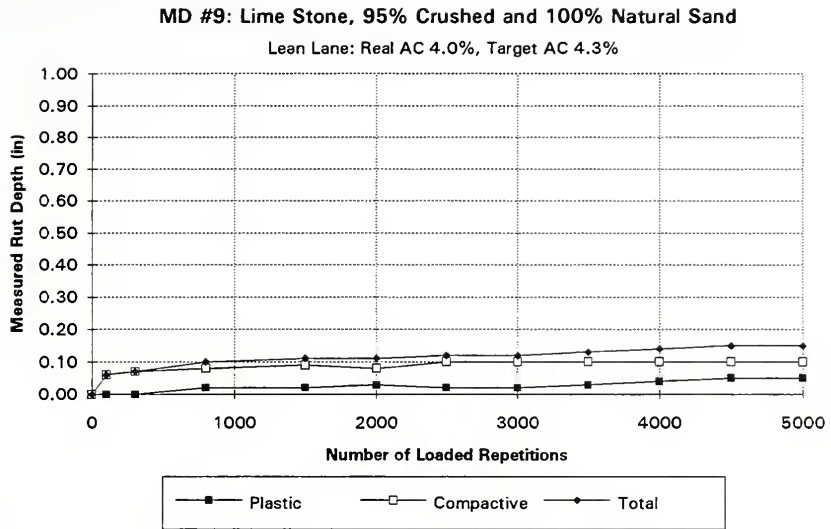


Figure B.25 Rutting of MD#9, Lean Lane



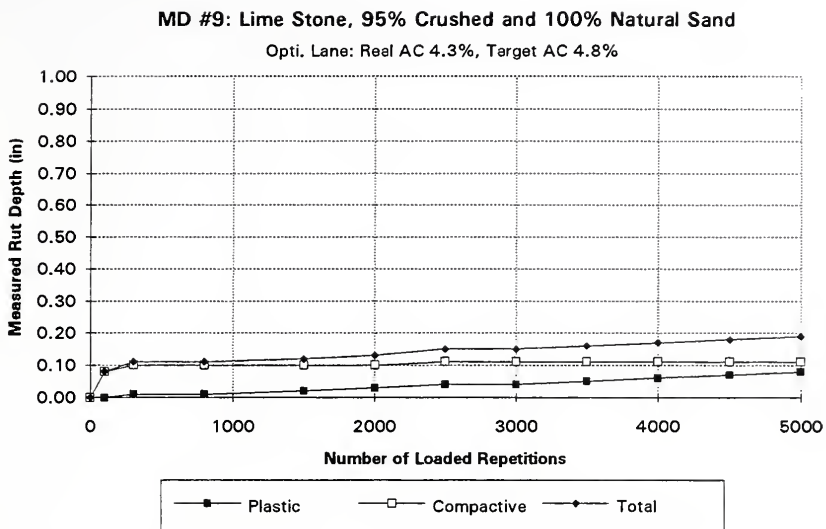


Figure B.26 Rutting of MD#9, Opti. Lane



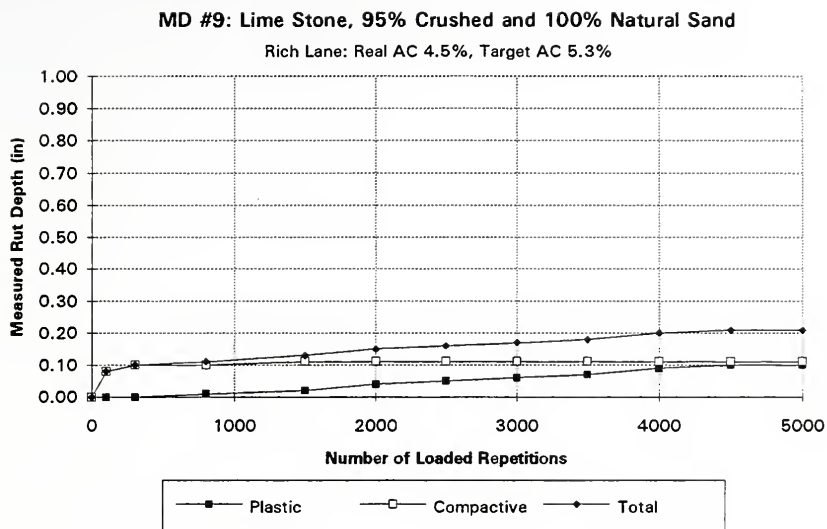


Figure B.27 Rutting of MD#9, Rich Lane



Appendix C Repeated APT Test Section Rutting Data





Table C.1 Rutting Data for Repeated APT Test Sections of MD#4 and MD#7

Load Repetitions	M D	Lean			Optimum			Rich		
		Plastic	Comp.	Total	Plastic	Comp.	Total	Plastic	Comp.	Total
0	4	0.00	0.00	0.00	0.00	0.00	0.00	0.00	0.00	0.00
100		0.05	0.06	0.11	0.03	0.01	0.04	0.07	0.08	0.15
300		0.09	0.09	0.18	0.07	0.02	0.10	0.09	0.14	0.23
800		0.16	0.14	0.30	0.13	0.04	0.16	0.20	0.17	0.37
1500		0.22	0.18	0.40	0.18	0.06	0.24	0.29	0.22	0.51
2000		0.25	0.20	0.45	0.22	0.08	0.29	0.36	0.26	0.63
2500		0.27	0.22	0.50	0.25	0.09	0.34	0.42	0.28	0.70
3000		0.30	0.24	0.53	0.27	0.10	0.37	0.47	0.31	0.78
3500		0.32	0.25	0.58	0.29	0.11	0.40	0.52	0.35	0.86
4000		0.35	0.26	0.61	0.32	0.11	0.43	0.55	0.37	0.93
4500		0.36	0.28	0.64	0.34	0.12	0.46	0.59	0.39	0.98
5000		0.39	0.30	0.68	0.36	0.12	0.48	0.63	0.43	1.05
0	7	0	0	0						
94		0.04	0.03	0.07						
262		0.06	0.04	0.10						
630		0.10	0.06	0.15						
1237		0.13	0.07	0.20						
1645		0.15	0.08	0.23						
2044		0.17	0.09	0.26						
2899		0.21	0.10	0.31						
3298		0.21	0.11	0.32						
4000		0.23	0.10	0.33						
4500		0.23	0.12	0.35						
5000		0.23	0.12	0.35						
0	7				0.00	0.00	0.00	0.00	0.00	0.00
100					0.05	0.04	0.09	0.06	0.07	0.12
300					0.08	0.06	0.14	0.10	0.09	0.19
800					0.13	0.09	0.22	0.17	0.12	0.29
1500					0.18	0.11	0.29	0.24	0.14	0.38
2000					0.21	0.12	0.33	0.28	0.16	0.44
2500					0.23	0.13	0.36	0.32	0.17	0.49
3000					0.25	0.13	0.38	0.35	0.18	0.54
3500					0.28	0.14	0.41	0.39	0.19	0.58
4000					0.28	0.14	0.42	0.41	0.20	0.61
4500					0.30	0.15	0.45	0.43	0.21	0.64
5000					0.32	0.15	0.47	0.45	0.22	0.67



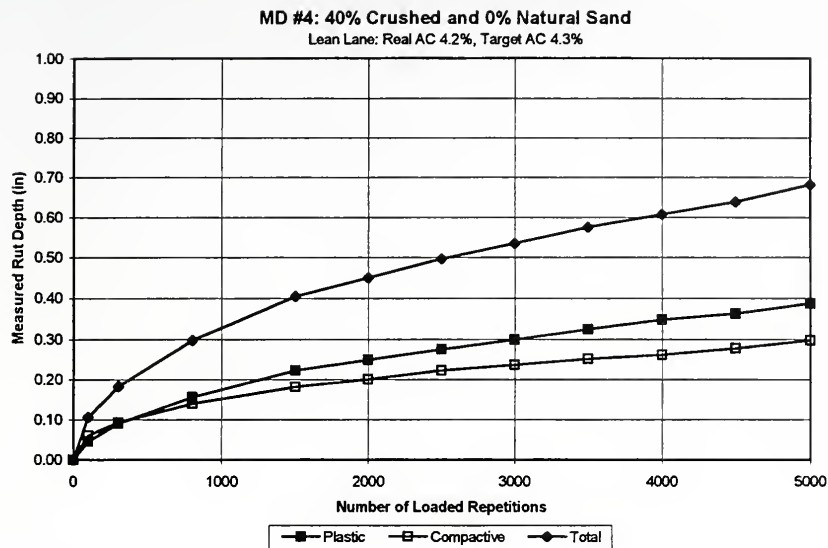


Figure C.1 Rutting of Repeated MD#4, Lean Lane



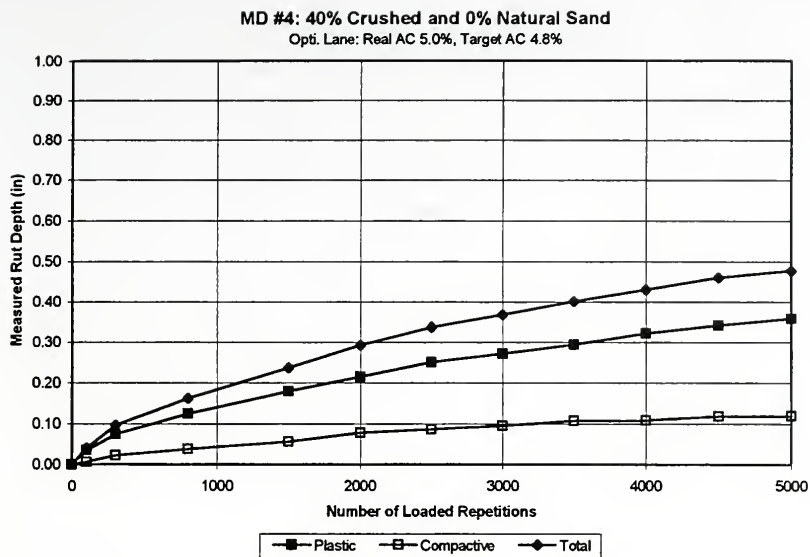


Figure C.2 Rutting of Repeated MD#4, Opti. Lane



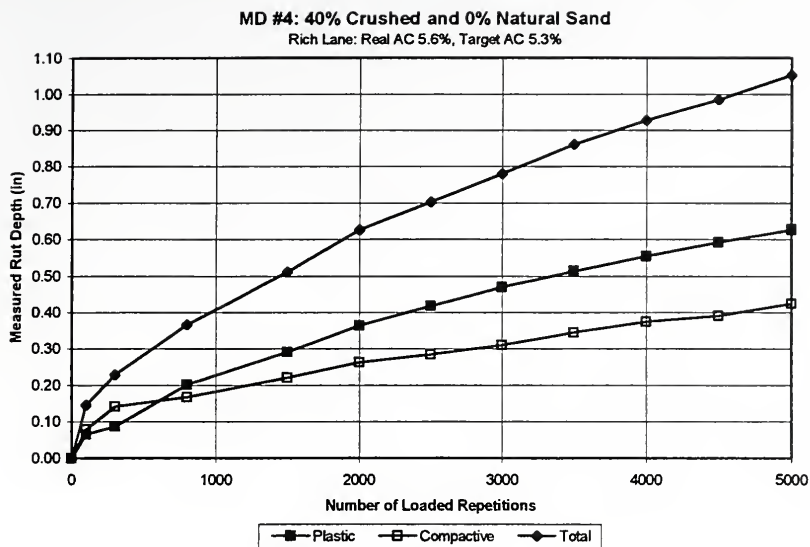


Figure C.3 Rutting of Repeated MD#4, Rich Lane





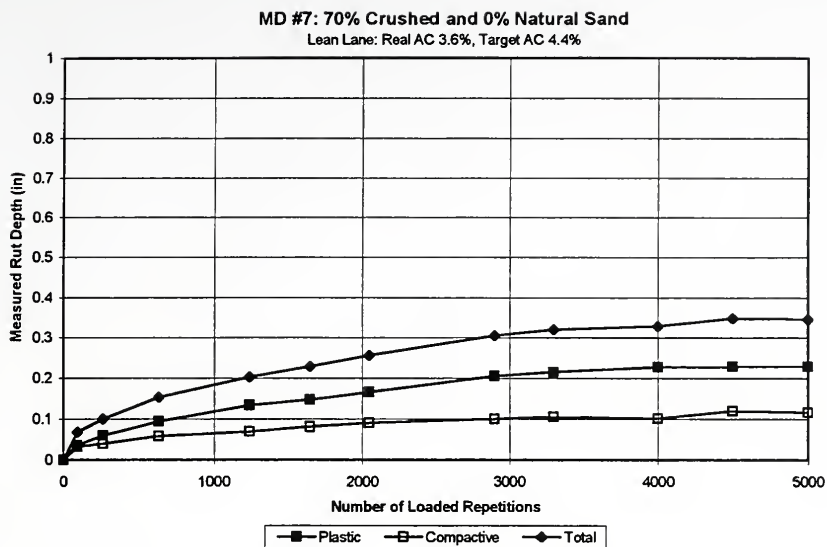


Figure C.4 Rutting of Repeated MD#7, Lean Lane



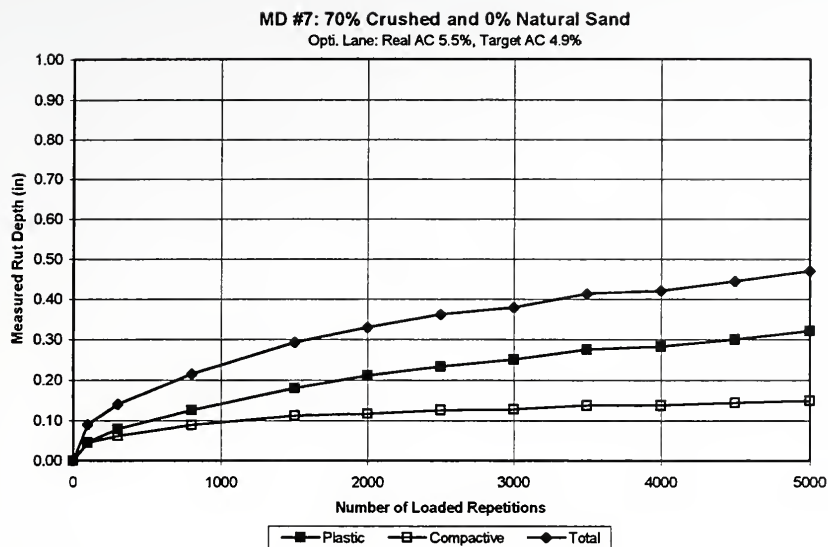


Figure C.5 Rutting of Repeated MD#7, Opti. Lane



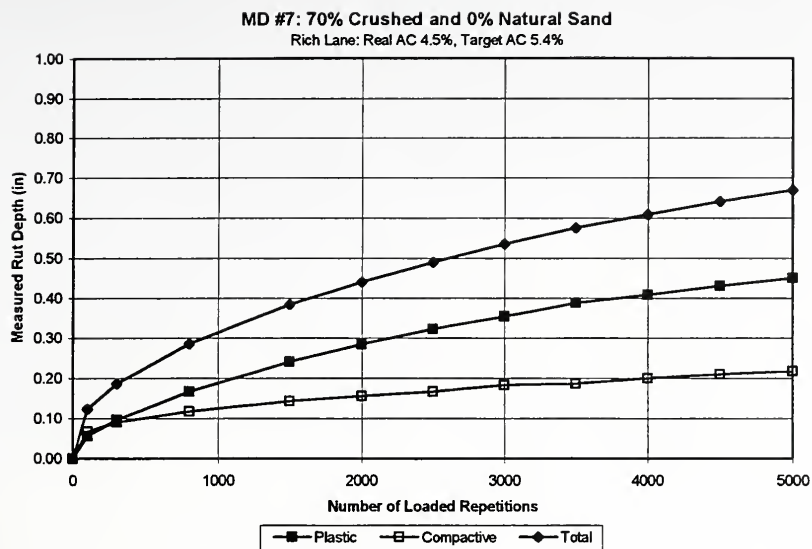


Figure C.6 Rutting of Repeated MD#7, Rich Lane





COVER DESIGN BY ALDO GIORGINI